A DYNAMIC SIMULATION APPROACH TO SOIL SALINITY AND SODICITY IN KONYA PLAIN OF TURKEY

by

Mehmet Can Tunca

B.Sc. in International Trade, Boğaziçi University, 2018

Submitted to the Institute of Environmental Sciences

in partial fulfillment of the requirements for the degree of

Master of Science

in

Environmental Sciences

Boğaziçi University

2021

ACKNOWLEDGEMENTS

Thanks to all who paved the path before me,
Who cleared the way for me,
Who showed the light to me,
Who supported and eased me…

I would like to express special thanks to the financial support of the TUBITAK Project (No: 118Y343).

ABSTRACT

A DYNAMIC SIMULATION APPROACH TO SOIL SALINITY AND SODICITY IN KONYA PLAIN OF TURKEY

Soil salinity and sodicity are twin problems potentially affecting soil fertility, farmers' livelihoods and food security. Management and control of these problems, particularly on irrigated farmlands require knowledge and expertise crafted through appropriate models and experiments. The accumulation of salts on the soil profiles may occur through natural processes as well as by human actions, that are mostly related to poor agricultural and irrigation practices. Accumulation of salt in soil water impedes crop evapotranspiration, sodicity threatens the soil structure and degrades its hydraulic qualities. These problems are more pervasive in arid and semi-arid regions. Therefore, irrigation and agricultural practices are crucial in controlling these problems to avoid their undesired consequences. In this research, a dynamic simulation model is built to represent salinization and sodification in soil layers so as to test the long-term impact of alternative irrigation practices with respect to water quality, quantity and schedule, on soil fertility and farm yields. The model is developed based on the system dynamics methodology. Model parameter values are selected as representative of the field conditions of Konya Plain in Turkey, which is a semi-arid region partially experiencing soil salinization problems. This study is completed as a part of the TÜBİTAK-funded research project entitled, "Soil Salinity and Sodicity Management by Sustainable Irrigation Practices in Konya Plain". Based on the scenario analyses performed in the research, irrigation water quality, irrigation method as well as crop rotations found to be important factors on soil salinization and sodification process in soil.

ÖZET

TÜRKİYE KONYA OVASI'NDA TOPRAK TUZLULAŞMASI VE SODİKLEŞMESİ: DİNAMİK BENZETİM YAKLAŞIMI

Toprak tuzlulaşması ve sodikleşmesi, toprak üretkenliğini, gıda güvenliğini ve çiftçilerin hayat koşullarını etkileyebilen ikiz problemlerdir. Bu problemlerin yönetimi ve kontrolü, bilhassa sulanan tarım arazilerinde, uygun model ve deney çalışmalarına dayanan bilgi ve uzmanlık gerektirmektedir. Tuzların toprak kesitlerinde birikimi, doğal süreçler sebebiyle gerçekleştiği gibi insan etkisiyle de gerçekleşmektedir. Toprak tuzlulaşması bitki su tüketimini engelleyebilmektedir. Bununla birlikte, toprak sodikliği ise toprağın yapısını tehdit etmekte, özellikle hidrolik özelliklerini zayıflatabilmektedir. Bu problemler yağış oranının buharlaşmaya göre yetersiz olduğu yarı-kurak ve kurak alanlarda yaygın olarak görülebilmektedir. Bu çalışmada, farklı sulama yöntemlerinin, sulama suyu kalitesine bağlı olarak gerçekleşebilecek toprak tuzluğu ve sodikleşmesi problemlerinin, toprak üretkenliği ve verim üzerindeki etkilerini uzun vadede test etmek amacıyla bir benzetim modeli geliştirilmiştir. Model dinamik sistem metodolojisi baz alınarak geliştirilmiştir. Model parametreleri, bazı kısımlarında toprak tuzlulaşmasına rastlanabilen, yarı-kurak iklime sahip Konya Ovası'nın koşularını temsil etmek üzere belirlenmiştir. Bu çalışma TÜBİTAK tarafından fonlanan "Konya Ovası'nda Sürdürülebilir Sulama Uygulamalarına Dayanan Toprak Tuzluluğu ve Sodikliği Yönetimi" isimli kapsamlı bir araştırma projesinin bir parçası olarak tamamlanmıştır. Bu çalışmada gerçekleştirilen senaryo analizleri, sulama suyu kalitesi, sulama metodu, uygulanan ekin tercihi ve de ekin nöbeti çeşitlerinin toprak tuzlulaşması ve sodikleşmesi süreçlerinde önemli etkilerinin olabileceğini göstermiştir.

TABLE OF CONTENTS

LIST OF FIGURES

LIST OF TABLES

LIST OF ABBREVIATIONS

Abbreviation	Explanation
DSI	State Hydraulic Institute
EC	Electrical Conductivity
ESP	Exchangeable Sodium Percentage
FAO	Food and Agriculture Organization of United Nations
KOP	Konya Plain Project
RCP	Representative Concentration Pathway
SAR	Sodium Adsorption Ratio
TAGEM	General Directorate of Agricultural Research and Policies
TUIK	Turkish Statistical Institute

1. INTRODUCTION

Soil salinity and sodicity are processes which pose threats to agricultural production and farmer livelihood through soil quality degradation and crop yield reduction. Salinity and sodicity often accompany each other, and emerge due to the accumulation of the various salts in the soil layers (Hillel, 2000).

Soil salinity and sodicity have been long-standing challenges for societies especially which reside in semi-arid and arid regions. Civilizations that are engaged in irrigated agricultural production have experienced these very problems for centuries. Mesopotamia region has been stated as one of the oldest examples of salinity challenge to the ancient societies. After long periods of irrigation, increased agricultural productivity helped Sumerians to prosper. However, starting from 2400 BC, accelerated soil quality degradation due to soil salinity and sodicity had severely affected productivity. Consequently, this major damage in agricultural production is emphasized an important factor contributing to the collapse of Sumerian civilization (Jacobson and Adams, 1958). The Harappan civilization of the plains of India and Pakistan and the Valley of Peru has been reported as other ancient cases with similar problems (Shahid et al., 2018).

Irrigation is a great facilitator to boost agricultural production. In the last 50 years, the area of irrigated lands has doubled and currently constitutes %20-25 percent of the total global harvested land. Nevertheless, irrigated lands provide %35-40 percent of the total crop production (FAO-ITPS, 2015; Meier et al., 2018).

Together with the augmentation of the irrigation practices in agricultural activity, the expansion of salt-affected areas worldwide also requires attention. Although the accuracy of the statistics of global salt-affected soils are open to dispute, the best available reports emphasized that the area of salinity and sodicity affected lands accounts for 1 billion ha in total (FAO-ITPS, 2015; Ivushkin et al., 2019). The estimations also highlighted that the salt-affected areas associated with the irrigation practices are around 60 million ha. Therefore, human induced salinity problems due to agricultural irrigation affects much less area than natural salinity. We can view the distribution of saline and sodic soil across the globe in Table 1.1.

Table 1.1. Continentally Share of Saline and Sodic Soils (FAO-ITPS, 2015).

Continent	*Saline Soils (Million ha)*	*Sodic Soils (Million ha)*	*Total (Million ha)*
Africa	122.9	86.7	209.6
South Asia	82.3	1.8	84.1
North and Central Asia	91.5	120.2	211.7
Southeast Asia	20	-	20
South America	69.5	59.8	129.3
North America	6.2	9.6	15.8
Mexico/Central America	2	-	2
Australasia	17.6	340	357.6
Total	**412**	**618**	**1030**

The problem is encountered in many different countries around the world. Pakistan, China, Iraq, Mexico, Spain, Australia among the countries that experience salt related problems (Shahid et al., 2018; Daliakopoulos et al., 2016). The concentration of salts in soil water can inhibit plant water uptake and bring reductions in crop yield rates. Even though all plants can tolerate salinity up to a certain threshold level, which is specific to crop type, yields decrease almost linearly above the threshold parallel to increase in salt concentration (Maas and Hoffman, 1977). Therefore, the extensive share of salt-affected areas leads to dramatic loss in agricultural production. The global loss of crop production due to salinity is assessed as US$ 27.3 billion annually according to a recent study which considers 2013 as the base year to extrapolate the global cost with current data. (Qadir et al., 2014).

Agricultural activity plays a key role in the economic production of Turkey. According to data reported by Turkish Statistical Institute, the value of marketable crop production is about 4% of GDP in 2020. Furthermore, the area of total arable land and land under permanent crops covered 23 million ha again in 2020 (TUIK, 2021b). Besides, in Turkey irrigated agricultural area is estimated as 6.3 million ha in 2018 (Kalkınma Bakanlığı, 2018). Therefore, around 27% of cultivated area is being irrigated in the country based on current available data. Euphrates Basin and Konya Closed Basin are among the regions where agriculture is one of the main sources of economic production and irrigation is widely applied in the country.

Turkey also has been experiencing salt-related problems in agricultural sector. The country hosts various climatic and environmental conditions, including semi-arid and arid climates which can facilitate the emergence of salt related problems. It has been stated that the area salinized by irrigation applications covered around 1.5 million area in 2004 (Frenken, 2009). Harran Plain, Konya Plain, and Amik Plain are some of the agricultural basins suffered from salt-related problems due to irrigation applications without proper and well-operating drainage systems (Kanber et al., 2005).

Konya plain plays a vital role in agricultural production with around 13% of the total cultivated area of the country in this region (KOP, 2020). Furthermore, the plain is in the leading position for various crop types for the country, where irrigation application has a long-standing history. Even before the establishment of the Turkish Republic, investments have been made to construct irrigation channels in some parts of the region. As a result of the excessive irrigation, salt accumulation was observed in agricultural fields during the 20th century. Some parts of the plain experienced yield losses due to salt-related problem for several decades (de Meester, 1970). Nevertheless, especially after 90s, the improvements in drainage infrastructure which facilitated the control and management of salt leaching alleviated the salt accumulation on farmlands. Yet, the Konya Plain of Turkey, where the irrigated area is large, highly-water demanding crops are planted and semi-arid climate conditions are dominant, still has a potential to face similar obstacles in the near future (Yılmaz and Okumuş, 2015) (WWF, 2014).

Soil salinity is defined as the concentration of various salt minerals dissolved in the soil water. The dissolved electrolyte minerals involve several cations (Na^+, Mg^{2+}, Ca^{2+}, K^+) and anions (Cl^-, $SO4^{2-}$, NO_3^-, HCO_3^-, and CO_3^{2-}) present in soil profiles. The standard measure for salinity of a soil sample is electrical conductivity (decisiemens per meter) of a saturation extract at 25°C (Tanji, 2002). Based on the measurement of electrical conductivity, soils are classified according to salinity levels. Although salinity evaluation for irrigation water is mostly carried out by the same method of measurement as electrical conductivity, there are other gauges in use such as total soluble salts, $mmol_{(c)}/l$ (millimoles of charge or milliequivalents per liter) and total dissolved solids (TDS) in mg/l units. In Table 1.2, we can view the categorization of soil salinity class according to their electrical conductivity and the varying impact of salinity class on the plant growth.

Table 1.2. Soil Salinity Classes (Richards, 1954).

Soil Salinity Class	Electrical Conductivity of The Saturation Extract (dS/m)	Effect on Crop Growth
Non-Saline	0-2	Salinity effects negligible
Slightly Saline	2-4	Yields of sensitive crops may be restricted
Moderately Saline	4-8	Yields of many crops are restricted
Strongly Saline	8-16	Only tolerant crops yield satisfactorily
Very Strongly Saline	>16	Only a few tolerant crops yield satisfactorily

Soil sodicity refers to the ratio of adsorbed Na^+ to all cations that are adsorbed to the clay particles of a soil complex (Tanji, 2002). Soil sodicity is mostly expressed by the concept of Exchangeable Sodium Percentage (ESP) which refers to the percentage of exchangeable sodium relative to total exchangeable cations in a complex structure (Equation 1.1). The soil samples that have values higher than 15 ESP, which means more than 15% of the adsorbed cations are Na^+, are classified as sodic (Richards, 1954).

$$ESP = \left(\frac{Exchangeable\ Na}{Cation\ Exchange\ Capacity}\right) * 100 \tag{1.1}$$

where Exchangeable Na, and Cation Exchange Capacity are measured in the units of meq/100 gr soil. On the other hand, sodicity level of a soil water is assessed by another standard which is the Sodium Adsorption Ratio, SAR, of a saturated extract from soil. SAR values exceeding 13 is considered as indicating sodic conditions. SAR is a measure of sodium, Na^+, amount relative to calcium (Ca^{2+}) and magnesium (Mg^{2+}) in the solute. The calculation of SAR values is given in Equation 1.2. Sodium Adsorption Ratio (SAR) is measured in $(mmol_{(c\ )}/L)^{-1/2}$ units.

$$SAR = \frac{Na^+}{\sqrt{\frac{Ca^{2+} + Mg^{2+}}{2}}} \tag{1.2}$$

In addition to this, irrigation water quality is also assessed to determine its salinity and sodicity levels. While salinity of irrigation water can be evaluated by the gauges stated above, Electrical Conductivity is a common way to indicate water salinity as well. On the other hand, sodicity level of irrigation water is only expressed by its Sodium Adsorption Ratio (SAR). The classification of salt-affected soils can be demonstrated as in Table 1.3.

Table 1.3. Classification of Salt-affected Soils, Adapted from (Davis et al., 2007) and (Kansas State University, 1992).

Soil Classification	Electrical Conductivity (EC) (dS/m)	Exchangeable Sodium Percentage (ESP)	Sodium Adsorption Ratio (SAR) ($(mmol_{(c)}/L)^{-1/2}$)
Saline	>4.0	<15.0	<13.0
Sodic	<4.0	>15.0	>13.0
Saline and Sodic	>4.0	>15.0	>13.0

The presence of soluble salts in the soil inhibits the growth of the crop by two main mechanisms: osmotic stress and specific ion effects (Butcher et al., 2016). Osmotic or drought stress refers to the increase of the osmotic potential of the root zone water by the dissolved salts which lowers the energy state of the water, resulting in problems of plant water uptake because uptake through root membrane become difficult and require more energy. The limited ability to use water prevents crops to grow or germinate, consequently, leads to reduction in the agricultural yield. Moreover, the responses of plants to the salt accumulation in the root zone differs based on their tolerance level (Foth, 1990). The salt tolerance of plants refers to the maximum salt concentration that the plant withstands without being exposed to any negative impact. The plants adapted to saline conditions are called *halophytes* (i.e. barley, sugar beet, cotton, tomato, spinach etc.), while the salt- sensitive ones are *glycophytes* (i.e. fruit trees, corn, beans, clovers etc.) (Hillel, 2000). On the other hand, there are individual effects of the excess salts, which can have toxic effects on the organisms. The common effects are the membrane damage, which results in cell death, inhibition of photosynthesis, closure of stomata etc. (Aslam et al., 2012).

Soil sodicity is another condition that would generate obstacles to germination or plant growth and degrade the hydraulic qualities of soil. The clay particles in soil solution usually demonstrate a negative charge. The neutralization of those particles occurs through adsorption of some cations such as Na^+, Mg^{2+}, Ca^{2+}, K^+. Therefore, the ratio of absorbed cations to other cations can play important role in determining soil characteristics. For instances, if presence of Mg^{2+} or Ca^{2+} is more than Na^+, the soil tends to be flocculated and, therefore, more porous, and permeable for water. However, when

Na^+ is more absorbed by soil solution, the soil composition would be deflocculated. In such conditions, aeration and infiltration of water would be hard and create ineligible conditions for plant growth (Shainberg and Letey, 1984).

The accumulation of salt minerals in the soil layers may arise through natural processes. The transportation of salts after the chemical and physical weathering of mineral rich magmatic rocks could be stated as an example for such processes. Moreover, the augmentation in the salinity level of groundwater sources due to sea water intrusion especially in areas where sea water level lies above the soil surface could be another source for natural salinization. Lastly, the seepage flows from saline groundwater aquifers may introduce significant amounts of salts to soil layers as well. While the natural processes of salt accumulation are interpreted as primary salinization, the salinity problems caused by human interventions are called secondary salinization (Vengosh, 2003).

The second form of salinization happens primarily in arid and semi-arid regions where the rates of precipitation are quite lower than evapotranspiration. Human-induced salinization processes are mostly related to inappropriate irrigation by farmers (Daliakopoulos et al., 2016). Various dissolved salt minerals introduced by irrigation practices into the rootzone may not be leached through the soil profile via percolation of water. Furthermore, the rise in the groundwater level due to excessive irrigation applications could increase the salinity concentration of soil water in fields especially where the evapotranspiration rate is high. In such cases, shallow level of water table below the rootzone can be another source for salinization as dissolved salt minerals can move upwards through capillary rise of water and be left there, after water is removed by evapotranspiration process. In addition to this, the quality of irrigation water may also be salt-rich, or excessive applications of certain fertilizers, usage in salty wastewater in irrigation may augment the salt load in soil layers. Consequently, certain soil properties, such as hydraulic conductivity, crop growth, and yield are prone to be negatively influenced by the accumulation of the salts in the root zone (Qadir and Oster, 2004). The primary and secondary salinity are well illustrated in Figure 1.1 where the left-side of the figure indicates the primary form of salinization process, yet the right side demonstrates the secondary drive of salinization.

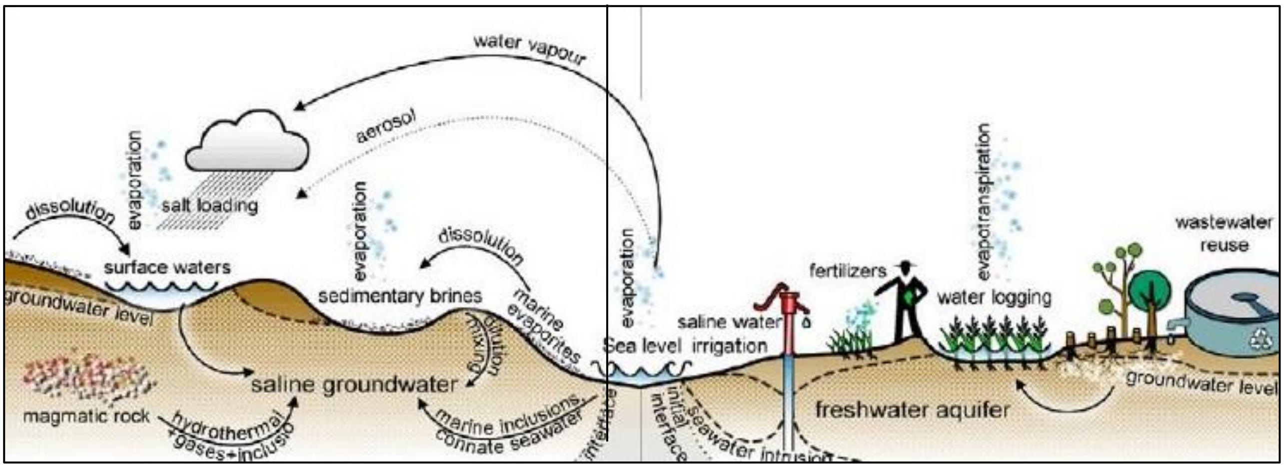

Figure 1.1. Salinization processes (Daliakopoulos et al., 2016).

The accumulation of salt minerals, soil sodification in agricultural fields and crop growth are highly interconnected and complex processes. Various scientific works from different disciplines have been carried out to better comprehend, manage, and control these problematic issues within this regard. Mathematical modelling and simulation is one of such disciplines which scholars developed to represent various realistic conditions that would help to uncover the underlying reasons for salt-related problems in agricultural production.

There are multiple mathematical models in software platforms that have been constructed to perform simulations of soil salinization with respect to agricultural activity. Hydrus 1-D (Simunek et al., 2018), Saltmod (Oosterbaan, 2002), SWAP (Kroes et al., 2009), Drainmod-S (Kandil et al., 1995) and SOTE (Kramer & Mau, 2020) are prominent and recent works in this area. We also aim to develop a model based on the system dynamics methodology to simulate soil salinization, sodification and crop growth processes which depends on soil properties, different irrigation methodologies and water quality, and crop types and rotations. Moreover, we aim to perform scenario-based simulation runs to observe how different farmer irrigation applications may impact the salt accumulation, quality of soil properties and crop yield by season in the long-term. For scenario-based simulation runs, we mainly focus on the Konya Plain of Turkey where salt-related problems have been experienced for decades and may get exacerbated in near future as well.

2. PROBLEM DESCRIPTION AND RESEARCH OBJECTIVES

The salinization and sodification processes have been examined by a large number of studies over decades. From soil column experiments to field research and observations, different approaches are introduced to develop an understanding about these problems especially with respect to agricultural activities. Furthermore, simple statistical models were produced to mathematically elucidate the interactions between different essential components of soil-water-crop nexus. For instance, the predictions for how various salt compositions of soil water can have impact on the hydraulic conductivity of a soil profile is mainly based on a long-standing statistical model which is built laboratory scale experiments. The model can express the possible reductions on hydraulic conductivity due to irrigation water quality (McNeal, 1968). Likewise, the prediction for crop yield rate by season is performed based on the measured or estimated actual evapotranspiration level in proportion to its potential throughout a season (Steduto et al., 2012). Nevertheless, such studies generally examine the relationships only between few selected factors in complex processes where numerous different elements are interconnected and simultaneously influence each other.

Geological and physical properties of soil profiles shape the fate of water movement through soil layers. On the other hand, various salt minerals accumulate in the rootzone or groundwater sources mainly via transportation by water in dissolved form. Moreover, soil sodification process through multispecies adsorption mechanism takes place between soil particles and the salt minerals in soil water. Varying levels of salt concentration in soil water and different proportions of adsorbed salt minerals in the soil particles may have influence on the soil hydraulic qualities, and, hence, on the water movement process. In the meantime, crop growth is continuously in relation with water movement and salt accumulation process in the rootzone, which is also prone to be negatively affected by them. Thus, we can state that there is a feedback rich mechanism building these complex processes. Simple statistical models are incapable of analyzing such intertwined relationships. Therefore, researchers focused on developing extensive mathematical models to enhance a comprehensive understanding about the soil salinity and sodicity problems in agricultural fields.

There are several simulation models which are used in software platforms to predict soil salinization processes over specific time horizons. Existing models are capable of long-term calculations for soil moisture, salt concentration of soil water, soil sodicity levels, crop yield loss rates by season, and the soil quality degradation due to the reduction on the hydraulic conductivity of soil. In addition to these, such models can be flexible to generate simulations for various kinds of soil types, crop types and rotations for multiple seasons. Plus, they can represent different geographical conditions including shallow groundwater and drainage capacities. Therefore, the existing simulation models can provide a wide variety of capabilities. Nevertheless, none of the existing models that are in use comprise all these features mentioned above. In fact, we can say that each model type has one or several focal points to represent in detail, and beside that they generally have quite simplistic approaches to other important processes or mostly drop those by model assumptions.

For instance, Hydrus-1D is capable of numerically solving complex equations to simulate hydraulic, solute transport and chemical process in the soil profile (Zeng et al., 2014). The model is a very useful tool for short-term accurate simulations. On the other hand, it is not suitable for long-term simulations which may require crop rotations and fast solving of cumbersome mathematical equations. Likewise, SWAP model is able to capture these processes and detailly solve such complex equations (Jiang et al., 2011). These models require theoretical knowledge to understand and operate. Therefore, both models can be considered as unhandy in terms of their practical usage by various kinds of audiences, such as policymakers, or farmers.

Models such as Saltmod and, Drainmod, which can address various audiences by its convenience in usage, can be employed to long-term simulation runs. Even though these models are more practical in use, they are created to represent a few key points and does not comprise the whole processes. While the Saltmod is more practical for long-term soil salinity predictions considering and also provides more social perspective through crop rotations and farmer’s response, Drainmod is more effective for simulating agricultural drainage systems and also calculates salinity level of the rootzone (Bahçeci et al., 2006; Kale, 2011). Nevertheless, both models do not comprise the soil sodification process and its’ negative impact on the hydraulic process.

Therefore, among the available simulation models in this area, we can say that none of them are capable of fast simulating for long-term durations to represent soil moisture, salinity concentration of the rootzone, soil sodification process and its negative impact on the soil properties along with the predictions for crop yield loss rates at the same time.

In this research, we aim to develop a simulation model based on dynamic systems methodology which can represent soil moisture, soil salinity and sodicity levels, and the crop yield loss by season in a feedback rich perspective. Moreover, we aim to create such a model with the capability of fast simulations for long-term durations and a user-friendly interface, that is also accessible on www. Thus, the model is aimed to be a useful tool to analyze the impact of alternative irrigation practices concerning water quantity, water quality and irrigation schedule on soil salinization, sodification and crop yields by season. Moreover, the model gives users various options to adopt different crop rotation types, precipitation regimes as well. We aim to represent how these various agricultural practices applied by farmers can generate different results in the long run. Therefore, the predictions that are made by our models would demonstrate various realistic patterns. Our ultimate goal is to provide an experimental platform, which can be used by a heterogenous audience such as farmers, policymakers, and local agricultural unions, to observe and control of soil salinity and sodicity, under various irrigation practices, soil, and crop-related parameters.

3. LITERATURE REVIEW

Modelling the hydraulic movement and solute transport processes within the soil profile requires familiarity with soil physics and modelling of hydraulic flows. In this section, we briefly summarize the scientific literature upon which our model is based. Furthermore, we introduce a summary of field conditions of the Konya Basin with respect to agricultural activity and salinity impact in the basin.

3.1. Theoretical Background of the Model

The water energy level within the soil profile is an important phenomenon which determines direction and rate of the water flow. The energy level is comprised of various types of forces which are influential on the hydraulic movement within the soil. The gravitation, osmotic difference, hydrostatic, and matric (adhesion) pressures are the main forces which are also conceptualized as the types of soil water potential energy. The gravitational potential, for instance, depends on the force of gravity which expresses the attraction of the water towards the center of the earth while the matric potential refers to the attraction of water to the solid surfaces within the soil. Water tends to move from a location where its total potential energy level is higher towards another location with lower potential energy (Weil and Brady, 2016). Furthermore, the textural and the structural characteristics of the soil profile also impact the water movement rate. The amount of clay in the soil augments its tendency to retain the water. Therefore, clay or clayey soils are likely to hold more water than other soil textures, sand, and loam namely. Likewise, the structural properties of soil play a role in the hydraulic flow. The pore volume and the pore size distribution within the soil profile are critical for hydraulic flow. The water moves more easily in the larger pores than small sized pores (Hillel, 1971). Consequently, the hydraulic movement within the soil profile depends on various kinds of factors and features of soil.

In the light of these, the mathematical expression of hydraulic flow is described by well-known formulations. Darcy’s law is the prevailing equation which mainly describes the water flow in saturated conditions (Eq. 3.1) (Dingman, 2015). On the other hand, the water flow in unsaturated conditions is explained by the adaptation of Darcy’s law or by the small modifications of it. The Richards Equation is the prominent formulation which adapts Darcy’s law into unsaturated condition where hydraulic conductivity and matric potential are expressed as a function of soil moisture level. The hydraulic flow in saturated soil is described by the Darcy’s law as below in Equation 3.1.

$$q = \frac{Q}{A} = K_{Sat} * \frac{dh}{dL} \tag{3.1}$$

Where q is referred as flux $(l.t^{-1})$; Q/A is the specific discharge rate $\left(\frac{l^3.t^{-1}}{l^2}\right)$; A is the cross-sectional area (l^2); K_{Sat} is the saturated hydraulic conductivity of the soil $(l.t^{-1})$; $\frac{dh}{dL}$ indicates the gradient of total hydraulic head (potential); h (length) is the difference of the total hydraulic potential (gravitational and matric) between the ends of two points in a hypothetical column where the distance among them is pointed out by L (length).

On the other hand, the Richards Equation aims to account for the hydraulic flow in unsaturated soil where hydraulic conductivity and matric potential levels are highly dependent on soil moisture level. The hydraulic conductivity is the transmission rate of the water through the soil pores. However, the rate of hydraulic conductivity depends highly on the soil textural and structural characteristics, and on the water content level of the soil (Dingman, 2015). The hydraulic conductivity rate is described by the formulations as a function of the saturation level of the soil which also comprise soil specific parameters (Brooks and Corey, 1964; Campbell, 1974; Mualem, 1976; van Genuchten, 1980; Rodriguez-Iturbe and Porporato, 2007). Likewise, the retention of water by the soil complex is highly dependent on the physical properties of the soil profile and the water content level. The matric potential is mathematically expressed by the soil water retention curves. The soil water retention curve is described by different studies over time as a function of soil water content (Campbell, 1974; Clapp and Hornberger, 1978; van Genuchten, 1980). Consequently, the hydraulic flow in unsaturated soil conditions is expressed regarding the hydraulic conductivity and water retention curve formulations (Dingman, 2015).

$$q = K(\theta) * \left(\frac{d\Psi(\theta) + z}{dL}\right) \tag{3.2}$$

Where $K(\theta)$ is the hydraulic conductivity as a function of water content $(l.t^{-1})$; $\Psi(\theta)$ is the suction head (matric potential) (l); z is elevation (l).

The solute movement within the soil profile mainly occurs along with the hydraulic flow. Primarily, the dissolved salt minerals, anions and cations, are transported within the soil water as an advective flux. Therefore, the dissolved minerals move with the hydraulic flow in proportion with the solute concentration in the soil profile. The advective transport of solute by soil water is described by the following formula, which is also referred as *Darcian flow* (Hillel, 1998).

$$J_c = q * c \tag{3.3}$$

Where J_c is the flux of the solute, mass per time $(m.t^{-1})$; q is the flux of the water which is explained above $(l.t^{-1})$; c is the concentration of the solute in the soil water $(m.l^{-1})$.

Nevertheless, the movement of the dissolved minerals does not occur only via advection. The dissolved minerals also tend to move within the solution, from the points with high concentrations towards lower concentration points. Similar to the Darcy's law, the spatial difference in solute concentrations generates a gradient which stimulates the diffusion of dissolved minerals within the solute. The diffusion of the solute is described by Fick's first law according to the following equation (Hillel, 1998).

$$J_d = D_0 * \frac{dc}{dx} \tag{3.4}$$

Where J_d is the diffusion rate of the solute $(m.t^{-1})$; D_0 is the diffusivity coefficient for a particular solute $(l^2.t^{-1})$; $\frac{dc}{dx}$ expresses the gradient of the concentration (m/l^2).

Furthermore, the process of solute motion within the soil profile can take not only for the concentration differences in the solute but also as a function of non-uniform flow with porous media environment. Therefore, the term hydrodynamic dispersion expresses the solute movement in the soil water where liquid is not stable and moves in different velocities (Hillel, 1998). All in all, the diffusion and hydrodynamic dispersion indicates the solute movement which occurs at the pore scale.

In addition to these transport mechanisms, salt minerals are in motion not only within the solution. The dissolved cations in the solution can translocate the cations adsorbed by soil complex through adsorption-desorption process. This mechanism, which is also referred as ion-exchange phenomenon, is a crucial part of the solute transport process (Huang et al., 2012b). Due to the negative charge of clay particles in the soil, the positively charged cations are attracted and adsorbed by the surface of colloids. The capacity of the soil for cation adsorption (cation exchange capacity) depends on the clay content and also on clay type. Therefore, cation exchange capacity signifies a chemical soil property. The level cation exchange capacity (meq/100 gr soil) is higher in clay soil than other soil textures (Hillel, 1998). Exchangeable cations are expressed in terms of cation charges. While the adsorbed cations are described by milliequivalents in soil mass (meq/100 gr), the exchangeable cations dissolved in solution is expressed as millimoles of charge per litre ($mmol_c$/l). Furthermore, the ionic composition of the soil water plays a major role in the ion-exchange process with the soil colloids. Depending on the composition of dissolved cations (readily exchangeable cations) and the cations adsorbed (exchanged cations) by the soil colloids, cations can replace each other. The cation exchange process between the soil water and the soil colloids is a key factor which can have impact on the physical properties of the soil (Huang et al., 2012b). The proportion of adsorbed Na^+ cations to all other adsorbed cations is crucial. As the more sodium is attached to the soil colloids, the clay particles start to swell and cause soil dispersion (deflocculation). This process can alter the pore structure of the soil and also impact the hydraulic conductivity rate. On the other hand, salinity concentration of the soil water has an inverse impact which can cause flocculation of soil aggregates in high concentration levels (Weil and Brady, 2016).

An example for ion-exchange mechanism between the solute and adsorbed cations is expressed in the following equation (Huang, et al., 2012a):

$$2XNa_{(s)} + Ca^{2+}_{(aq)} = X_2Ca_{(s)} + 2Na^{+}_{(aq)} \tag{3.5}$$

Where “s” refers to the cation adsorbed by soil, while “aq” describes the cations dissolved in solution. “X” represents the negative charge carried by the exchanger in soil. The main principle of the ion-exchange mechanism is the equivalence of charge. The equation above represents that two monovalent Na^+ cation adsorbed by soil complex can be displaces by one divalent Ca^{2+} cation present in the solution.

Measuring the impact of soil sodicity and salinity levels on the hydraulic conductivity is an important challenge. McNeal (1968) studied this question and tried to formulize reduction in the hydraulic conductivity by a parameter, referred as to the relative hydraulic conductivity. Through a series of experiments with various solution compositions, he could predict the reduction on the hydraulic conductivity with respect to different SAR and salinity rates (McNeal, 1968). Nevertheless, another study recently tested validity with other measurements and improved the mathematical expression of formulation which are used in predicting relative hydraulic conductivity (Ezlit et al., 2013).

On the other hand, plants grow in a soil profile within which these hydraulic and solute process take place unceasingly. As a matter of fact, these complex processes provide appropriate conditions for plant development. The plant needs to uptake water from the porous media of soil which is necessary for growth. The process of water uptake by plants, and vaporization from leaves after its' usage is termed as transpiration (Weil and Brady, 2016). However, the presence of salt minerals and/or, absence of water molecules within the rootzone may inhibit or lower the transpiration rate which can inhibit plant grow with respect to its potential. The reduction on the potential transpiration due to the water deficit in soil is termed as the water stress, while salt stress refers to negative impact on the plant transpiration based on the salt concentration in the soil water. Furthermore, plants may experience ion-toxicity due to the presence of specific ions in the soil water (Wallender & Tanji, 2011). In agricultural fields, these stresses on the crop types can lead to severe yield losses. Nevertheless, the crop stress and yield loss rates can be estimated based on some prominent works in the literature (Feddes and Zaradny, 1978; Van Genuchten, 1987; Allen et al., 1998).

Upon these basics of the scientific literature, various studies were carried out to model sub-surface hydraulic and solute processes. Consequently, there are different models which simulate water movement and soil salinity processes. However, each model work differs from the others. Different research objectives can specify their scope, focus points, level of detail, and also simulation durations.

Hydrus 1-D and SWAP are long-established models which can represent hydraulic and solute process within the soil profile. They can account for sub-surface water movement, soil salinity and sodicity problems. Plus, they consider the crop stress. These models are capable of simulating these processes accurately especially within small spatial and time resolutions. Both models solve Richards Equation for unsaturated hydraulic flow and incorporate advection and, diffusion for solute transport. Besides, these models can represent additional dynamic processes such as plant root growth or consider factors such as soil temperature. Nonetheless, numerical solution of such processes accurately requires parameter estimations considering the relevant soil characteristics. Related to these, understanding and operating these detailed models also demand scientific knowledge based on the literature.

On the other hand, Saltmod and Drainmod-S, which is an extension of Drainmod, are simulation models which also represent hydraulic flow and solute transport processes. Unlike Hydrus 1-D and SWAP, they do not represent adsorption-desorption mechanism. While Drainmod-S adopts the Darcy's law for its hydraulic equations, Saltmod uses more simplistic approach to account for water balance. Furthermore, both models adopt advection for solute transport yet, Drainmod also consider dispersion processes. These models are less detailed, and they can carry out long-term simulations much faster. Additionally, their simplistic approach allows them to address larger audience with variety of different backgrounds. These models offer different options to adopt various irrigation practices. However, they have different focal points. Saltmod is more oriented towards soil salinization process over the long-term, it also contains more options for farmer's behaviors such as different crop rotations and, irrigation scheduling. Nevertheless, it neglects the crop stress and potential yield loss rates. On the other hand, Drainmod-S is generated mainly to represent sub-surface drainage systems in agricultural fields. Therefore, soil salinization is the subsequent focus of interest. All in all, these models are useful tools with specific focal points to represent hydraulic, solute transport processes to simulate salt-related problems in farmlands.

In dynamic systems approach, there are several studies which focus on hydraulic flow, soil salinity, sodicity problems in agricultural areas variably. The water balance and movement through rootzone is conceptually analyzed and modeled (Khan et al., 2007). Along with this, the conceptual model is applied to practically test different irrigation conditions in paddy fields (Luo et al., 2009). In addition, the dynamics of soil salt accumulation in irrigated lands over long-term regarding different irrigation practices is represented by another system dynamic model (Saysel and Barlas, 2001). Lastly, the published works of Yair Mau deepen the understanding of soil salinity and sodicity problems based on dynamic systems approach. In these models, hydraulic flow and solute transport in soil profile is represented in terms of simple terms (Mau and Porporato, 2015; Mau and Porporato, 2016). Furthermore, the impact of soil sodicity on the hydraulic processes is also studied by the recently published model SOTE which also emphasizes the impact of irrigation water quality and changing climate change conditions (Kramer and Mau, 2020). In these works, hydraulic flow is not based on Richards Equations for unsaturated soil conditions, yet the average conditions of the rootzone are considered and represented. Besides, the solute transport is simulated based on the advection of the solute. This simplistic approach provides an ability to fast simulate these processes over long-term. Nevertheless, none of these works highlights the crop stress and yield loss rates based on the hydraulic and solute processes, nor do they represent farmers' response to changing crop and soil conditions.

Therefore, this study contributes to the literature by representing hydraulic flow, soil salinization and, sodification processes with their impact on the seasonal crop growth and yield rates in farmlands. The model, which is developed based on the system dynamics literature, has fast-simulating ability to generate long-term outputs to test and research alternative policy implications.

3.2. Konya Plain of Turkey

The model developed in this research is conceptualized and parametrized according to the field conditions of Konya Plain in Turkey. The plain plays an important role in agricultural production for the country. Besides, irrigation practices are widely applied in this area where semi-arid climate is dominant. We consider the plain as a vulnerable region for salt related problems in agriculture. Therefore, we represent the field conditions of the plain and perform different simulations for scenario analysis based on these conditions. Here, we present an overview of the agricultural activity, climate conditions of the plain along with its experience in soil salinization in farmlands.

The Konya Plain of Turkey, which covers a major share of land and agricultural production of the country, is located in a closed basin in the center of the Anatolian region. Surrounded by high mountains, the basin has a unique characteristic as no surface water flow can feed the water reserves within its boundaries or drain away the excess use. The rainfall that helps to feed groundwater sources and few surface reserves, is the main supply for the water budget of the Konya Closed Basin along with the groundwater water recharge, supplied by the melting of snow on top of Taurus Mountains on the south. In the Basin, more than 3 million people currently live (Orman ve Su Işleri Bakanlığı, 2015). Land cover contains around 5.5 million ha area which corresponds to 7% of the total land cover of Turkey. Konya, Karaman, Aksaray, and Niğde are the main cities that constitute more than 90% of land cover of the region (WWF, 2014). The basin is also one of the most drought regions of Turkey. The dominant climate condition is classified as continental, where the precipitation occurs generally in winter and springtime while very low rates are recorded during summer. In addition to that, according to long-term records of climate data, this semi-arid region can have 300-350 mm precipitation per year on average while the annual evapotranspiration rate is around 1100 mm per year around the basin (TAGEM and DSI, 2017) .

Konya plain has always been a key part for the agricultural production of the country. Likewise, agriculture is one of the most essential sources of economic activity within the region. For decades, the plain has been known for its capacity especially in cereal production which constituted more than 15% of the total production of the country. Along with the importance of agricultural production in the plain irrigation application has a long-standing history. Even before the establishment of the republic, there have been investments to build irrigation technologies, especially around the Çumra Province in Konya, in the late Ottoman era (de Meester, 1970). Nevertheless, the access to irrigation water was not accompanied with the development of proper irrigation methods in the field. As a result, the improvement of accessibility to irrigation water, and the increased need for food due to population growth enlarged the extent and deepened the severity of salt-affected soils. Throughout the 20th century, various parts of the basin faced problems due to salinization and sodification processes (Kanber et al., 2005; de Meester, 1970). The excessive amount of irrigation water applications and inadequate drainage infrastructures were the prominent factors for salt accumulations in some parts of the plain. However, during the 1990s several projects have been carried out to ameliorate conditions of the salt-affected soils and improve the drainage abilities of the plain. These projects are reported to make positive contributions to the efforts for easing the relevant problems (Bahceci, 2021).

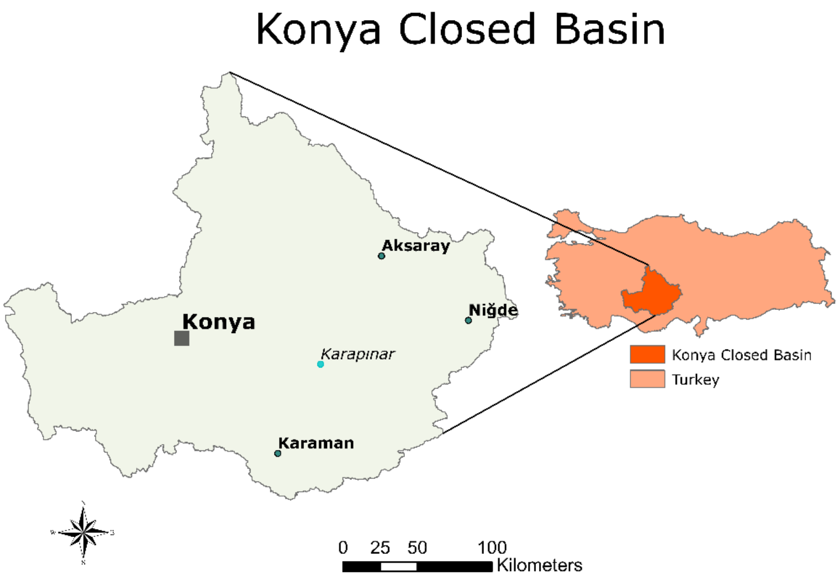

Figure 3.1. Konya Closed Basin.

Agricultural production maintains its importance in the Konya basin. In 2019, studies report that around 13% of the total cultivated area of the country is planted in this region which corresponds to around 2.8 million ha (KOP, 2020). The plain is in the leading position for production of many crop types of Turkey. Sugar beet, maize, potato, haricot bean, wheat, barley, sunflower are among the crops that farmers mainly cultivate and produce a major supply for the country (KOP, 2017).

The agricultural area of the plain can be categorized into two segments as irrigated and rainfed fields. Barley and wheat are two traditional crops that are preferred by farmers who cultivate their plants without irrigation. However, farmers who can access irrigation water also plant barley and wheat. Yet these crop types do not require much irrigation water due to sufficient precipitation that would somewhat meet their needs during their sewing-harvesting schedule. Based on the report of the regional development institute stated in 2017, the region contributes for %20 for wheat and %23 barley of total production of the country (KOP, 2017).

On the other hand, it is stated that around 30% of the total agricultural area is irrigated in the closed basin (WWF, 2014). Maize, sugar beet, sunflower, beans, potato, and clover are among the crops that are mostly cultivated by farmers who are able to regularly irrigate their fields. Even though the region is in poor conditions for water supply, these crop types require a considerable amount of irrigation water which is mostly delivered from the groundwater reserves. Furthermore, there is a %12 increase in the planted area in the last 15 years only within the Konya’s boundaries, where more than 1.5 million ha area is now used in agricultural production (TUIK, 2021a). Nevertheless, this extension mainly enlarged the area of total irrigated fields. There is a huge enlargement on the land cover of the area where irrigated crops, maize, sunflower, potato, and sugar beet are planted. This enlargement surely requires more irrigation water application in the plain.

In Figure 3.2 below, the monthly reference evapotranspiration and precipitation rates are presented in units of millimeters for different meteorological stations around the plain. These meteorological stations are selected to represent the climate variations around this quite large basin. While Cihanbeyli is in the north of the basin, Aksaray is in the east and Karaman which is at the other edge of the plain, is in the south. Konya, Karapınar, and Çumra are located within the center of the plain where intense agricultural activity is performed. Regarding these graphs, it is very clear that there is a huge gap between the evapotranspiration and precipitation rates around the plain particularly during the summer period. This gap is inevitably closed down by the irrigation by farmers to secure agricultural productivity.

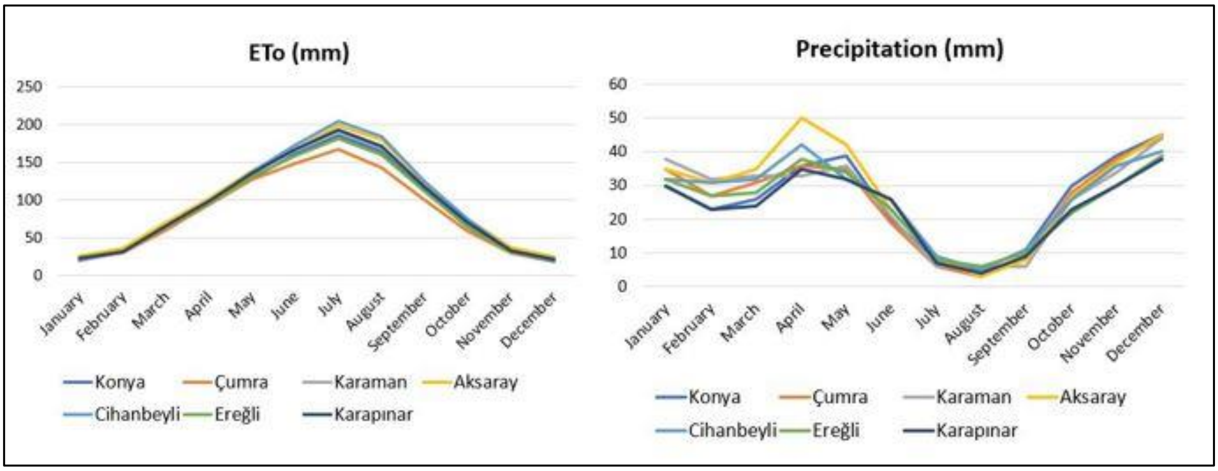

Figure 3.2. Monthly Evapotranspiration and Precipitation Rates in Konya Province (mm) (TAGEM and DSI 2017).

The surface irrigation methods which are popular for their lower applications efficiencies against the modern methods, are applied in the closed basin for a long period. Such methods played an important role in deteriorating agricultural conditions in the field. Combining with the great irrigation need considering the low precipitation levels, farmers made irrigation applications affluently when they do not face any constraints to the irrigation water accessibility. However, these methods not only caused salt-accumulation in the soils but also built up a great pressure on groundwater sources (WWF, 2014). Although the drainage infrastructures helped improve the quality of salt affected soils to some extent, the groundwater levels kept falling down (WWF, 2014). Considering the rising pressure on the groundwater levels, the plain has experienced a major transition from surface irrigation methods to closed-channel irrigation methods, particularly to sprinkler and drip irrigation in the last decade as we are able to confirm based on the field works that we conducted.

The efforts for adopting efficient irrigation application methods pave the path for reduced water consumption in the fields. In this way, farmers hope to sustain the accessibility to water from wells and cultivate irrigated crop types in coming decades. Nevertheless, we suspect of recurring of salt-accumulation problems in the fields since the diminishing amount of irrigation water would also reduce the leaching rates of salts from root zone. Therefore, the plain may encounter similar problems in near future, particularly in relation the climate change.

4. METHODOLOGY

Models are generated and employed to examine various types of problems through depicting selected aspects of the real systems. Physical, symbolic, static or dynamic, each modelling approach aims to provide better understanding of a problem in question (Barlas, 2002). Different modelling approaches introduce various and useful insights about a problem which stems from the real-life conditions. For instance, physical models are used to illustrate physical objects such as an architectural construction, while the non-complex mathematical models express static relationships between two or several variables. However, dynamic models are formed to represent the changes in the selected variables over time. Statistical models which predict population growth in future, or a numeric model which simulate customer orders for a private company in certain conditions can be stated as examples for dynamic models.

System dynamics approach, which is a scientific modelling methodology, aims to introduce a better understanding and management of complex dynamic systems. System dynamics methodology is concerned to reveal underlying causes of problems through its unique approaches such as examining the non-linear behaviors of systems and assessing the causal relations which can form endogenous feedback loops within a system (Sterman, 2000). In this approach, causal relationships rather than strong correlations are aimed to be identified. Studying interrelated causal relationships can induce an endogenous perspective upon a system. Therefore, one of the essential advantages that system dynamics methodology can offer is to diagnose and analyze the circular causalities within the system which characterize the behaviors of dynamic problems. Furthermore, the methodology allows us to assess the causes of problematic patterns and to propose new, and alternative policies which can ameliorate the existing complications (Barlas, 2002).

The interaction between the hydraulic, solute and crop yield processes within the soil profile has a dynamic and complex nature. Moreover, the circular causality between the hydraulic movement and the accumulation and transport of salt minerals within the soil forms an internal structure which requires elaborate assessment. We adopt the system dynamics methodology to explore and analyze the soil salinization and sodification problems in farmlands due to different irrigation applications in terms of different irrigation water quantity and quality based on a feedback rich model. Furthermore, we assess the crop yield ratios by season based on the accumulation levels of water and salt minerals within the soil profile. Consequently, this methodology provides a useful approach to better understand dynamic salt-related problems in agricultural lands and to propose alternative irrigation practices to improve problematic conditions.

Causal loop diagrams depict the important causal links and internal feedback structures of the system. The causal links between the variables are pointed out by the arrows between them which also indicates the direction of the relationship. The arrow is linked from cause variable to the effect. Furthermore, the type of the causal relationship between the variables are expressed by the polarity of the arrows. While the plus sign describes a positive relationship, the negative relationship between two variable is demonstrated by the minus sign. In addition to that, the causal loop diagrams can illustrate the links between open and, or closed loops as in Figure 4.1. The arrows demonstrate the direction of causal links between two variables, from cause towards the effect. The relationship between transpiration and crop yield variables is illustrated as an open loop causality. Other things being equal, an increase in the transpiration is expected to increase the crop yield rate.

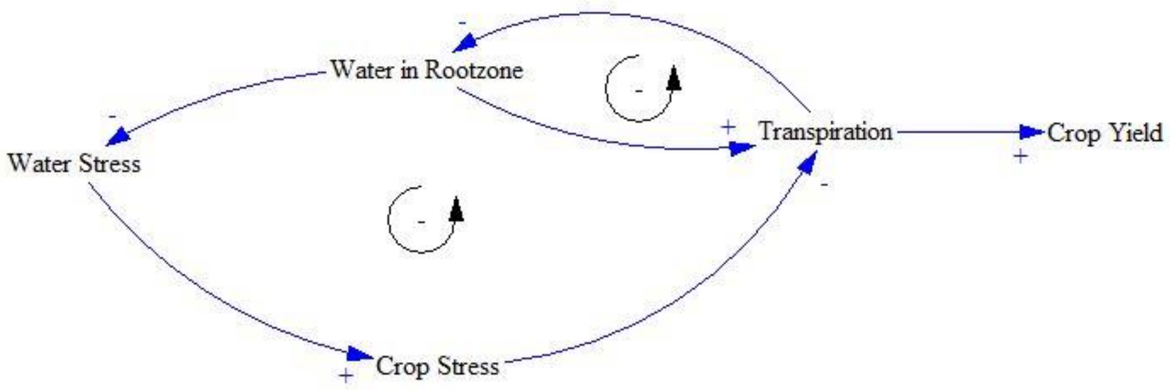

Figure 4.1. Open and Closed Loop Diagrams.

On the other hand, feedback loops offer more in understanding the dynamic behaviors and the complex structure of problems. The dynamic behaviors can be generated by two types of feedback loops: reinforcing and balancing (Sterman, 2000). The reinforcing causal feedback loops are indicated with the positive sign in the middle in the loop with the direction arrow. In reinforcing feedback loop, other things being equal, a change, decrease or increase, causes the same impact on itself at the end. However, the balancing feedback loops, which are indicated with negative sign around the direction arrow as in the figure above, points out a balancing behavior. For instance, other things being equal, an increase in the water in rootzone decrease the water stress which further reduces the crop stress level. Yet, a reduction in the crop stress variable increases the transpiration rate which cause a decrease in the water in rootzone level.

In addition to these, stock and flows are the essential variables in the dynamic systems. Stocks express the accumulations in the system which are formed by the inflow and outflow variables Outflows are used to deplete the accumulation amounts in the stock variables. However, stock variables are key for generating information about the system upon which important insights and decision making process are based (Sterman, 2000). While the stock variables are represented by the rectangle shaped symbols, the flow variables are illustrated with pipelines which are attached towards (inflows) or stemmed from stock variables (outflows). In the Figure 4.2 below, a basic example of a stock-flow structure is illustrated.

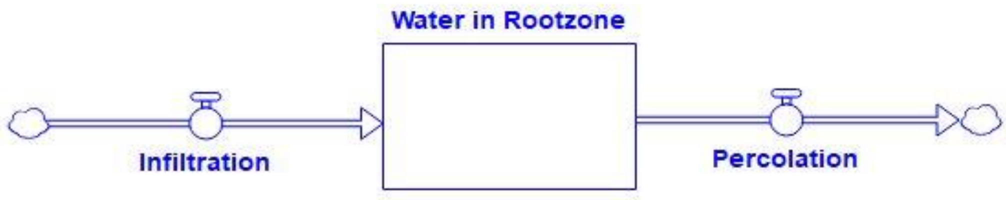

Figure 4.2. Illustration of a Stock-Flow Structure.

The accumulation of water in the rootzone is accounted by the stock variable. While the accumulation is fed through the infiltration rate (inflow), it is reduced by percolation (outflow). The stock-flow structure maps the mathematical formulation in Equation 4.1. The rate of change in the stock variable is expressed by the net flow into the stock. Therefore, the change in a stock variable can be solved according to the following equation (Sterman, 2000):

$$\frac{d(stock)}{dt} = Inflow(t) - Outflow(t) \tag{4.1}$$

The model development in system dynamics methodology is guided by the methodological steps, illustrated below based on Barlas (2002). Through these steps, a structure of analyzing complex problems is provided. Therefore, the main methodological steps are stated as:

- Problem identification and definition:

The very first step gives details about the determination of important basic points for research. It is suggested that the problem in question should have a dynamic characteristic and also a feedback nature. Furthermore, the analysis of dynamic behaviors of key variables, the setting of time unit and time horizon of the study should be defined. Along with these points, the definition of the dynamic problem and the purpose of the study should be precisely defined.

- Development of the dynamic hypothesis and the model conceptualization:

The second step suggests formulating the hypothesis which causes the problematic dynamics. In this step, diagnosing all variables which contribute the dynamic behaviors with respect to defined problem, identifying the circular causalities and constructing causal loop diagrams are the main activities. Moreover, identifying the main stock and flow variables is another essential point.

- Formal model construction:

In this step, the formal structure of simulation model is developed. The stock-flow structure is constructed, and the cause-effect relationships between the variables are described by the mathematical equations. In addition to that, initial values for stock variables are determined and the numerical values of parameters are estimated. Lastly, the internal consistency of the model is verified with respect to the dynamic hypothesis.

- Model credibility (validity) testing:

The validity tests are performed to assess the reliability of the model outputs. The level of representativeness of the model generated outputs is questioned considering the real problem. Two types of validation tests are used to assess the model credibility. The structural validity tests assess the internal structure of the model whether it can generate meaningful representations with respect to the real system. On the other hand, pattern tests are employed to evaluate the model behaviors against the pattern components in the real behaviors of the real systems. The slopes, minimum and maximum points, number, period and the amplitudes of the oscillations are useful tools to perform patterns tests.

- Analysis of the model:

In the fifth step the model is analyzed to understand important dynamics of the model. Sensitivity tests are performed to better comprehend the degree of responsiveness of the outputs based on the changes in the selected parameters, inputs and initial conditions.

- Design Improvement:

After the credibility of the model is ensured and its essential dynamics are understood, alternative policy settings can be simulated in the model. The main purpose of this step is to improve policy implementations and decision-making processes.

- Implementation:

The last step is the implementation of the alternative policies suggested by the simulation model. This step highlights the importance and success of dynamic systems methodology. Nevertheless, policy implementations cannot always be applicable due to various constraints in the real-life conditions. Therefore, it is important to emphasize that the useful results or the model itself should be presented to enhance establishment of better policies in future.

According to these fundamental steps, we study the dynamics of soil salinization and sodification in farmlands due to the various irrigation applications. Based on the literature review and the interviews conducted with representatives of various stakeholders during the field visits, we identify the key variables and feedback mechanisms within the system. Formal model is constructed considering the mathematical equations described in the literature and estimated parameters to represent field conditions. The credibility of the model is ensured through the structural validity and behavior pattern tests. The relationship between variables which construct formal model and validity tests is expressed in the next section. We prepared and simulated different policies which represent different irrigation methods and precipitation regimes for 30 years of durations. The simulation results will be presented to eliminate problematic irrigation applications in farmlands and improve the existing practices.

5. MODEL DESCRIPTION

The model is built to simulate soil salinization and sodification processes based on different soil types, irrigation water qualities, amounts and methods, and also various crop types. The model represents water movement through soil profile, solute transport in days, and crop yield loss by season. With this work, we aim to simulate a feed-back rich and complex processes where hydraulic, solute and crop growth processes simultaneously influence each other. Furthermore, we intend to carry out long-term simulation runs to observe how alternative irrigation practices and crop rotations may impact salt accumulation, soil sodification, and also crop yields with specified soil properties. Therefore, the model provides results to enrich our understanding and support improved farm practices that would control salt-related problems. The model calculations are made considering representative point in the rootzone. The model is simulated on daily basis. The time horizon of the model is set as 30 years starting from 2021. The computational time step is set as 0.0625 (1/16) days. We employ the STELLA Architect software (ISEE Systems) to solve numerical equations for the mass balance and flow equations which are described in next sections. The model is named as "SAMIMI" with respect to research project of which our study is a part.

5.1. Overview of the Model

The model consists of two-way interacting modules of hydraulic flow (Hydraulic Model) and solute transport (Solute Model). While crop yield is influenced by the water and solute conditions, the water and solute conditions are influenced by farmer practices. Figure 5.1 depicts these modules in boxes and their interactions with arrows showing the direction of influence.

The hydraulic model represents the water movement through soil profile depending on physical properties of soil profiles. Meanwhile, various salt minerals accumulate in the soil profile via advective transport by water in dissolved form. Moreover, adsorption mechanism between soil particles and the salt minerals dissolved in soil water can lead to sodification, under the conditions of excess sodium cations. Therefore, the hydraulic flows generated in the hydraulic model influence the salinity and sodicity generated in the solute model. In the meantime, varying levels of salt concentration in soil water and different proportions of adsorbed salt minerals in soil complex have influence on the hydraulic properties of soil layers, affecting the water flow between soil layers.

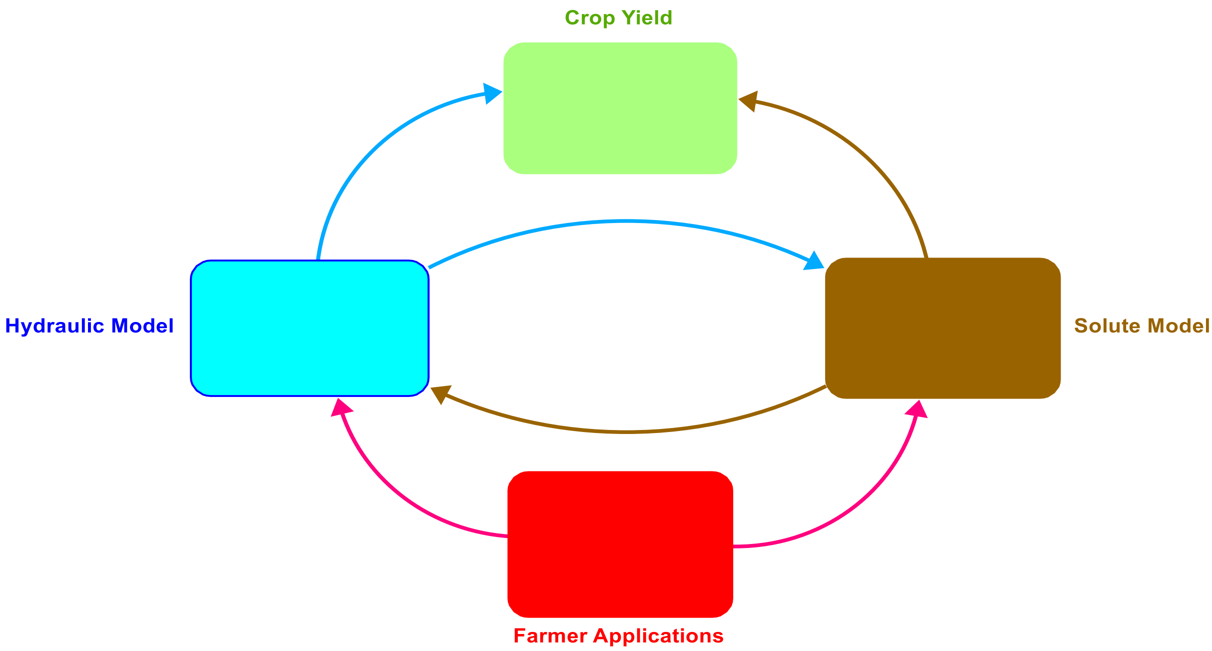

Figure 5.1. The Overview of the Model.

These build up a feedback mechanism between hydraulic and solute models which simultaneously influences the two models. Moreover, low levels of soil water and high salt concentration may induce stress on crops and would leads to yield losses.

Various farmer practices affect the processes of water and salt. Irrigation water amount, water quality, and irrigation method are important factors which impact hydraulic flows, solute transport, and crop yield. Furthermore, different crops and their rotations are adopted by farmers, which lead to different water application rates over the seasons. The model user is able to set these parameters accordingly and test their impact on salinity, sodicity and crop yields in the long-term.

5.2. Descriptions of the Model Sectors

5.2.1. Hydraulic Model

The physical compartmental representation of the hydraulic model is demonstrated in Figure 5.2 The soil profile is demonstrated in three compartments. The top layer represents the soil surface water that can accumulate on top of the soil profile and the rootzone is represented as a single vertical compartment below the soil surface. The saturated zone stands for the water table in the soil profile at the bottom. The rootzone has a 50 cm depth, whereas the soil surface only accounts for the processes that would occur on top of the soil profile. As the groundwater level is too deep in the field conditions, we priorly worked on the first two layers and neglected the impact of shallow water table level on the rootzone. Still, even though we do not observe such low levels of water table in our case, shallow saturated zone is a very common phenomenon in agricultural field conditions and experienced in many cases elsewhere. Therefore, we intend to focus on the impact of shallow water table considering the groundwater irrigation and sub-surface drainage options as a further work. The soil texture is specified as clay loam in the field work. We also assume that the area of the field corresponds to 1 ha (10.000 m^2).

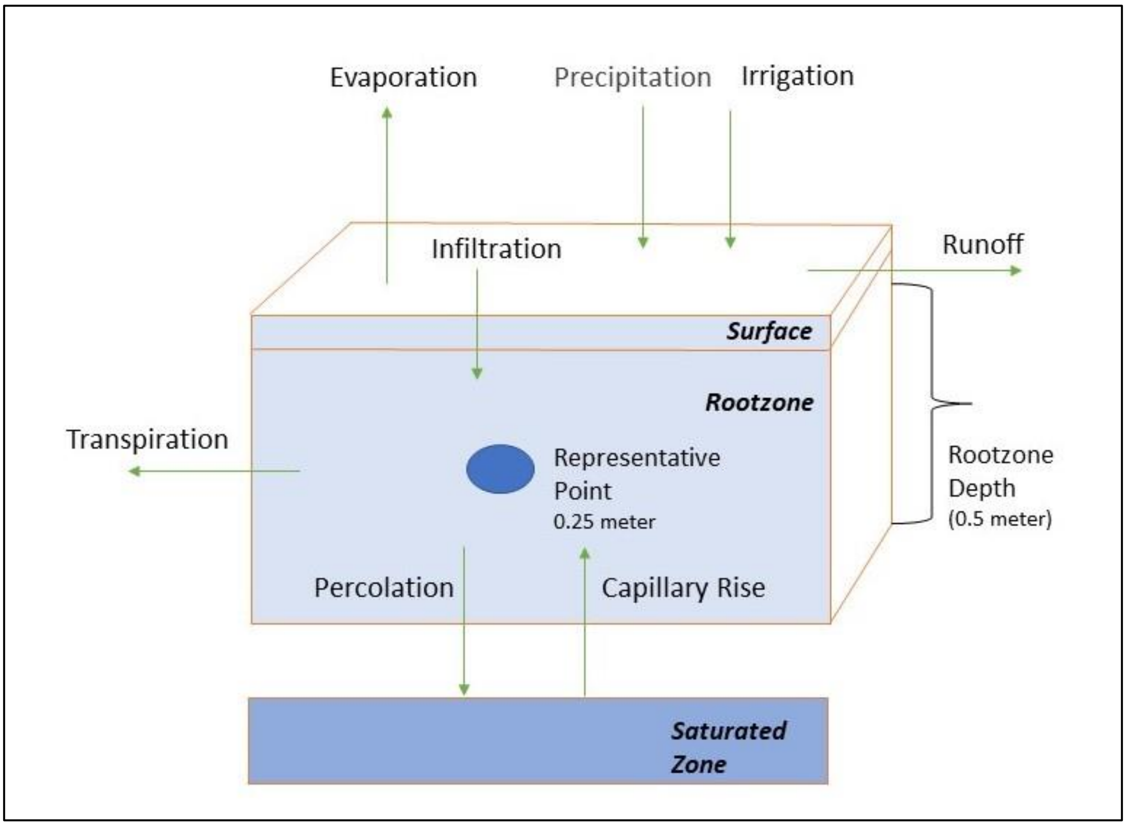

Figure 5.2. Physical Model of Hydraulic Model.

In hydraulic model, the water can accumulate in the soil compartments, surface, rootzone and saturated zone, respectively. Vertical movement of the water between the soil compartments is governed by flows (irrigation, precipitation, evaporation, runoff, infiltration, transpiration, percolation and capillary rise) as illustrated by arrows in the Figure 5.2.

In Figure 5.3, the stock-flow structure is illustrated on STELLA software. The square variables are the stocks (accumulations), while the variables with valves and arrows either embedded between the stocks or connected to the clouds are the flows (rates). The hydraulic model contains two stocks, and eight flow variables.

The water accumulation in the stocks is measured in units of cubic meter (m^3). The water flows are in units of m^3/day units.

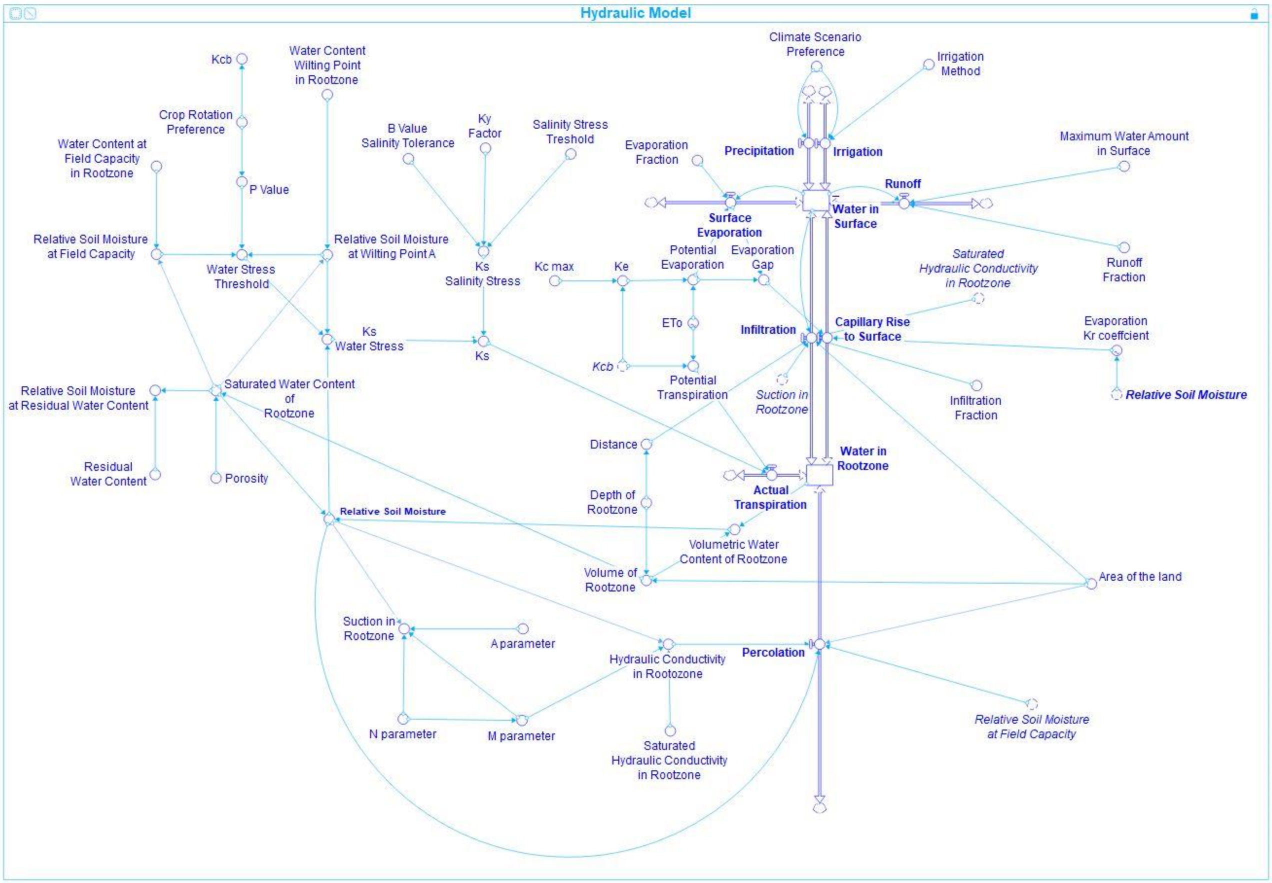

Figure 5.3. The Stock-Flow Diagram of Hydraulic Model.

In the hydraulic model, there are one reinforcing and seven balancing feedback loops. The causal loop diagram of the hydraulic model is illustrated in Figure 5.4.

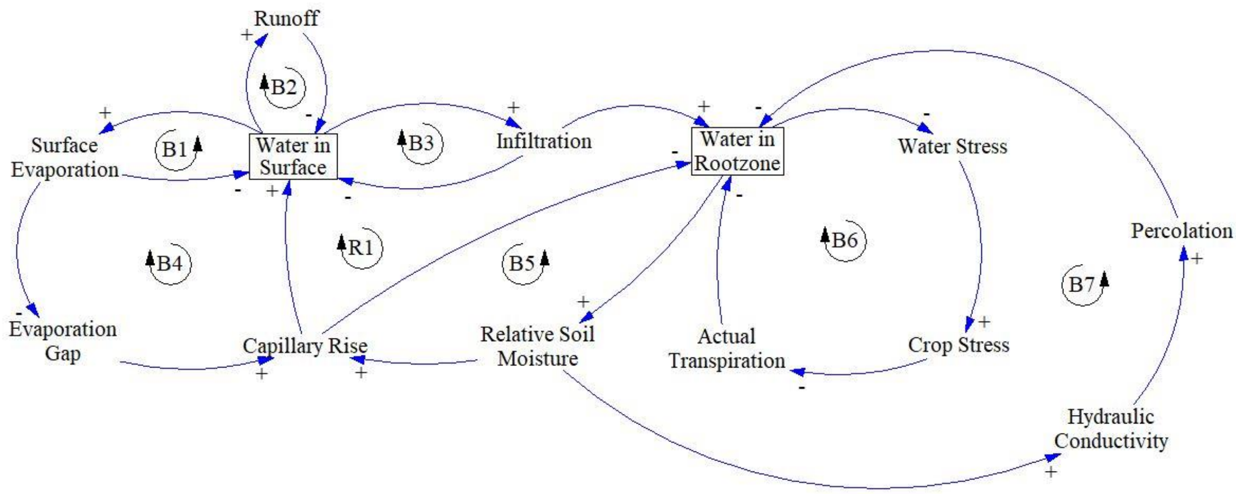

Figure 5.4. Casual Loop Diagram of the Hydraulic Model.

In the first balancing loop (B1), the relationship between the surface evaporation and the water amount in the surface is depicted. As water in the surface increases, the evaporation rate from the surface also increases. However, the increase in the surface evaporation reduces the amount of water in surface. B2 loop demonstrate that the increase in the water in surface leads to an increase in the runoff while the augmentation in the runoff diminishes the water amount in the surface. Similarly, in B3, we see another balancing loop where the water in surface rises the infiltration rate hikes, yet the increase in infiltration reduces the water in surface. Moreover, the fourth balancing loop (B4) indicates a counteracting relationship between capillary rise of water amount to the surface and the accumulated volume of water in the surface. The increase in water in surface stock leads to an augmentation in the surface evaporation. As the surface evaporation increases, evaporation gap diminishes (Eq. 5.3). However, an increase in the evaporation gap amplifies the water amount of capillary rise to surface.

On the other hand, B5 demonstrates a balancing loop between water in rootzone stock and capillary rise. As the water in rootzone increases, the level of relative soil moisture (Eq 5.10) rises. The rise in the relative soil moisture leads an augmentation in the capillary rise of water from rootzone which decreases the water amount in the water in rootzone stock. The balancing loop B6 illustrates the relationship between the water in rootzone and actual transpiration amount in the rootzone. The augmentation in the water amount in the rootzone reduces the water stress which has a positive relationship between the crop stress variable. However, the rise in the crop stress decreases the actual transpiration amount that takes places in the rootzone. Yet, an increase in the actual transpiration generates a decrease in the water in rootzone stock. The last balancing loop in the hydraulic model (B7) expresses the relationship between the water in rootzone and the percolation variables. A rise in the water in rootzone stock augments the relative soil moisture level which further increases the hydraulic conductivity in the rootzone. As the hydraulic conductivity increases, the volume of water that percolates also enlarges. However, the increase in the percolation flow leads to decrease in the water amount in rootzone. In addition to these, there is one reinforcing loop (R1) in the hydraulic model. R1 indicates the positive relationship between the two stocks through related flows and variables. The increase in the water in surface uprises the amount of water in infiltration flow which also augments the water in rootzone. As the water in rootzone increases the level of relative soil moisture rises which leads to an increase capillary rise. The capillary rise from rootzone towards the surface raise the water amount in the surface.

In order to simulate this stock flow structure which contains multiple feedback loops we employ scientific equations based on the literature. The equations used in the hydraulic model are expressed below. Firstly, we indicate the mass balance equations of water stocks. While water in surface (S_s) corresponds to the water amount in the surface layer, water in rootzone (S_r) indicates the soil water quantity that rootzone stores. The water balance in the surface and rootzone stocks is expressed by the equations (1) and (2) (Khan et al., 2007).

$$Water\ in\ Surface\ (t) = Water\ in\ surface\ (t-dt) + (I + R + CR - E - SR - F) * dt \tag{5.1}$$

$$Water\ in\ Rootzone\ (t) = Water\ in\ root\ zone\ (t-dt) + (F - CR - T - P) * dt \tag{5.2}$$

Where I indicates the irrigation water introduced into the surface (m^3/day); R is the amount daily precipitation (m^3/day); CR is the capillary rise from rootzone to soil surface (m^3/day); E is the amount of water evaporated from surface (m^3/day); SR is the surface runoff (m^3/day); F is the water infiltrating from surface layer to the rootzone (m^3/day); T is the daily transpiration amount of the plant (m^3/day); and P corresponds to the percolation of water from rootzone to deep layers (m^3/day).

Surface Evaporation

Surface evaporation refers to the vaporization of the water amount that is present in soil surface considering potential evaporation rate based on climatic conditions, and the available water amount in the soil surface. The surface evaporation is calculated through adaptation of the partitioning method of reference evapotranspiration (ETo) into separate processes as evaporation and transpiration. The partitioning of the evapotranspiration through implying the dual crop coefficient method is described in FAO’s Irrigation and Drainage Paper No:56 (Allen et al., 1998). Reference evapotranspiration rates express the evapotranspiration from a soil profile covered with grass (reference crop) where soil water is not in abundance, yet the reference crop does not experience any stress due to the water deficit in the soil. The reference evapotranspiration (ETo) is computed based on the Penman-Monteith equation which requires local climatic parameters such as wind speed, radiation, air density etc. Nevertheless, we do not calculate the climate specific ETo rates as we can access these publicly available data from many meteorological stations across Turkey including the Konya Basin based on a report published by state institutions (TAGEM and DSI, 2017). In the model we employ the ETo rates which are specific to Karapınar, Konya.

We calculate the daily surface evaporation rate from the soil surface according to the equation 5.3. Therefore, the surface evaporation is specified as the minimum of potential evaporation and the water in surface stock. By this means, evaporation equals to its potential when water on the soil surface can meet atmospheric demand for evaporation. However, the available water amount in surface stock becomes the governing variable when it is less than the potential evaporation.

$$E = MIN\ (PE, S_s * Ef) \tag{5.3}$$

Where PE is Potential Evaporation (m^3/day); S_s is the water in surface (m^3/day); and Ef refers to the Evaporation Fraction (1/day).

Considering the specified reference evapotranspiration value in the TAGEM's report, potential evaporation (PE) is determined by ETo (reference evapotranspiration) and Ke (soil evaporation coefficient). In Figure 5.5, we can view the daily reference evapotranspiration rate along the time horizon of a year. In the simulations, we employ this one year of daily ETo values repetitively. The report that we conduct to employ evapotranspiration data indicates the values in 10 days of intervals.

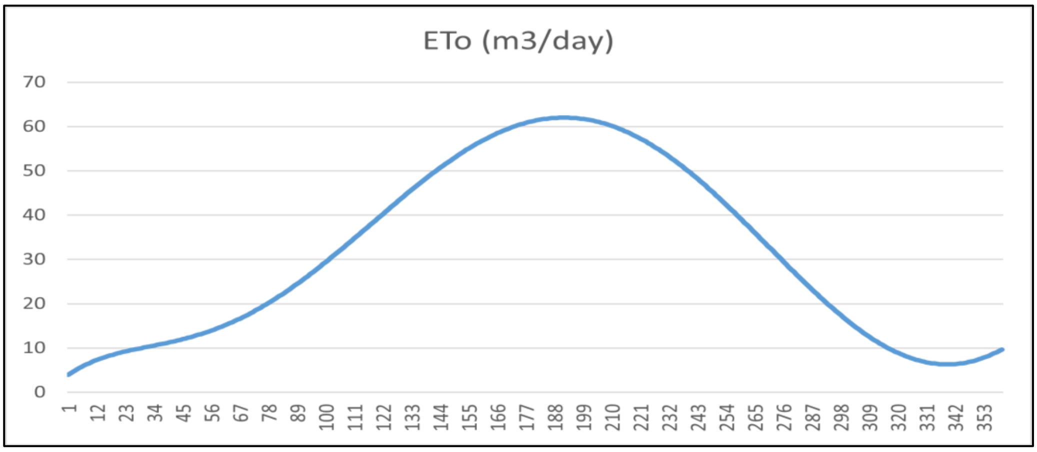

Figure 5.5. Daily Reference Evapotranspiration Data TAGEM and DSI (2017).

However, we used a parabolic trendline to convert the data into daily numbers so that we can insert it as a table function into the model. Moreover, this smoothed trendline prevents us from observing discontinuous behaviors in the model. Based on the location specific reference evapotranspiration rate, we can formulate the potential evaporation as follows:

$$PE = ETo * Ke \tag{5.4}$$

Where ETo (m3/day) is the reference evapotranspiration rate; Ke is the dimensionless soil evaporation coefficient that is used for partitioning of ETo.

The soil evaporation coefficient calculated through the difference between two other parameters employed in partitioning of ETo.

$$Ke = Kc_{max} - Kcb \tag{5.5}$$

Where Kc_{max} in another dimensionless parameter, represents a natural limit for evaporation and transpiration processes considering the energy balance difference between the air and soil surface. Kcb refers to the FAO's basal crop coefficient which corresponds to crop transpiration, the other part of the evapotranspiration process. Kcb values which have positive values when crop is planted, vary over time depending on the crop developmental stages. The FAO suggests three different values for Kcb coefficient for one season which would represent initial, middle and the end of the growth season in order (Allen et al., 1998). However, we again use table functions with smooth trendlines to represent Kcb similar to ETo data.

Surface Runoff

Surface Runoff (SR)(m^3/day) occurs when water amount in the water in surface stock exceeds a specified maximum value. Therefore, a specified amount of water can accumulate on the top of the soil surface which is also be named as ponding. However, after having reached that maximum amount, surface runoff takes place, and the accumulated water is discharged according to the Equation 6.

$$SR = MAX\ (((S_s - S_s max) * Rf), 0) \tag{5.6}$$

Where $S_s$max is the Maximum water amount in surface (m^3) and Rf is the Runoff Fraction (1/day)

Infiltration

Infiltration is the penetration of the accumulated water amount on the soil surface into the soil profile. In other words, infiltration stands for the water influx from water in surface stock into water in rootzone. There are different interpretations for infiltration calculations in the literature. We adapt the simplistic way of Green and Ampt (1911) equation which was originally developed for homogenous soil profiles (Mein, R.G and Larson, 1973). In addition to that, we introduce a modification to involve the negative impact of the soil sodicity on the infiltration rate of the soil profile.

$$F = A * K_{sat} * RK_{sat} * (\frac{\Psi_R + Z_R}{Z_R}) \quad (5.7)$$

Where A is the area of the land (m^2); K_{sat} refers to the saturated hydraulic conductivity of the rootzone (m/day); RK_{sat} is the rate of reduction on hydraulic conductivity which is discussed later in the solute model; Ψ_R is the matric potential in the representative point in the rootzone (m) and Z_R is the depth of the representative point (m).

Capillary Rise to Surface

In this model structure, capillary rise of water from rootzone to soil surface can only occur due to high evaporation demand of the atmosphere since we neglect a shallow water table below the rootzone. As it is mentioned, surface evaporation takes place depending on the data based potential evaporation and the water amount in the soil surface. However, it is suggested that water can evaporate not only from the top of the soil, soil surface, but also from a very shallow depth of the soil layer as well (Allen et al., 1998). Therefore, we consider the gap between potential evaporation and the amount of surface evaporation as a gradient which can draw soil water upwards, into the soil surface.

$$CRs = E_{gap} * Kr \quad (5.8)$$

Where CRs is the capillary rise to surface (m^3/day); E_{gap} expresses the evaporation gap (m^3/day); and the Kr is the evaporation reduction coefficient (dimensionless).

$$E_{gap} = PE - E \quad (5.9)$$

Evaporation reduction coefficient (Kr) is inserted as a table function which depends on the relative soil moisture level of the rootzone. Kr serves as a varying fraction considering the moisture level of the soil profile. In this way, a small fraction of evaporation gap can rise up to soil surface from the rootzone. However, as relative soil moisture of the rootzone declines, Kr coefficient diminishes as well. The less the soil water level becomes in the rootzone, the harder water can move upwards due to the tendency of water retention of the soil particles. The numerical values for Kr coefficient are calibrated during the model validation process.

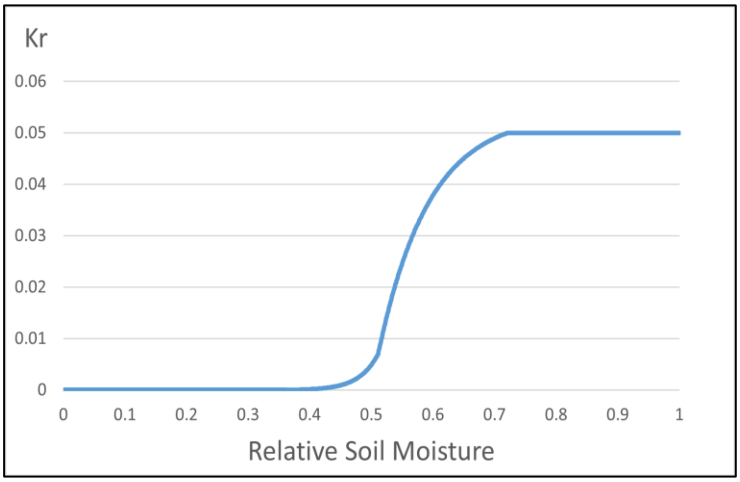

Figure 5.6. Evaporation Reduction Coefficient (Kr) (dimensionless).

Relative soil moisture is an indicator for water amount within the soil profile. It indicates the fraction of water which fills the void volume in the soil profile. Relative soil moisture is a dimensionless variable which calculated according to Equation 5.10 (Rodriguez-Iturbe and Porporato, 2007).

$$\Theta = \frac{V_W}{V_w + V_A} \tag{5.10}$$

Where, Θ represents relative soil moisture (dimensionless); V_W is the volume of water within the soil profile (m^3); and the V_A stands for the volume of air in the pores(m^3). Therefore, relative soil moisture equals to 1 when the all pores are occupied by water, and it is zero if pores do not contain any water.

Along with the relative soil moisture parameter, volumetric water content is also commonly used to measure soil moisture level. Volumetric water content, which is also called water content, is the ratio of water volume to soil volume (Dingman, 2015).

$$\theta = \frac{V_W}{V_S} \tag{5.11}$$

Where θ represents the volumetric water content of the soil (m^3/m^3); V_W is the volume of water within the soil profile (m^3); and the V_S refers to the volume of soil (m^3).

Transpiration

The process of soil water uptake and use by plant or, vaporization from the plants' stomata in leaves is defined as transpiration (Weil and Brady, 2016). Transpiration is another way of soil water loss to the atmosphere which constitutes the evapotranspiration process when it is combined with evaporation. Therefore, we benefit from the partitioning method of evapotranspiration to achieve crop transpiration values (Allen et al., 1998).

$$T_{Ac} = T_P * K_S \tag{5.12}$$

Where T_{Ac} is the actual transpiration amount that the crop performs (m^3/day); T_P is the potential transpiration the crop can make under ideal conditions (m^3/day); K_S is the stress on the crop which emerges either from the water deficit in the soil or the high soil salinity conditions and would limit the transpiration ability of the crop (dimensionless).

The potential transpiration is derived from the reference evapotranspiration rate (ETo) through the basal crop coefficient (Kcb) as a part of the dual crop coefficient method of the FAO. Therefore, the potential transpiration is the amount that a crop type can make without experiencing any stress as a limiting factor through the growth season.

$$T_P = ETo * Kcb \tag{5.13}$$

Basal crop coefficient (Kcb) is a crop specific parameter to represent crop water requirement during the developmental process. Kcb values vary from one crop type to another, which are used to transform the reference crop evapotranspiration rates (grass) into the crop specific vales. Moreover, Kcb values also changes during the developmental stages for the crop type in question. As the crop grows, its' water requirement increases, and the value of the coefficient rises as well. However, after having passed the middle of the growth season, the crop water requirement, and the coefficient begin to decline. Therefore, the basal crop coefficient is also a time-dependent variable that depends on the crop development stages as well.

We inserted the Kcb parameters for various types of crops as time dependent table functions. We benefitted from the FAO's (1998) and TAGEM's (2017) documentations to determine crop specific values for Kcb parameters, to identify the local seeding and harvest times, and also to set the vegetation duration. In addition to these, we again avoided the linear and discrete functions, rather tried to adapt smooth and non-linear ones while representing the basal crop coefficients. The figure below illustrates the comparison of FAO's suggestion and our adaptation for the time dependent Kcb functions for one specific crop type.

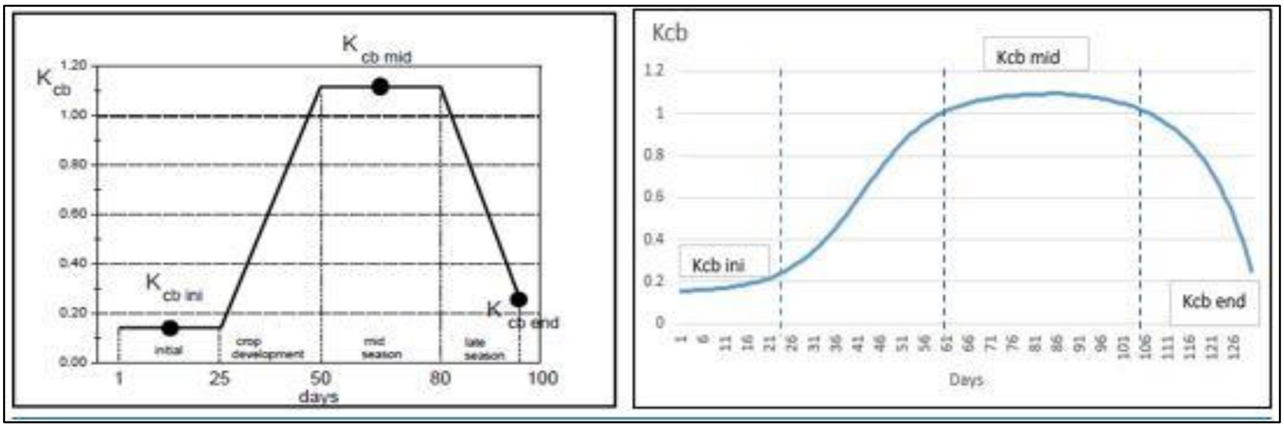

Figure 5.7. Dry bean Kcb comparison (Allen et al., 1998).

In Figure 5.7, we demonstrate changes in the Kcb values of dry bean for one season in two different graphics. On the left, we view the Kcb values for dry bean according to the FAO's document. This graph comprises four developmental stages within each we can observe a linear trend. However, the right graphic in the figure, which we employ in our simulations, shows a non-linear and a continuous trend throughout the growth season in Karapınar. We believe that the non-linear curve better represents the generalized crop curve than the formulated discontinues values (Allen and Pereira, 2009). In addition to these, the crop may struggle to uptake the water amount from soil which is required to maintain its' growth. One reason for limiting the uptake of required water for the crop growth is water stress, which is defined as the water deficit in soil profile. Plus, crop can experience another way of stress due to high saline conditions in the rootzone as well. We consider the impact of these two kinds of crop stresses together. Therefore, the crop stress coefficient is calculated as follows (Allen et al., 1998):

$$K_S = K_{WS} * K_{SaS} \tag{5.14}$$

Where K_S is the crop stress coefficient (dimensionless); K_{WS} is the water stress on the crop (dimensionless), while K_{SaS} is the salinity stress (dimensionless).

K_{WS} comes into force when water amount in the rootzone is less than the water stress threshold, therefore equals to 1. However, water stress coefficient (K_{WS}) is expressed in Equation 5.14 in the condition of soil water level falls below the water stress threshold (Luo et al., 2009).

$$K_{WS} = \begin{cases} 1\,, & \Theta_{threshold} \leq \Theta \\ \dfrac{\Theta - \Theta_{WP}}{\Theta_{threshold} - \Theta_{WP}}\,, & \Theta_{WP} \leq \Theta < \Theta_{threshold} \end{cases} \tag{5.15}$$

Where Θ is the relative soil moisture as described in the Equation 5.10; Θ_{WP} is the relative soil moisture at the wilting point (dimensionless); and $\Theta_{threshold}$ is the relative soil moisture at the water stress threshold which is calculated as shown below (Luo et al., 2009).

$$\Theta_{threshold} = (1 - p) * \Theta_{FC} + p * \Theta_{WP} \tag{5.16}$$

Where Θfc is the volumetric water content at field capacity (dimensionless); “P” parameter indicates the fraction of the total available water in the rootzone that the crop can extract without experiencing water stress (dimensionless).

Total available water (TAW) concept refers to the maximum amount of soil water that a crop can uptake after the soil profile is naturally drained away from the excess water and reached its field capacity. Total available water corresponds to the difference between the field capacity and the wilting point of the soil profile which is stated as the level of soil moisture that crop water uptake reaches zero. On the other hand, the total water amount that crop can uptake without encountering any water stress is expressed as the readily available water (RAW). The relationship between total available water and the readily available water is described in equation 5.16 (Allen et al., 1998).

$$TAW = P * RAW \tag{5.17}$$

On the other side, KSaS points out the crop stress that originates from the accumulated salt minerals in the soil profile. Similar to the water stress on the crop, salinity stress (KSaS) also can be effective when the salinity of the rootzone rises above the salinity stress threshold of the crop type. Therefore, KSaS is equal to 1 when the salinity of the rootzone is below the salinity stress threshold. However, the salinity stress coefficient is expressed below when the rootzone salinity achieves higher values than the threshold (Allen et al., 1998).

$$K_{SaS} = \begin{cases} 1 & , \ EC_R \leq \ EC_T \\ MAX(1 - B * \left(\frac{1}{Ky * 100}\right) * (EC_R - EC_{threshold}), 0), & EC_T < EC_R \end{cases} \quad (5.18)$$

Where, EC_T is the salinity stress threshold which is a specific value for crop types (dS/m); EC_R is the salinity level of the rootzone (dS/m); "B" is a crop specific parameter indicating the reduction in yield per increase in EC_R $\left(\frac{\%}{dS/m}\right)$; Ky is the yield response factor depending on the crop type (dimensionless).

Percolation

The downward flux of soil water from the rootzone towards deeper layers is defined as percolation. After a wetting event, such as rainfall or, irrigation, a certain amount of the water is held in the void volume of the soil profile and the rest of the water is discharged. The field capacity of the soil refers to the water level of a soil profile after the excess water naturally drains away (Weil and Brady, 2016). Therefore, we can say that the percolation takes place when the soil water level exceeds its field capacity. The percolation rate is highly depending on the soil texture and the moisture level of the soil profile. The numerical solution of Richards Equation is computationally cumbersome challenge which interferes with the fast simulation purposes. Therefore, we are inspired to use a simple formulation for percolation which can helps us to represent water flow in unsaturated conditions as in the valuable work of modelling soil salinity (Mau and Porporato, 2015). In this work percolation is represented mainly through accounting unsaturated hydraulic conductivity in the rootzone. However, we do not adopt the same formula from their work to calculate hydraulic conductivity in unsaturated conditions yet, we apply prominent work of Van Genuchten which is the commonly employed approach in the literature. In addition to that, we include the reduction in the hydraulic conductivity due to the varying composition of the soil salinity and sodicity conditions as in the infiltration process (Kramer and Mau, 2020).

$$P = \begin{cases} 0 & , \Theta \leq \ \Theta_{FC} \\ A * K(\Theta) * RK_{Sat} & , \Theta_{FC} < \Theta \end{cases} \quad (5.19)$$

Where P is the percolation of the water from the rootzone (m^3/day); and $K(\Theta)$ is the hydraulic conductivity of the rootzone depending on its soil moisture level (m/day); A is the area of the land (m^2).

According the Van Genuchten-Mualem model, soil hydraulic conductivity in unsaturated conditions is expressed below (van Genuchten, 1980).

$$K(\Theta) = K_{Sat} * \Theta^{\left(\frac{1}{2}\right)} * \left\{1 - \left[1 - \Theta^{\left(\frac{1}{m}\right)}\right]^{m}\right\}^{2} \tag{5.20}$$

Where K_{Sat} is the saturated hydraulic conductivity (m/day); “m” is the soil specific parameter (dimensionless).

Precipitation

Precipitation values are inserted as time-dependent table functions in units of cubic meter per day (m^3/day). The model provides options to adapt different precipitation regimes in the simulations. These regimes try to represent different climate change scenarios which are based on the well-known RCP (Representative Concentration Pathways) scenarios, RCP 2.6, RCP 4.5, and RCP 8.5. In each precipitation regime, there are daily precipitation values for 30 years of duration. These precipitation regimes differ in their annual average rates. The thirty years of average annual precipitation corresponds to 296 (mm/year) for RCP 2.6, 281 (mm/year) for RCP 4.5 and, 260 (mm/year) for RCP 8.5 scenarios, respectively. We benefitted from an open source, online weather data generator named MarkSim to create these daily precipitation values specific to any geographic location. (Jones et al., 2002). MarkSim provides an opportunity to generate weather data based on the selected location. Herein, Karapınar, Konya is selected to generate and employ precipitation data to represent field conditions. In the Figure 5.8 below, we present a daily precipitation amounts which is based on the RCP 4.5 scenario for 30 years long as an example.

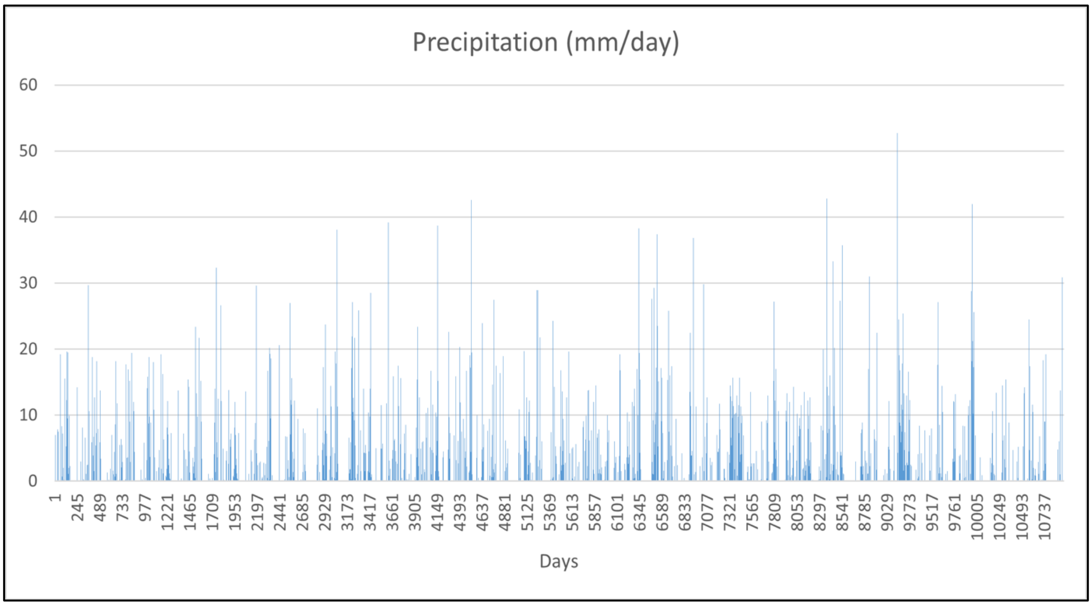

Figure 5.8. Daily precipitation values (mm) for RCP 4.5.

Irrigation

In the model, irrigation water amounts also inserted as time dependent table functions very similar to the precipitation flow. It is also possible to select irrigation method in the simulations. There are two types of irrigation methods, as sprinkler and drip irrigation.

Daily irrigation amounts are specified according to the irrigation guideline handed out to farmers that we achieved during the field visit. The guidelines suggest monthly irrigation amounts for several crop types which are commonly planted in the field but only for sprinkler irrigation method. Therefore, the water applications with sprinkler irrigation method are carried out regarding the guideline. Nevertheless, considering the suggestions of this guideline and the FAO's irrigation scheduling guideline, we created the application amounts for drip irrigation method (Brouwer et al., 1989). However, both methods consider the crop water requirement, which is conceptualized based on the difference of crop evapotranspiration and precipitation rate, and the common efficiencies for these methods. While the 75% of sprinkler irrigation meets the crop water requirement, this ratio is stated as 90% for drip irrigation (Brouwer et al., 1989). Therefore, we can conclude that sprinkler irrigation water brings more water amount than drip irrigation. Furthermore, we paid attention to avoid overlapping days of irrigation and precipitation. There is no irrigation application day when precipitation occurs. On the other hand, irrigation table functions are generated considering the various crop rotations that can be selected in the model, which will be described in next sections.

5.2.2. Solute Model

In the solute sector of the model, the transport of the solute through the soil profile is represented. The salinity concentration in the soil layers, and the soil sodicity is calculated. Through the soil salinity and sodicity rates of the soil, we can estimate the reduction on the hydraulic conductivity.

The salt minerals can accumulate in the soil compartments, in soil surface, in rootzone and in the saturated zone very similar to the hydraulic model. The vertical transport of the salt minerals is carried out by the advection process assisted by the water movement (flows) in the hydraulic model. The salt minerals can be introduced into the soil profile in dissolved form in the irrigation water. The salts can be stored on top of the soil surface, as well as they can penetrate into the rootzone by the infiltration water. The accumulated salt minerals on the soil surface can also be flushed out by the runoff water. Likewise, salt minerals can accumulate in the rootzone layer from where they can be leached down to deeper layers. As mentioned before, we neglect the presence of a shallow water table, i.e., a saturated zone below the rootzone. However, theoretically dissolved salt minerals can rise to the rootzone from the saturated zone by the capillary rise of the water.

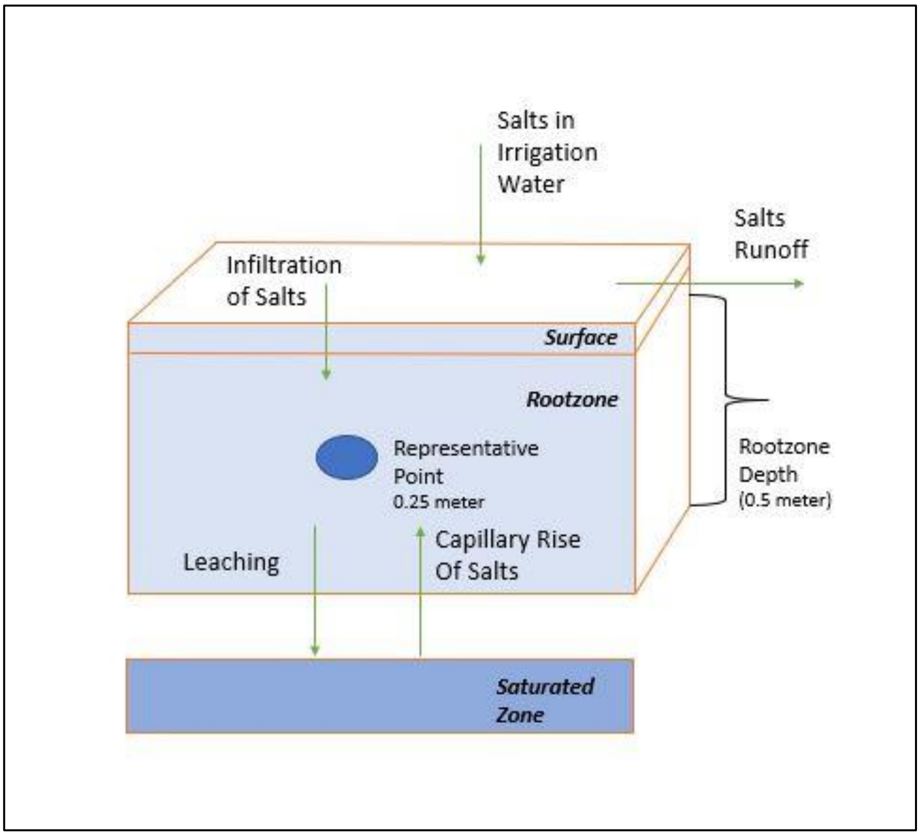

Figure 5.9. Physical Model of Solute Model.

The main cations that are present in the soil water are Ca^{2+}, Mg^{2+}, Na^{+} and, K^{+}. On the other hand, even though all cations take part in the adsorption-desorption process, Mg^{2+} and, Ca^{2+} behave very similarly. Consequently, Ca^{2+} in the model represents the aggregation of Mg^{2+} and Ca^{2+} in the soil profile. Moreover, K^{+} cation may be present in negligible amounts in the soil. Therefore, we only employ Ca^{2+} and Na^{+} to represent the main cations to avoid solving cumbersome equations and to keep the simplicity of the model for fast simulating purposes (Mau and Porporato, 2015).

The solute model consisted of four stocks, and ten flow variables. The accumulations of salt minerals (cations) in the solute model are accounted by the salt stocks, in the units of equivalents. The transportation of the Ca^{2+} and Na^{+} cations are governed by the flows which are in equivalent/days units. The stock-flow structure of the solute model is depicted in the Figure 5.10, as generated in the STELLA software.

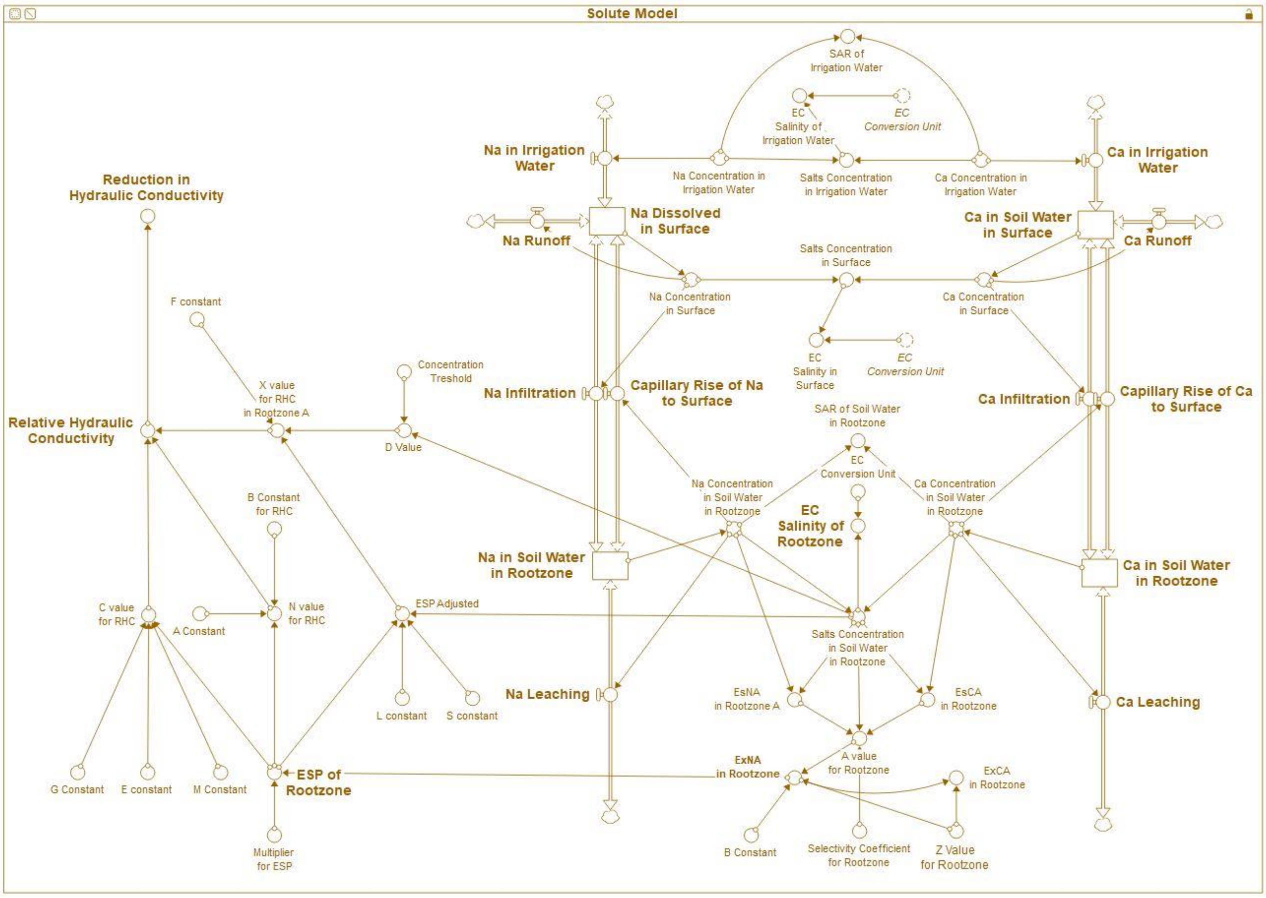

Figure 5.10. The Stock-Flow Structure of the Solute Model.

The causal loop diagram of the solute model is illustrated below, in Figure 5.11. The causal diagram of the solute model contains eight balancing and, two reinforcing feedback loops.

The first balancing loop of the solute model (B8) indicates the relationship between the Na^+ dissolved in surface stock and Na^+ infiltration. As the dissolved Na^+ amount increases in the surface, the concentration of the cation also rises. Rise in the concentration of Na^+ leads to an increase in the infiltration of Na^+. However, augmentation of Na^+ infiltration diminish the amount of Na^+ in the surface stock.

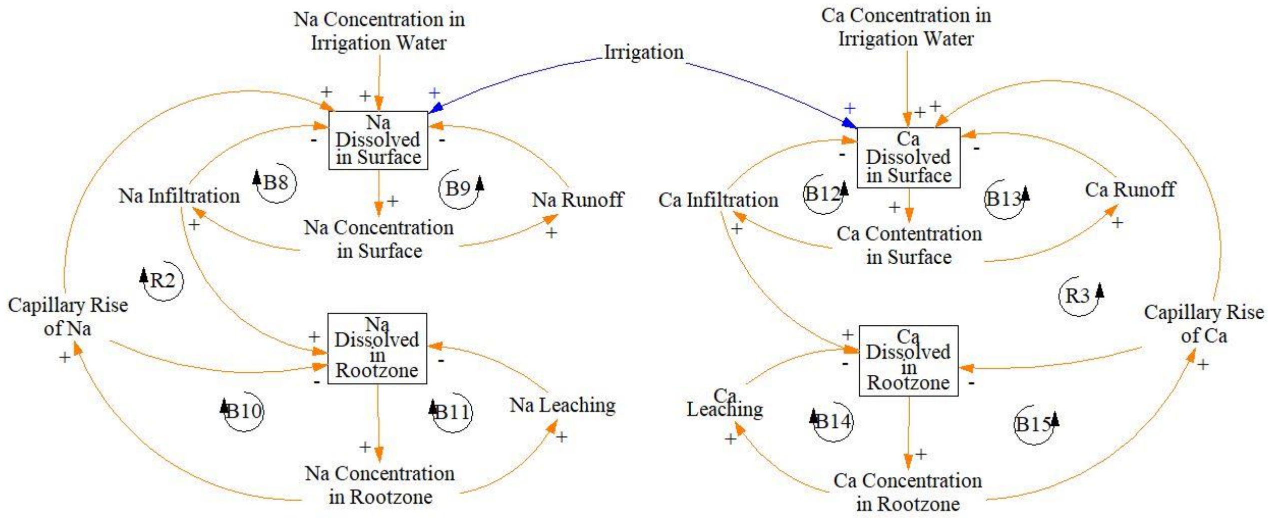

Figure 5.11. Causal Loop Diagram of Solute Model.

The second balancing loop (B9) indicates the relationship between the Na^+ dissolved in surface stock and Na^+ runoff outflow. As in the B8, an augmentation in the Na^+ dissolved in surface stock raises the concentration of Na^+ in the surface which also leads to an increase in the runoff of Na^+. Yet, the increase in the Na^+ runoff reduces the amount of Na^+ dissolved in surface. Another balancing feedback loop (B10) exists between the Na^+ dissolved in rootzone stock and the capillary rise of Na^+. Increase in the Na^+ dissolved in rootzone stock also further increases the capillary rise of Na^+. Yet, the rise in the capillary rise of Na^+ reduces the amount Na^+ cations dissolved in rootzone. Moreover, similar mechanism takes place between the dissolved Na^+ cations in rootzone and the leaching of Na^+. The increased amount of dissolved Na^+ cations in rootzone also rises the leaching of Na^+ through the Na^+ concentration in the rootzone. However, leaching of Na^+ decreases the amount of Na^+ dissolved in the rootzone.

Balancing feedback loops which express the causal relationships between the stocks and flows of dissolved Ca^{2+} cations also indicate the same types of liaisons as in the Na^+ cation. B12 and B13 point out the counteractive relationships between the dissolved Ca^{2+} cations in the surface and their transportation through infiltration and runoff, respectively. In addition to that, B14 and, B15 represent two other balancing relationships which express the transport of dissolved Ca^{2+} from rootzone stock to surface (B15) and the leaching of the Ca^{2+} from rootzone towards deeper levels (B14).

On the other hand, there are two reinforcing loops, R2 and R3, in the causal loop diagram of the solute model. Both reinforcing loops indicate same type of relationship; one represents it for the dissolved Na^{+} cations while the other displays it for dissolved Ca^{2+} cations. In R2, increase in the dissolved Na^{+} cations in the surface leads to an increase in Na^{+} infiltration which further augments the amount of dissolved Na^{+} in the rootzone. However, the augmentation in the dissolved Na^{+} cations in rootzone inflates the amount of capillary rise of Na^{+} from rootzone to surface which increases the amount of Na^{+} cations in the surface stock. The similar mechanism can be found between the dissolved Ca^{2+} cations in surface and rootzone stocks through infiltration and capillary of Ca^{+} variables.

Solute Transportation

The stock-flow structure and the causal feedback loops of the solute models are governed by equations mainly described in the literature. The mass balance equations for the salt minerals in soil compartments are described below. The transport of the dissolved cations (Na^{+} and Ca^{2+}) is generated by the advection process with soil water. Diffusion of the minerals in the soil water is neglected as transport is commonly controlled by advection and to keep the simplicity of the model structure.

The Na Dissolved in Surface (Q_S^{Na}) indicates the Na^{+} cations present in soil water on the soil surface while Ca Dissolved in Surface (Q_S^{Ca}) refers to the Ca^{2+} cations dissolved on surface. Likewise, Na Dissolved in Rootzone (Q_R^{Na}) represents the Na^{+} cations in the soil water in rootzone. Furthermore, Ca Dissolved in Rootzone (Q_R^{Ca}) refers to the Ca^{2+} cations in the soil water in rootzone. The mass balance equation for these cations in the surface and rootzone stocks are based on the work of Mau (2015) to generate mass balance equations for these cations in the surface and rootzone stocks (Mau and Porporato, 2015).

The equations 5.19 and 5.20 suggest the equilibrium of cations in the surface, for Na^{+} and Ca^{2+}, respectively.

$$Q_S^{Na}(t) = Q_S^{Na}\,(t - dt) + (Q_I^{Na} + Q_{Cr}^{Na} - Q_{Sr}^{Na} - Q_F^{Na}) * dt \tag{5.21}$$

$$Q_R^{Na}(t) = Q_R^{Na}\ (t - dt) + (Q_F^{Na} - Q_{Cr}^{Na} - Q_L^{Na}) * dt \tag{5.22}$$

Where, Q_I^{Na} refers to the flux of Na^+ cations introduced in the irrigation water (eq/day); Q_{Cr}^{Na} is the of Na^+ cations present in the capillary rise flow from rootzone to surface (eq/day); Q_{Sr}^{Na} is the rate of Na^+ cations that is flushed out from the soil surface through surface runoff (eq/day); $Q_F^{Na}$is the infiltration flow of the Na^+ cation from surface to rootzone (eq/day); Q_L^{Na} is the leaching rate of the dissolved Na^+ cations from rootzone to the deeper soil layers (eq/day).

$$Q_S^{Ca}(t) = Q_S^{Ca}\ (t - dt) + (Q_I^{Ca} + Q_{Cr}^{Ca} - Q_{Sr}^{Ca} - Q_F^{Ca}) * dt \tag{5.23}$$

$$Q_R^{Ca}\ (t) = Q_R^{Ca}\ (t - dt) + (Q_F^{Ca} - Q_{Cr}^{Ca} - Q_L^{Ca}) * dt \tag{5.24}$$

Where Q_I^{Ca} stands for the flow Ca^{2+} cations in the irrigation water (eq/day); Q_{Cr}^{Ca} indicates the rate of Ca^{2+} cations that rise to surface from rootzone via capillary rise (eq/day); Q_{Sr}^{Ca} represents the flux of dissolved the Ca^{2+} cations in the surface runoff (eq/day); Q_F^{Ca} stands for the infiltration flow of Ca^{2+} cations from surface into rootzone (eq/day) Q_L^{Ca} is the flux of dissolved Ca^{2+} cations that is leached out by percolation of water from rootzone towards deep soil.

The transport of the cations through soil profile is formulated as the multiplication of the relevant water movement, a flow variable in the hydraulic model, with the concentration of the cation present in the soil water in the soil compartment (Hillel, 1998; Mau and Porporato, 2015). Therefore, we can express the movement of the cations in the solute model regarding the following equations.

The runoff of the cations is formulated as such:

$$Q_{SR}^{Na} = C_S^{Na} * SR \tag{5.25}$$

Where SR is the surface runoff water (Eq 5.6), C_S^{Na} is the concentration of the Na+ cation in the surface (eq/m^3). The concentrations of the cations are considered as the dissolved cation amount in a soil compartment in proportion to the soil water. The cation concentration in the soil surface refers to the division of the cation quantity dissolved in the soil surface by the soil water amount in the surface. The concentration of the dissolved the Na+ cation in the surface (eq/m^3) can be found according to the following equation.

$$C_S^{Na} = \frac{Q_S^{Na}}{S_S} \tag{5.26}$$

On the other hand, the runoff of the Ca2+ cation from the soil surface is calculated as follows, in a very similar way with the Na+ cation.

$$Q_{SR}^{Ca} = C_S^{Ca} * SR \tag{5.27}$$

Where C_S^{Ca} is the concentration of Ca2+ cation in soil water in the soil surface (eq/m3). The dissolved Ca+ concentration in soil surface can be found regarding the following equation.

$$C_S^{Ca} = \frac{Q_S^{Ca}}{S_S} \tag{5.28}$$

The penetration of dissolved cations from soil surface into the rootzone compartment is assessed as the cation's infiltration. The infiltration of the cation in question is formulated as the multiplication of the infiltration flow in the hydraulic model with the cation's concentration in the soil water in soil surface. Therefore, the formulations of cations are described below for Na^{+} and Ca^{2+} respectively.

$$Q_F^{Na} = C_S^{Na} * F \tag{5.29}$$

$$Q_F^{Ca} = C_S^{Ca} * F \tag{5.30}$$

Furthermore, capillary rise of the cations from rootzone to the soil surface occurs via the capillary movement of the soil water. However, we consider the cations' concentration in the rootzone to calculate their capillary movement in the soil water. Therefore, the capillary rise of the Na+ cation is calculated according to the following equation.

$$Q_{CR}^{Na} = C_R^{Na} * CR \tag{5.31}$$

Where, C_R^{Na} is the concentration of the Na^{+} in soil water in the rootzone (eq/m^3) which is described in the equation 5.30:

$$C_R^{Na} = \frac{Q_R^{Na}}{S_R} \tag{5.32}$$

On the other hand, the capillary rise of the dissolved Ca^{2+} cation is expressed below.

$$Q_{CR}^{Ca} = C_R^{Ca} * CR \tag{5.33}$$

Where, C_R^{Ca} is the concentration of the dissolved Ca2+ in soil water in the rootzone. The concentration of Ca+ in soil water in the rootzone is formulated likewise.

$$C_R^{Ca} = \frac{Q_R^{Ca}}{S_R} \tag{5.34}$$

Furthermore, the cations can be removed from the rootzone to the deeper levels of soil profile via leaching process. Leaching takes place by means of percolation water as well as the amount is assessed considering the cations' concentration in soil water in the rootzone. The formulation of the leaching process of the Na^{+} and Ca^{2+} cations is described as follows, respectively.

$$Q_L^{Na} = C_R^{Na} * P \tag{5.35}$$

$$Q_L^{Ca} = C_R^{Ca} * P \tag{5.36}$$

On the other hand, the cation amount in the irrigation water is also achieved through the irrigation flow variable in the hydraulic model. In addition to that, we specify cations' concentrations in the irrigation water to set the water quality with respect to its' saline and sodic characteristic. In simulation runs, we set the cations' concentrations in irrigation water to represent the field conditions. However, it is also testing parameter to examine the effects of different water qualities on the soil salinization and sodification process. Therefore, the cations in the irrigation water can be expressed as in the following equations for Na+ and Ca2+ cations accordingly.

$$Q_I^{Na} = C_I^{Na} * I \tag{5.37}$$

$$Q_I^{Ca} = C_I^{Ca} * I \tag{5.38}$$

Along with the transport of salt minerals through the soil profile, the solute model also generates the parameters to estimate soil salinity, sodicity and the reduction in the hydraulic conductivity due to the salinity and sodicity rates of the soil profile. Firstly, the standard parameter of the soil salinity is the Electrical Conductivity of the saturated extract at 25^0C degree. However, the stock-flow structure of the solute model accounts for the cation equivalents. Therefore, we convert the salt concentration in the model into the Electrical Conductivity terms based on the rule of thumb described in the literature (Huang et al., 2012).

$$10 * EC = C_R^S \tag{5.39}$$

Where EC stands for the electrical conductivity $\left(\frac{dS}{m}\right)$; C_R^S refers to the salt concentration in the rootzone $\left(\frac{eq}{m^3}\right)$.

The salt concentration in the rootzone can be achieved through the additive calculation of the cations present in the rootzone.

$$C_R^S = C_R^{Na} + C_R^{Ca} \tag{5.40}$$

On the other hand, the soil sodicity conditions described by two measurements as mentioned in the introduction section is based on the well-known formulations in the literature (Eq 1.1 and 1.2). Nevertheless, it is important to note the implementation of these formulations in our model. In the first place, the sodium adsorption ratio (SAR) is formulated based on the presented cations in the models. Ca^{2+} cation represents the Mg^{2+} as well. Therefore, we can state the SAR formulation in the solute model in $\left(\frac{eq}{m^3}\right)^{-1/2}$ as follow:

$$SAR = \frac{Na}{\sqrt{\frac{Ca}{2}}} \tag{5.41}$$

Exchangeable Sodium Percentage (ESP) level indicates the ratio of adsorbed Na^+ cations in the soil complex to all adsorbed cations (Eq 1.1). Nevertheless, achieving the ESP ratio requires considering the ion-exchange equilibrium. The adsorption-desorption process occurs in very short time steps. Therefore, we assume that there is a thermodynamic equilibrium in soil conditions (Mau and Porporato, 2016). We employ the following approach to represent ion-exchange process in the soil complex (Yaron et al., 1973).

$$K_{SC} = \frac{E_X^{Ca} * (E_S^{Na})^2 * C_R^S}{(E_X^{Na})^2 * E_S^{Ca}} \tag{5.42}$$

Where K_{SC} is the selectivity coefficient which is specific to soil type $\left(\frac{eq}{m^3}\right)$ (Levy and Hillel, 1968); E_X^{Ca} is the fraction of adsorbed Calcium (dimensionless); E_S^{Na} is the fraction of Na^+ cation in the salt concentration (dimensionless); likewise E_X^{Na} is the ratio of adsorbed Na^+ in the cation exchange capacity (dimensionless); E_S^{Ca} indicates the portion of dissolved Ca^{2+} cations in the salt concentration (dimensionless).

The fraction of a cation in the soil water the ratio of concentration of each cation over the total salt concentration in the rootzone. Therefore, E_S^{Na} and E_S^{Ca} is described respectively:

$$E_S^{Na} = \frac{C_R^{Na}}{C_R^S} \tag{5.43}$$

$$E_S^{Ca} = \frac{C_R^{Ca}}{C_R^S} \tag{5.44}$$

Moreover, the fraction sodium adsorbed by the soil complex (E_X^{Na}) is calculated through mathematical rearrangement of the equation 5.40. We assume that the amount of total adsorbed cations in the soil complex is always equal to the cation exchange capacity. Therefore, the sum of the fraction of the adsorbed cations, E_X^{Na} and E_X^{Ca} equals to 1. Consequently, E_X^{Na} can be expressed as "1-E_X^{Ca}" as well. Having in mind these assumptions and equalities, we can convert the equation 5.40 into a quadratic formula:

$$A * (E_X^{Na})^2 + B * E_X^{Na} + Z = 0 \tag{5.45}$$

Where A value (dimensionless); B constant (dimensionless); and Z value (dimensionless) are generated to solve the quadratic formula.

$$A = \frac{E_S^{Ca} * K_{SC}}{(E_S^{Na})^2 * C_R^S} \tag{5.46}$$

$$Z = E_X^{Na} + E_X^{Ca} \tag{5.47}$$

Therefore, the fraction of adsorbed Na^+ (E_X^{Na}) can be found by the solution of the equation 5.46:

$$E_X^{Na} = \frac{-B + \sqrt{B^2 + 4 * A * Z}}{2 * A} \tag{5.48}$$

Nevertheless, we stated that the standard expression of the soil sodicity is the exchangeable sodium percentage (ESP). Within this regard, we can note the simple relationship between the E_X^{Na}fraction and the exchangeable sodium percentage. Hence, the fraction numerically expresses the share of adsorbed sodium in the soil complex between 0 and 1 values while, the ESP indicates the very same share in a percentage rate, between 0 and 100. As a result, we can simply note the following equation.

$$ESP = E_X^{Na} * 100 \tag{5.49}$$

Furthermore, the salt concentration in the soil water and the composition of adsorbed cations can impact the physical structure of the soil profile and degrade its hydraulic qualities. Thus, the hydraulic conductivity rate of the soil profile highly depends on the salinity and sodicity conditions of the soil. The prediction for the reduction on hydraulic qualities due to the salinity and sodicity rates is made based on the valuable work of Ezlit's which improves the well McNeal's Clay Swelling Model (Ezlit et al., 2013). Therefore, the reduction on the hydraulic conductivity is expressed by another parameter, namely relative saturated hydraulic conductivity. This parameter indicates the relative reduction in the hydraulic conductivity as a ratio which can take values between 0 and 1. Accordingly, we do not observe any degradation in the hydraulic qualities while the RKsat equals to 1. Yet the lower values point out the fractional reduction in the hydraulic conductivity respectively. Furthermore, the RKsat is highly dynamic parameter which can reincrease due to the soil conditions even after the serious reduction in the parameter level. Consequently, the RKsat parameter is calculated according to following equation:

$$RK_{sat} = 1 - \frac{c * x_0^n}{1 + c * x_0^n} \tag{5.50}$$

Where c and n are soil specific constants which can take different values in a range with the specified rate of ESP. Yet, x_0 is the adjusted clay swelling factor that represents the swelling and dispersion processes within the soil. Therefore, c and n constant can be determined based on the following functions, respectively:

$$c = g * e^{m*\left(\frac{ESP}{100}\right)} \tag{5.51}$$

$$n = \left(\frac{ESP}{100}\right)^{a} + b \tag{5.52}$$

Where a, b, g and m empirical fitted constants which depend on the soil type.

Furthermore, the adjusted clay swelling factor (x_0) is described through the equation below.

$$x_0 = f * ((3.6 * 10^{-4}) * ESP^*) * d^* \tag{5.53}$$

Where, f corresponds to the fraction of montmorillonite (dimensionless) which constitutes the clay particles in the soil; d^*refers to the adjusted interlayer swelling of montmorillonites (dimensionless); ESP^* indicates the adjusted ESP value (dimensionless).

The adjusted interlayer spacing of montmorillonites d^* is expressed based on the following equation.

$$d^* = \begin{cases} d^* = 0 & , C_R^S > 300\ \frac{eq}{m^3} \\ d^* = 356.4 * (C_R^S)^{-\frac{1}{2}} - 20.58 & , C_R^S \leq 300\ \frac{eq}{m^3} \end{cases} \tag{5.54}$$

Besides, the adjusted exchangeable sodium percentage level (ESP^*) stands for the ESP rate that becomes influential on the hydraulic conductivity.

$$ESP^* = ESP - [l + s\ln(C_R^S)] \tag{5.55}$$

Where, l and s are also empirical parameters which depend on the soil type and condition.

Furthermore, based on the calculation of relative hydraulic conductivity, we formulate a reduction percentage which simplifies the language of the model outputs.

$$RHC = (1 - RK_{Sat}) * 100 \tag{5.56}$$

Where RHC indicates the reduction in hydraulic conductivity as a percentage.

Therefore, through the works of McNeal (1968) and Ezlit (2013) we can analyze that how the salt concentration in the soil water and the ESP level in the soil profile can impact hydraulic conductivity of the soil profile. In this way, we emphasize that the two-way interaction between the hydraulic and solute models contains multiple feedback mechanisms. The causal loop diagram of the feedback mechanism between hydraulic and solute model is illustrated below, in Figure 5.12. The causal loop diagram comprises six balancing and four reinforcing loops. The first balancing loop is the B7 which expresses the counteracting relationship between the water in rootzone stock and the percolation variable, which is mentioned in Figure 5.4 as well. The second balancing loop (B16) in this causal loop diagram indicates the interaction between the infiltration of water into the rootzone and soil salinity. The increase in the infiltration raises the amount of water in the rootzone which decreases soil salinity. However, soil salinity has a positive causality with the relative hydraulic conductivity variable. Augmentation in the relative hydraulic conductivity rises the infiltration. B17 points out another balancing feedback loop. The rise in the infiltration also increases the infiltration of the Na^+ cation which further augments the amount of dissolved Na^+ in the rootzone. The increase in the dissolved Na^+ cations in the rootzone cause an increment in the level of exchangeable sodium percentage which has a negative relationship with the relative hydraulic conductivity parameter. Due to the positive causal link between relative hydraulic conductivity and infiltration variables, a decrease in the relative hydraulic conductivity also reduces the rate of infiltration.

In addition to these, another balancing causal loop (B18) is present between the percolation variable and dissolved Ca^{2+} in rootzone stock. Percolation flow in the hydraulic model has a positive relationship with the leaching flows in the solute model. Therefore, the rise in the percolation leads to increase in the Ca^{2+} leaching. However, the augmentation in the leaching of Ca^{2+} dissolved from rootzone reduces the amount of dissolved calcium in the rootzone stock. Yet, the reduced level of Ca^{+2} dissolved in rootzone variable increases the rate of exchangeable sodium percentage in the rootzone. The exchangeable sodium percentage has a negative causal relationship between the relative hydraulic conductivity. Moreover, a reduction in the relative hydraulic conductivity also diminishes the percolation rate. Likewise, B19 indicates a balancing loop between percolation flow and the Ca^{2+} dissolved in rootzone stock. However, this causal loop emphasizes the role of salts concentration in the rootzone rather than exchangeable sodium percentage as mentioned above. The increase in the amount of dissolved Ca^{2+} cations in the rootzone also rises the level of salts concentration. Furthermore, an increment in the salt concentration augments the relative hydraulic conductivity level. As mentioned above, there is a positive relationship exists between relative hydraulic conductivity and percolation. The last balancing feedback loop (B20) in Figure 5.12 depicts the relationship between percolation and Na^+ dissolved in rootzone variables. In the same way, increased the level of percolation rises the Na^+ leaching rate. Nevertheless, the raise of leaching rate reduces the amount of dissolved Na^+ in the rootzone. Yet, an augmentation in the Na^+ dissolved in rootzone variable also increases the salt concentration in the rootzone. As expressed above, the increased level of salt concentration in the rootzone rises the relative hydraulic conductivity which further increments the percolation rate.

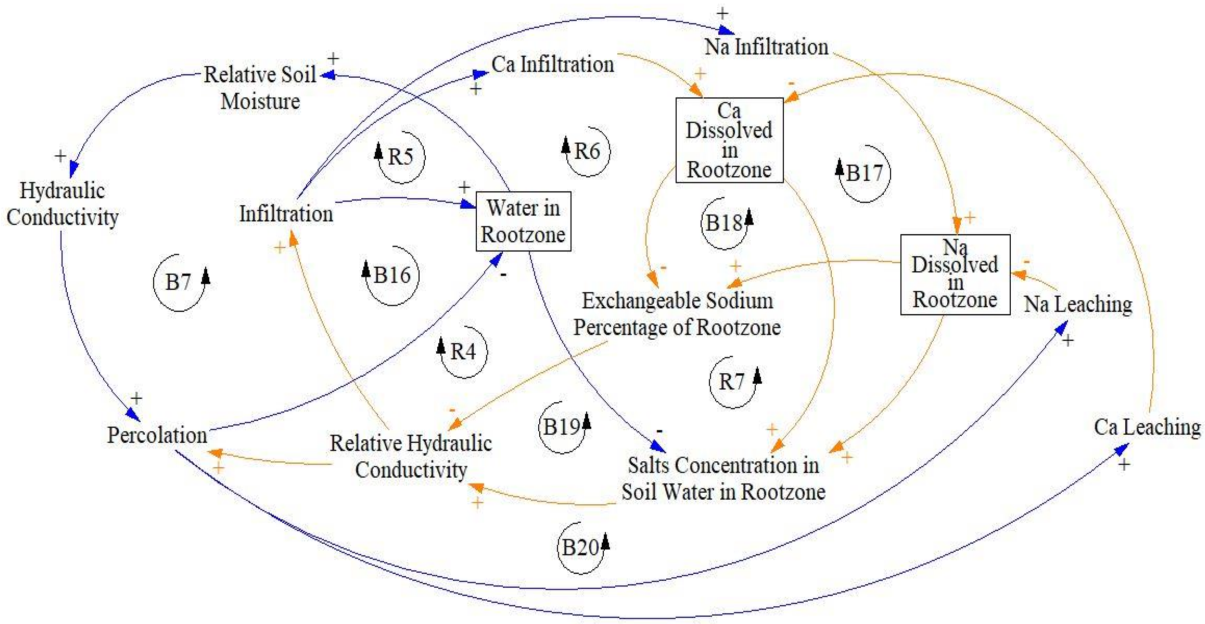

Figure 5.12. Causal Loop Diagram of Feedback Mechanism between Solute and Hydraulic Model.

Besides, there are four reinforcing feedback loops in the causal loop diagram in Figure 5.12. The first reinforcing loop (R4) points out the interaction between infiltration and dissolved Ca2+ in the rootzone. The increase in the infiltration level also rises the infiltration of Ca2+ cation. The rise in the infiltration of Ca2+ cation augments the quantity of Ca2+ dissolved in the rootzone stock. However, the increase the Ca2+ dissolved in the rootzone stock reduces the degree of exchangeable sodium percentage of the rootzone. Additionally, the decrease in the exchangeable sodium percentage level increases the relative hydraulic conductivity. As previously mentioned, the rise in the relative hydraulic conductivity also increases the infiltration rate. Moreover, the second reinforcing loop (R5) in this causal loop diagram also indicates the relationship between infiltration and the Ca2+ dissolved in the rootzone stock. Yet, R5 emphasize the impact of soil salinity in this relationship since the increase in the Ca2+ dissolved in the rootzone stock also rises the salt concentration in the rootzone which further augments the relative hydraulic conductivity.

On the other hand, another similar causal feedback loop (R6) highlights the relationship between infiltration and the Na+ dissolved in the rootzone. As the increase in the infiltration rate rises the infiltration of Na+ cation. The rise in the infiltration of Na+ cation also augments the amount of the dissolved Na+ cations in the rootzone which further increases the salt concentration in the rootzone. The aforementioned links between salt concentration in the rootzone and relative hydraulic conductivity; and the infiltration completes the loop, respectively. The last reinforcing loop in the Figure 5.12 (R7) indicates the interaction between percolation and the dissolved Na+ cations in the rootzone. The increase in the percolation rate also augments the level of Na+ leaching. The augmentation in the Na+ leaching rate reduces the quantity of dissolved Na+ in the rootzone. The reduction in the Na+ dissolved in the rootzone also diminishes the exchangeable sodium percentage in the rootzone. However, the decrease in the exchangeable sodium percentage rises the degree of relative hydraulic conductivity which further increases the percolation rate.

5.2.3. Crop Yield

The model generates a yield response which aims to anticipate the loss of crop yield rate by season. As mentioned in the description of the hydraulic model, the transpiration is the rate of plant water uptake from the rootzone and use it for the crop growth process. Nevertheless, there can be limits to water uptake by plant which would prevent its potential growth. Water deficit in the rootzone is stated as the one source of stress on the crop, while salt concentration in the soil profile is another stress which introduce limits to plant water uptake. Within this regard, the daily actual and potential transpiration rates are accumulated throughout a growth season. These accumulations enable us to compare them with each other at the end of the season for yield predictions. Therefore, crop production process can be considered over a simple linear function which is introduced in the FAO's Irrigation and Drainage Paper N0:33 (Doorenbos and Kassam, 1979).

$$\left(1-\frac{Y_a}{Y_m}\right)=\left(1-\frac{T_{ac}}{T_p}\right)*Ky \tag{5.57}$$

Where Y_a indicates the actual yield rate at the end of the season (dimensionless); Y_m is the maximum yield crop can achieve without experiencing any kinds of stress; Ky is the yield response factor depending on the crop type (dimensionless).

On the other hand, the interaction between the crop transpiration and various stress types due to the amount of water and salt minerals in the rootzone creates feedback processes. The Figure 5.13 demonstrate the causal loop diagram of crop stress due to water deficit and/or salinity concentration in the rootzone. As expressed before, B6 indicates the relationship between actual transpiration and water amount in the rootzone. Decrease in the water in rootzone stock raises the water stress which further increase the crop stress. However, as the crop stress augments the actual transpiration diminishes. Yet, there is another negative relationship between actual transpiration and water in rootzone stock. An increase in actual transpiration reduces the amount of water in the rootzone.

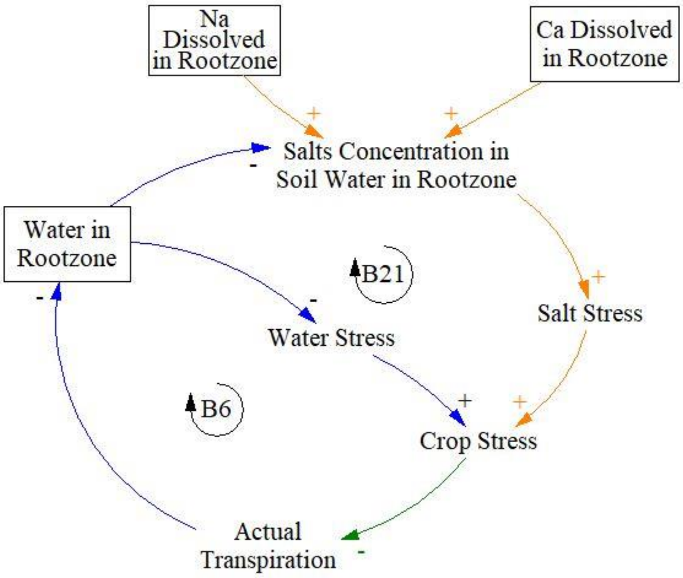

Figure 5.13. Causal Loop Diagram of Crop Stress.

The second balancing loop (B21) related to crop stress reveals the liaison between the salt concentration and actual transpiration through the salt stress variable. The salt concentration is linked to three different stock variables. Two of them represents the dissolved salt minerals present in the rootzone, Na+ and Ca+ respectively. Salt stocks are exogenous variables for these causal loop diagram while both have positive relationship between the salinity concentration variable. Nevertheless, water in rootzone stock variable is negatively linked to the salinity concentration. As the water amount in rootzone increases the salinity concentration decreases. The reduced rate of salinity concentration also diminishes salt stress level. As the salt stress level decreases, the crop stress level also reduces. However, a reduction in the crop stress level causes an augmentation in the actual transpiration rate. As explained above, the negative liaison between the actual transpiration and water in rootzone suggests that the rise in the actual transpiration rate diminishes the water volume in the rootzone stock.

6. MODEL VALIDATION

Model validation is an essential part of studies which aim to develop models and/or employ different kinds of models in their methodological analysis. The reliability of the outputs generated by a model and, the credibility of the policy suggestions developed based on the model outputs are highly dependent on the validity of the model employed. The models, which are built based on the system dynamics literature, are identified as causal-descriptive (Barlas, 1996). These models aim to represent the relevant structure of the real-life systems that are responsible for the analyzed systems behavior. They are developed upon the causal relationships expressed by scientific theories in the relevant literature. Therefore, the system dynamics model should not only generate the right outputs but also generate “right output behavior for the right reasons” (Barlas, 1996).

Model validation is performed throughout the model development process. Thus, validity of the model is ensured step by step rather than an ultimate assessment at the end. In formal validation procedure, two types of tests are applied to assess the model validity. Firstly, the structural validity is examined through direct structure tests and structure-oriented behavior tests. In addition, the behavior pattern tests are performed after the credibility of the model structure is enhanced. Behavior pattern tests enable us to evaluate the representativeness of model generated behavior patterns with respect to real-life patterns in question.

Direct structure tests are carried out based on the knowledge about the real system. In this phase, the simulation results are not considered. This step comprises structure confirmation, parameter confirmation and direct extreme condition tests and dimensional consistency test (Barlas, 1996). Therefore, we aim to ensure the structure and equations of the model that are determined based on theoretical knowledge about the real system. Furthermore, the parameters should be checked both conceptually and numerically. Direct extreme-condition test is carried out by noting the plausible anticipations of the model outputs under extreme conditions. Lastly, dimensional consistency of each equation is checked. Within this regard, we can state that the model is constructed based on the available scientific literature. Therefore, the model structure is determined, and the equations are taken from according to the existing literature. The dimensional consistency of the equations is checked before embedding into the model structure.

Furthermore, structure-oriented behavior tests are employed to assess the validity of internal structure of the model. In this phase, simulation runs are performed and assessed. Extreme condition tests are applied by setting too high or low numerical values to selected parameters. In this way, the expected results and model generated outputs are compared for the same extreme condition. Moreover, behavior sensitivity tests are performed to detect the parameters which can highly impact the model outputs (Barlas, 1996).

After having ensured the structural reliability of the model, behavior pattern tests are done by comparing the model outputs by available data. Such data can be provided by historical recordings of selected parameters, as well as by generated outputs of other robust models to compare selected parameters under the same simulation conditions.

The simulation runs for extreme condition tests, behavior sensitivity tests and behavior pattern tests are presented in following sections. In these simulation runs for validation tests parameters related to soil properties are selected from the literature (Carsel and Parrish, 1988). The simulations duration in validation tests is one year, 360 days. The water inflow into the soil compartments is supplied only by irrigation, precipitation flow is excluded. Irrigation, potential evaporation, and potential transpiration rates are set as constant variables. Potential evaporation is set as 15 m^3/day, while potential transpiration rate is determined as 10 m^3/day in all simulation runs. However, irrigation rate is varied based on the purpose of validation tests. Furthermore, in these simulations soil type is assumed as clay loam. The initial condition of soil water is always set at field capacity level. On the other hand, initial condition for soil salinity is determined as 1.5 dS/m EC and, soil sodicity level is fixed to 6.3 SAR value. The hypothetical crop typed is assumed as maize in all simulation runs for validation tests. The classification of these parameters across the validation tests are listed in Table 6.1. Classification of Parameters in Validation Tests below.

Table 6.1. Classification of Parameters in Validation Tests.

Validation TEST / Parameter	6.1.1	6.1.2	6.1.3	6.2.1	6.2.2	6.3	6.4
Irrigation Rate (m^3/day)	0	250	250	250	250	Table Function	Table Fuction
Irrigation W. Salinity (EC)	-	1.5	6.5	1.5	1) 0.3 2) 3 3) 8	1.5	0.75
Irrigation W. Sodicity (SAR)	-	6.3	25	6.3	1) 3 2) 22 3) 30	6.3	1.5
Potential Evaporation (m^3/day)	15	15	15	15	15	15	Table Function
Potential Transpiration (m^3/day)	10	10	10	10	10	10	Table Function
Soil Type	Clay Loam	Clay Loam	Clay Loam	1)Clay Loam 2) Sandy Cay Loam 3)Sandy Loam	Clay Loam	Clay Loam	Clay Loam
Crop Type	Corn	Corn	Corn	Corn	Corn	Corn	Corn
Simulation Time Horizon (days)	360	360	360	360	360	360	10950
Initial Water Content of Soil (m^3/m^3)	0.3	0.3	0.3	0.3	0.3	0.3	0.3
Initial Soil Salinity (EC)	1.5	1.5	1.5	1.5	1.5	1.5	1.5
Initial Soil Sodicity (SAR)	6.3	6.3	6.3	6.3	6.3	6.3	6.3

6.1. Extreme Condition Tests

6.1.1. Extreme condition test - No precipitation & No irrigation

In this test, precipitation and irrigation rates are set to zero. Therefore, neither water nor salt minerals are introduced. In this condition, we expect that water volume in the soil pores should decrease until a level where plant can no longer uptake the soil water. In other words, volumetric water content of the rootzone is expected to decrease and reach an equilibrium at water content at wilting point level. In Figure 6.1, we can observe that the blue line which represents the volumetric water content of rootzone is reduced to water content at wilting point level indicated by green dotted line.

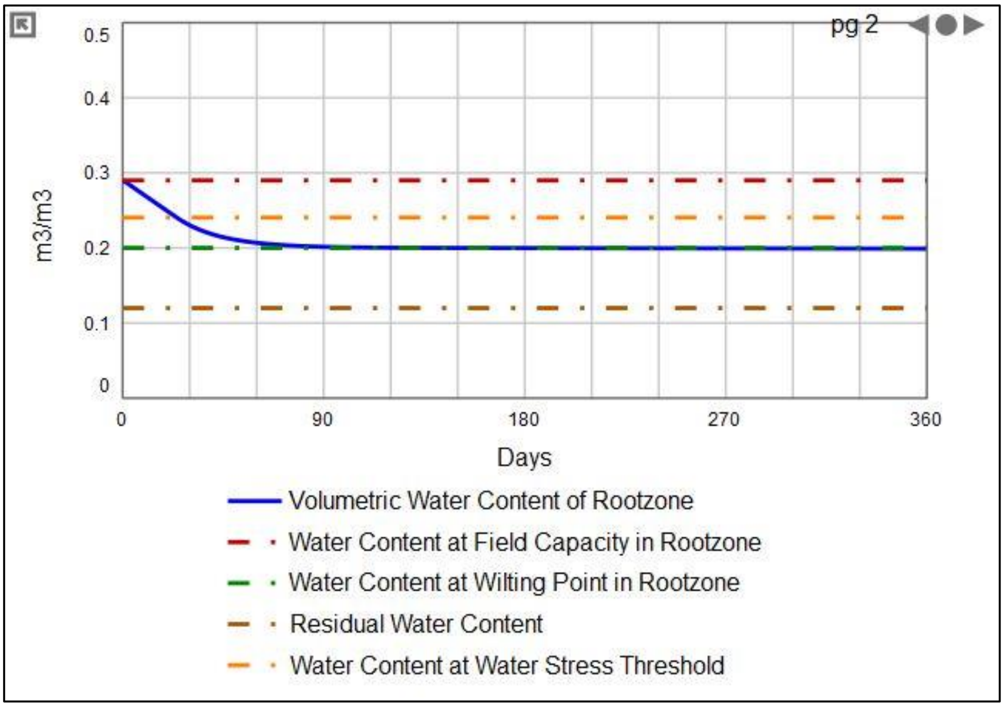

Figure 6.1. Extreme Condition Test 1: Volumetric Water Content of Rootzone.

Parallel to the behavior of volumetric water content of rootzone, actual transpiration rate of the crop should trace a similar pattern. Therefore, we expect that actual transpiration rate, which represents the plant water uptake, should reduce to zero and achieve an equilibrium. In Figure 6.2, we observe that actual transpiration rate, identified by the green line, can perform its potential until the volumetric water level falls below the water stress threshold as depicted in Figure 6.1. However, the actual transpiration rate decreases to zero as the water content in rootzone reaches wilting point.

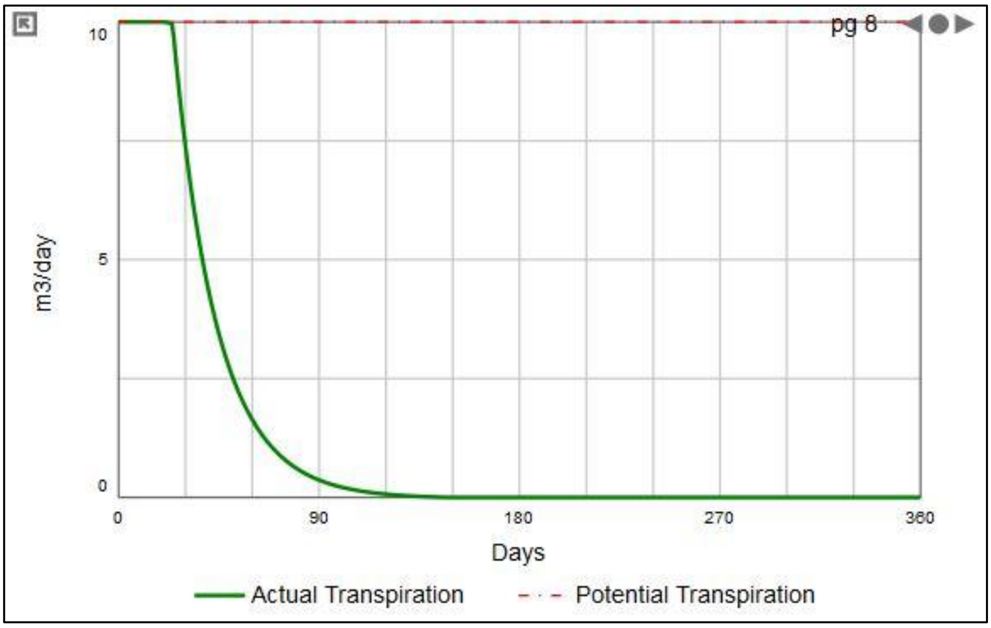

Figure 6.2. Extreme Condition Test 1: Transpiration.

On the other hand, we expect a minor increase in soil salinity and sodicity levels. Since the water content never exceed field capacity level, there is no percolation, therefore there is no leaching of salt minerals. In addition to that, there is no dissolved salt minerals introduced to the soil profile as no irrigation water applied. Therefore, the amount of dissolved salt minerals does not change, while the volumetric water content diminishes as depicted above. Consequently, we expect an increase in the salinity level of the rootzone until the time when volumetric water content stabilizes. We also expect that soil salinity level should also be balanced as long as volumetric water content stays in equilibrium. In Figure 6.3, we observe the changes in soil salinity, Electrical Conductance of soil water, and soil sodicity rates, Sodium Adsorption Ratio of soil water. On the left, the change in the salinity of rootzone is depicted, while soil sodicity of soil water is illustrated on the right with red line. Therefore, the soil salinity of rootzone, the brown line, rises as the water amount is diminished and the salt concentration increased as we expected. However, it stabilized in correlation to the volumetric water content level in rootzone, as it is anticipated. Furthermore, SAR value in Rootzone traces a similar pattern. As the nature of its' formulation, which is expressed by square root of the ratio sodium concentration to half of calcium concentration in soil water, the same rate of augmentation in the concentration of two cations should increase the SAR value. Thus, the increase and the equilibrium in the SAR value illustrated with red line, confirm our expectations.

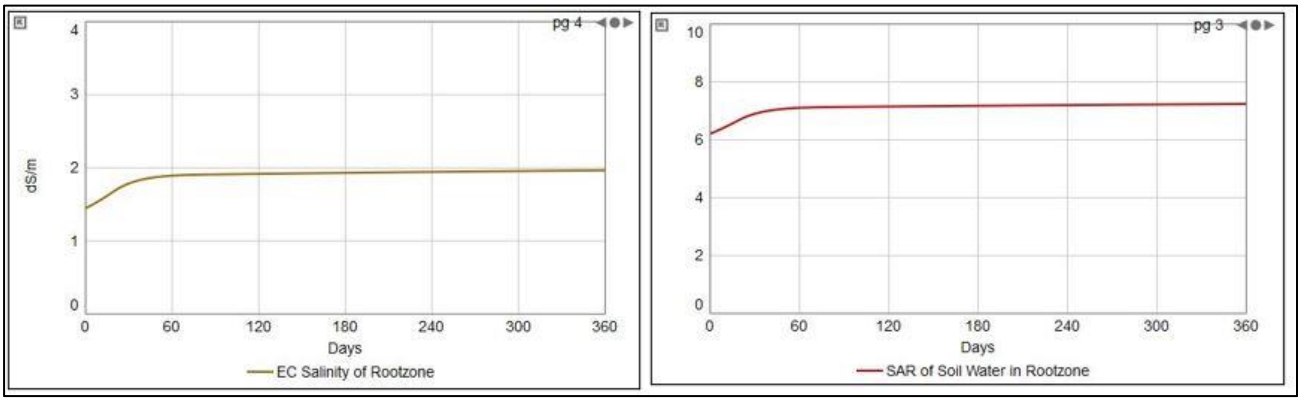

Figure 6.3. Extreme Condition Test 1: EC and SAR of Rootzone.

Beyond these soil salinity and sodicity conditions, we can observe the potential changes in hydraulic conductivity. As the soil sodicity is not sufficiently high and the salinity level is not too low, we do not expect any reduction on the hydraulic conductivity rate (Weil and Brady, 2016). In Figure 6.4, we can observe that reduction in hydraulic conductivity does not increase above zero as we anticipated.

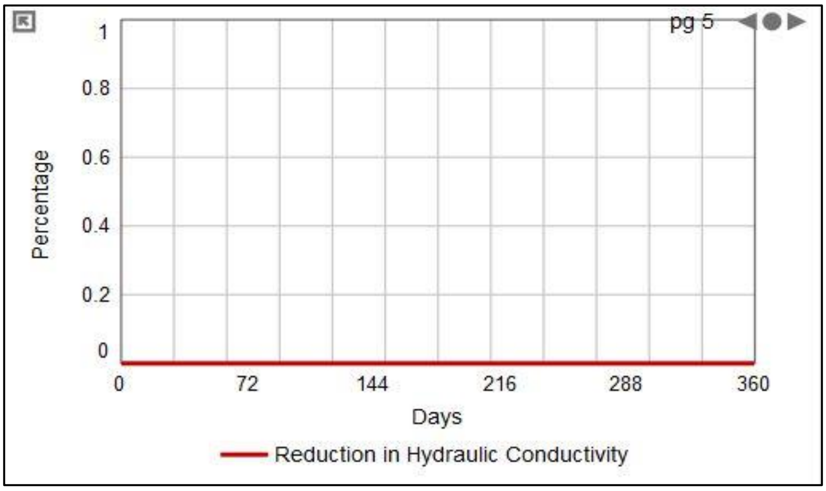

Figure 6.4. Extreme Conditions Test 1: Reduction in Hydraulic Conductivity.

6.1.2. Extreme condition test - Excessive constant irrigation with non-saline and non-sodic Water

In this test, we apply an excessive constant irrigation rate. Nevertheless, precipitation is not included. The rate of the irrigation is 250 m^3/day, while the salinity of irrigation water is 1.5 dS/m and SAR level is 6.3. In these conditions, we expect an abrupt increase in the volumetric water content in the rootzone. Thereafter, an equilibrium should be achieved at the saturated water content. In Figure 6.5, the change in the volumetric water content of rootzone is illustrated. We can observe that excessive irrigation leads to a sudden increase and the water content reaches to saturation as we expected.

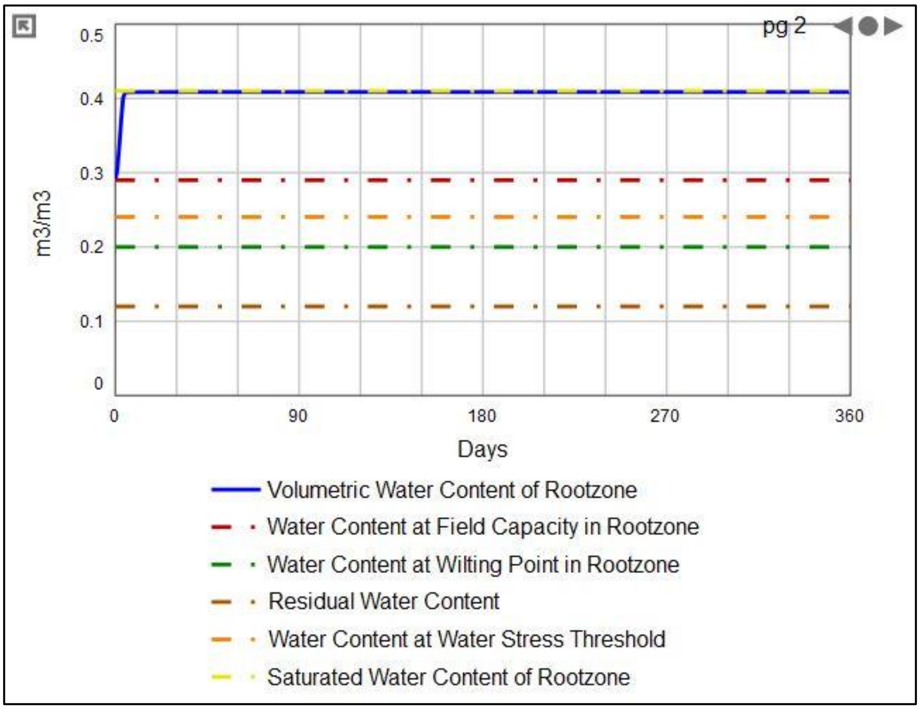

Figure 6.5: Extreme Condition Test 2: Volumetric Water Content.

Irrigation water quality parameters for salinity and sodicity are slightly above the initial conditions of the rootzone. Therefore, we expect a minor increase initially. Thereafter, a steady-state condition should be achieved for both salinity and sodicity parameters over time. In Figure 6.6, we observe the changes in the EC and SAR rates over time. On the left, Electrical Conductance of rootzone is depicted, while Sodium Adsorption Ratio of soil water in rootzone is illustrated on the left. Additionally, the salinity stress threshold is indicated with the horizontal dotted line. The changes in EC and SAR levels meets our expectations.

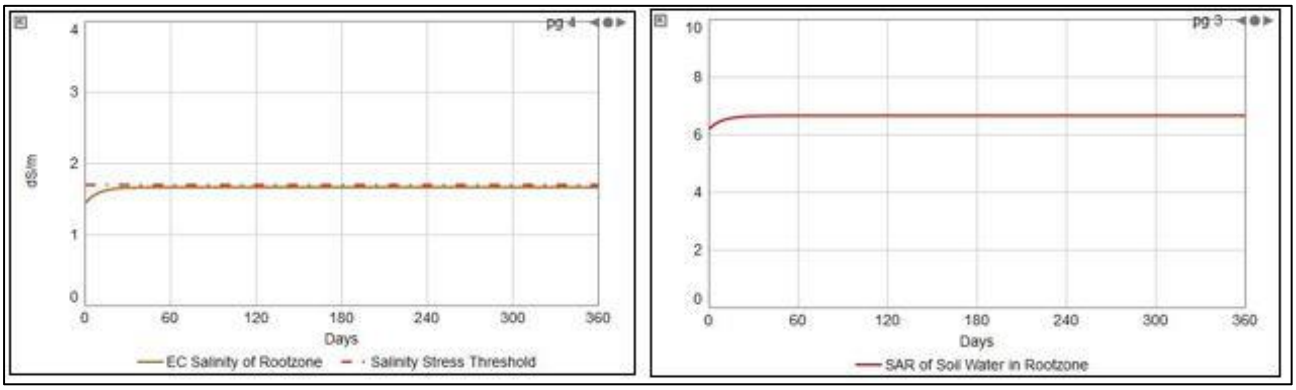

Figure 6.6. Extreme Condition Test 2: EC and SAR of Rootzone.

Based on these conditions, we anticipate that the crop should perform its' potential transpiration. Since excessive irrigation is applied, water is abundant in the rootzone and also there is stress source assumed other than water deficit and saline soil conditions. Furthermore, we can observe that volumetric water content never falls below the stress threshold in Figure 6.5. Likewise, we can notice that salinity rate reaches the salinity stress threshold, but never exceed it. Therefore, there is no stress condition which would inhibit the transpiration rate. In Figure 6.7, we can view that actual transpiration rate, which is depicted by the green line, behaves equal with the potential transpiration rate demonstrated by red dotted line.

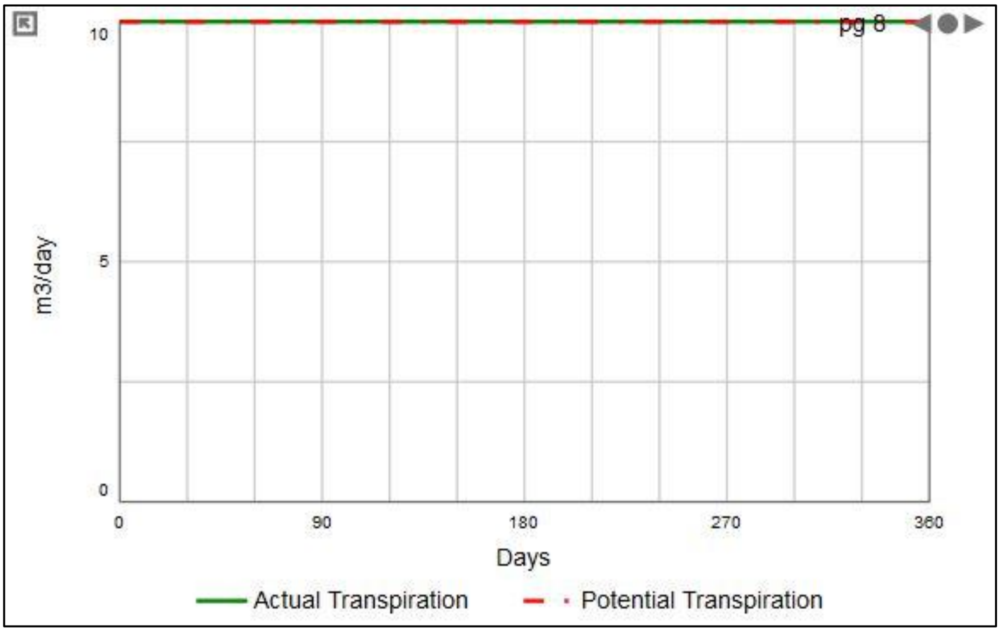

Figure 6.7. Extreme Condition Test 2: Transpiration.

Based on the SAR and EC levels illustrated in Figure 6.6, we do not expect any reduction in the hydraulic conductivity rate. Similar to the previous extreme condition test, soil sodicity level does not augment adequately, and/or, soil salinity is not too low to cause reduction in hydraulic conductivity. Thus, we observe that the percentage of reduction equals to zero as in Figure 6.8.

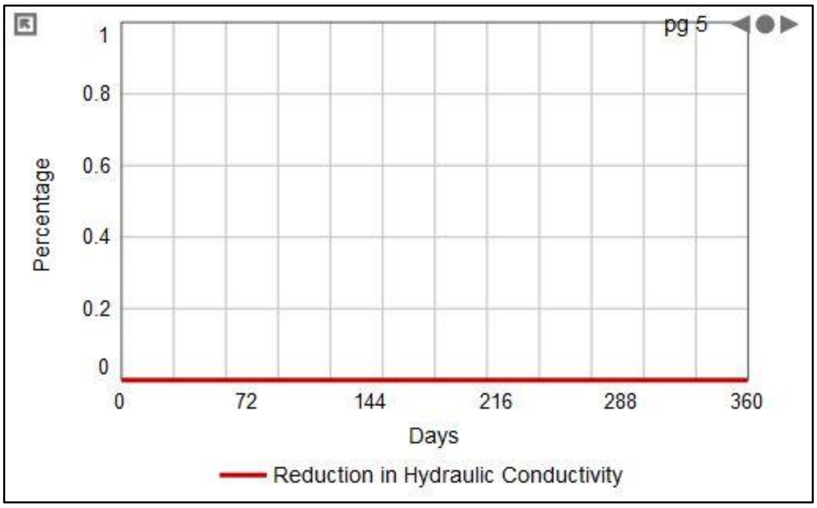

Figure 6.8. Extreme Test 2: Reduction in Hydraulic Conductivity.

6.1.3. Excessive irrigation water with sodic and saline water

In this extreme condition test, we apply excessive amount of irrigation water which has a high sodic and saline quality. The constant rate of irrigation water is 250 m^3/day. However, EC value equals to 6.5 dS/m while, the SAR value of irrigation water is 25. Precipitation is not included as a water inflow. As the water inflow is the same as previous extreme condition test, we expect the same behavior in water content of the rootzone. The abrupt increase and steady state condition at saturated water content is observed in volumetric water content of rootzone as depicted in Figure 6.9. Therefore, we can state that our expectation is satisfied.

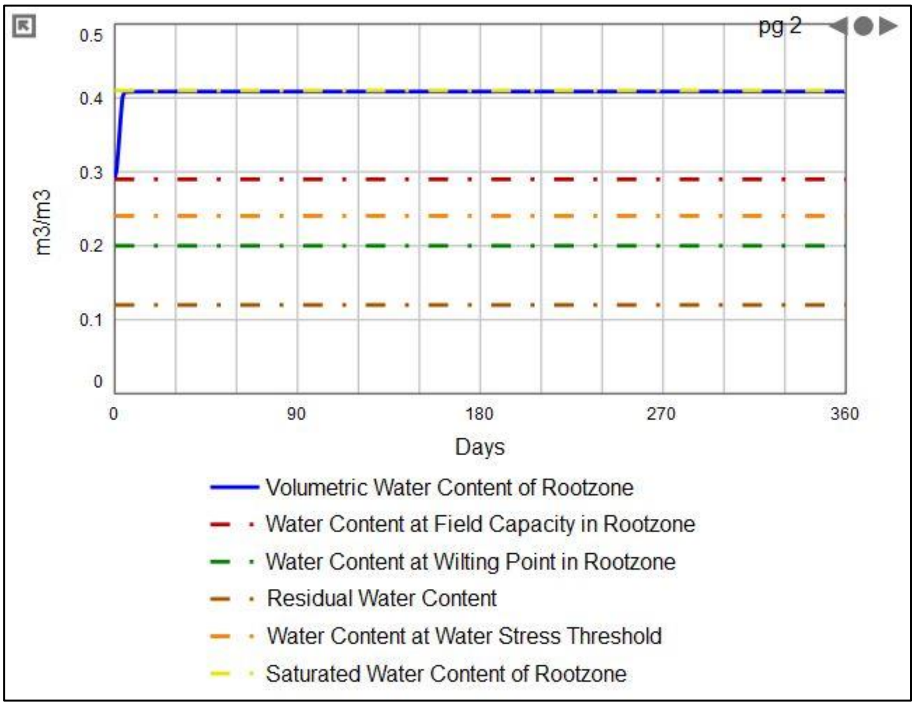

Figure 6.9. Extreme Condition Test 3: Volumetric Water Content of Rootzone.

On the other hand, irrigation water has high saline and sodic characteristic. The EC and SAR value of irrigation water are well above the initial conditions of soil water in rootzone. Therefore, an increase should be achieved in both parameters in the beginning of the time horizon. Since the saline and sodic irrigation water continuously flow across the soil profile, equilibrium should be achieved over time, close to the irrigation water quality in both EC and SAR values of rootzone. In Figure 6.10, EC and SAR values of rootzone are illustrated. On the left, EC value of rootzone is depicted, while on the right SAR value of rootzone is indicated. We can view that both parameters initially augment and afterwards stabilize around the values which irrigation water quality also has. Therefore, the results for these parameters match with our expectation.

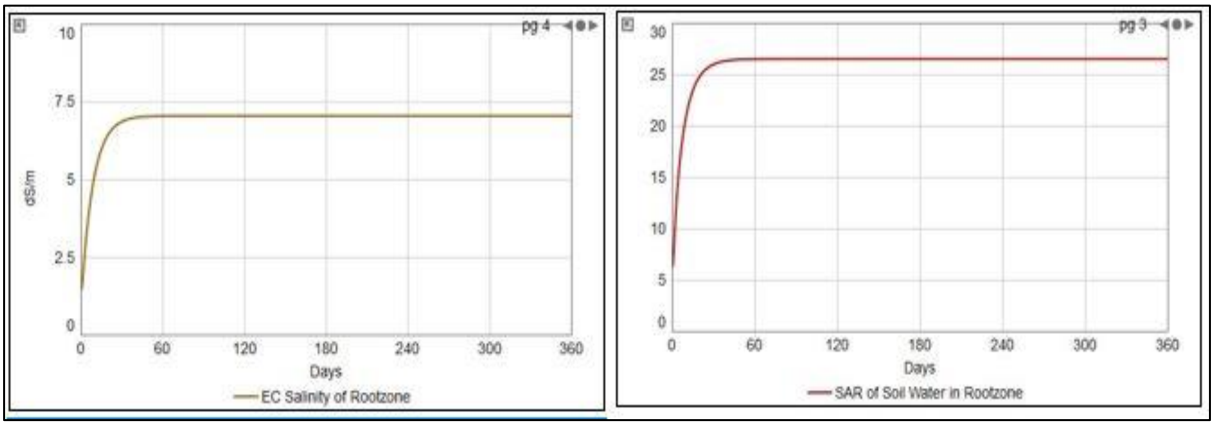

Figure 6.10. Extreme Condition Test 3: EC and SAR values of Rootzone.

Furthermore, in Figure 6.10 we can observe that the soil salinity condition augments and stays in a value which is much higher than salinity stress threshold. Therefore, we expect that plant water uptake should be negatively impacted by the high soil salinity rate. In Figure 6.11, we can monitor that the actual transpiration rate falls quite below the potential transpiration rate as it is anticipated.

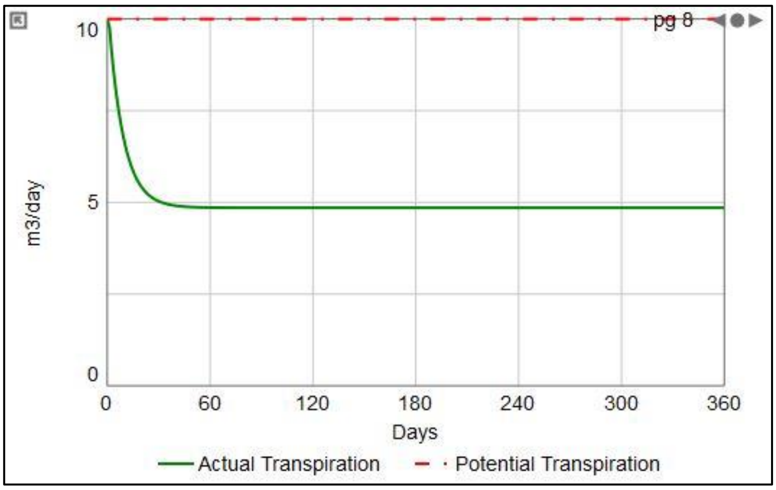

Figure 6.11. Extreme Condition Test 3: Transpiration.

On the other hand, we may also presume that hydraulic conductivity is to be influenced negatively due to the high SAR values of rootzone which indicates increased soil sodicity conditions. Similar to the pattern of SAR and EC parameters of rootzone, reduction in hydraulic conductivity is expected to rise initially and thereafter, should achieve the steady-state condition. In Figure 6.12, we can see that the percentage of reduction in hydraulic conductivity augments initially and then stabilizes.

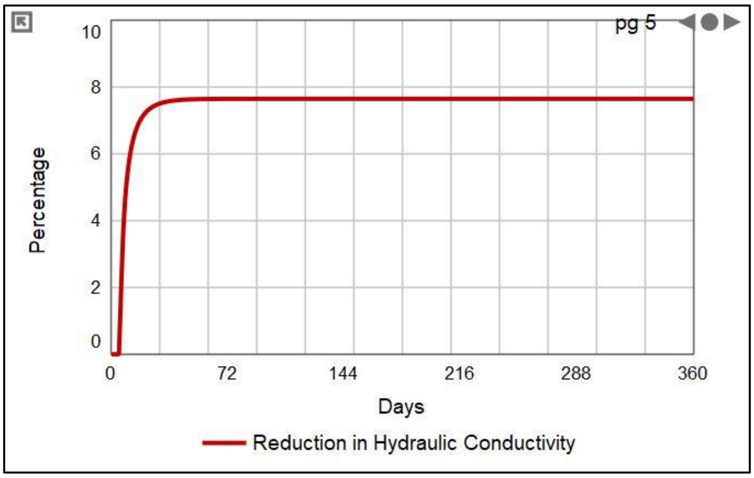

Figure 6.12. Extreme Condition Test 3: Reduction in Hydraulic Conductivity.

6.2. Behavior Sensitivity Tests

We carried out two different sensitivity analysis tests to assess behavior sensitivity of the model. Firstly, we tested to what extent the hydraulic model is sensitive to different soil properties. We applied the same irrigation water quantity and quality to three different soil type. Thereafter, we investigated the impact of change in irrigation water quality on reduction in hydraulic conductivity and actual transpiration.

6.2.1. Behavior sensitivity of hydraulic model to different soil types

In this test, we run three simulations with three different soil types. The first simulation run is done with the properties of clay loam soil, then the soil properties represent sandy clay loam and sandy loam, respectively. The parameters for this soil types are acquired from the literature (Clapp & Hornberger, 1978). In these simulation runs; initial value of volumetric water content is 0.3 m3/m3, and irrigation rate is 75 m3/day. Irrigation water quality corresponds to a non-sodic and non-saline characteristic with 1.5 EC (dS/m), and 6.3 SAR values. Therefore, three different soil types are tested with the same irrigation water quantity and quality. As each soil type has different hydraulic conductivity rate and water retention characteristics, we expect that each should reach a steady-state conditions with different volumetric water levels. In Figure 6.13, we observe the change in volumetric water content and percolation rate over time for different simulation runs, and different soil types as well. As the sandy loam is the most permeable one within these soil types, we expect that initially percolation rate should be highest for this soil type and the equilibrium for volumetric water content should be at the lowest level. On the contrary, clay loam is the less conductive one. Therefore, we expect that initial percolation rate should be the lowest for this soil type and the equilibrium for volumetric water content should be reached at higher level than others.

In Figure 6.13, we can view that the steady state condition for volumetric water content is at the highest level for clay loam soil and at the lowest level for sandy loam, as it is anticipated.

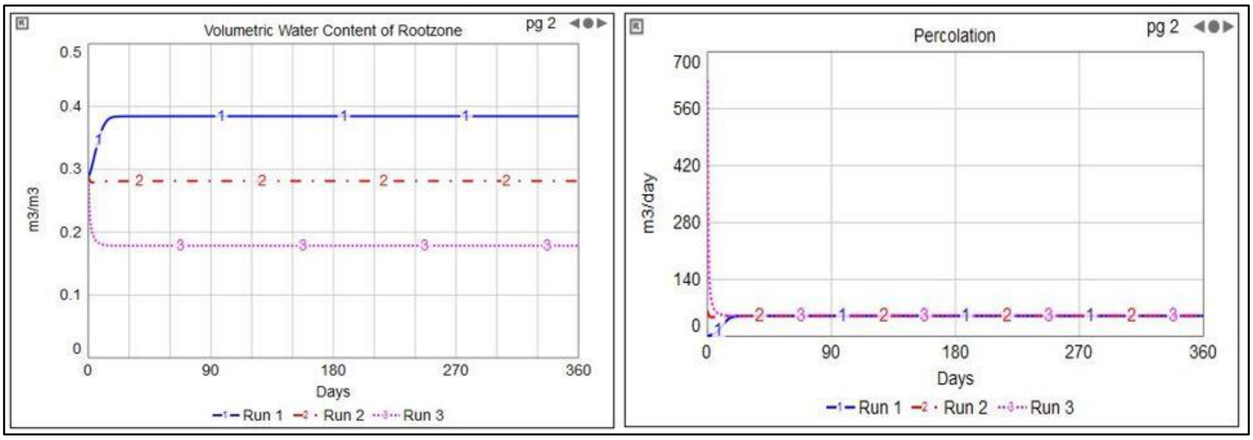

Figure 6.13. Sensitivity Test 1: Volumetric Water Content and Percolation.

6.2.2. Behavior sensitivity of transpiration and reduction in hydraulic conductivity to different irrigation water qualities

In this test, we investigated the sensitivity of reduction in hydraulic conductivity and actual transpiration rate to different irrigation water qualities. In this regard, we performed three different simulation runs with three different irrigation waters. The first simulation is run with non-sodic and non-saline water which has 0.3 EC (dS/m) and 3 SAR values. The second simulation is carried out with sodic and slightly saline water whose parameters corresponds to 3 EC (dS/m) and, 22 SAR values. Plus, the last simulation run is conducted with highly sodic and saline water which has 8 EC (dS/m) and, 30 SAR values. Irrigation water rate is 75 m^3/day for all simulation runs.

Table 6.2. Irrigation Water Qualities for Sensitivity Test Runs.

	EC	SAR
RUN 1	0.3	3
RUN 2	3	22
RUN 3	8	30

Based on these conditions, we expect that EC and SAR values of rootzone should diminish as irrigation water quality has lower values for these parameters than initial conditions of rootzone in the first run. On the other hand, in the second and third simulation runs, EC and SAR values of rootzone should increase since the irrigation water quality has higher saline and sodic characteristics than initial condition of the rootzone. Nevertheless, the equilibrium in both parameters should be higher in the third simulation runs since the EC and SAR values are the highest in irrigation water for this run. In Figure 6.14, we can view the changes in the EC and SAR values of rootzone over time for three simulation runs. We can state that changes in these parameters occurs parallel to our expectations.

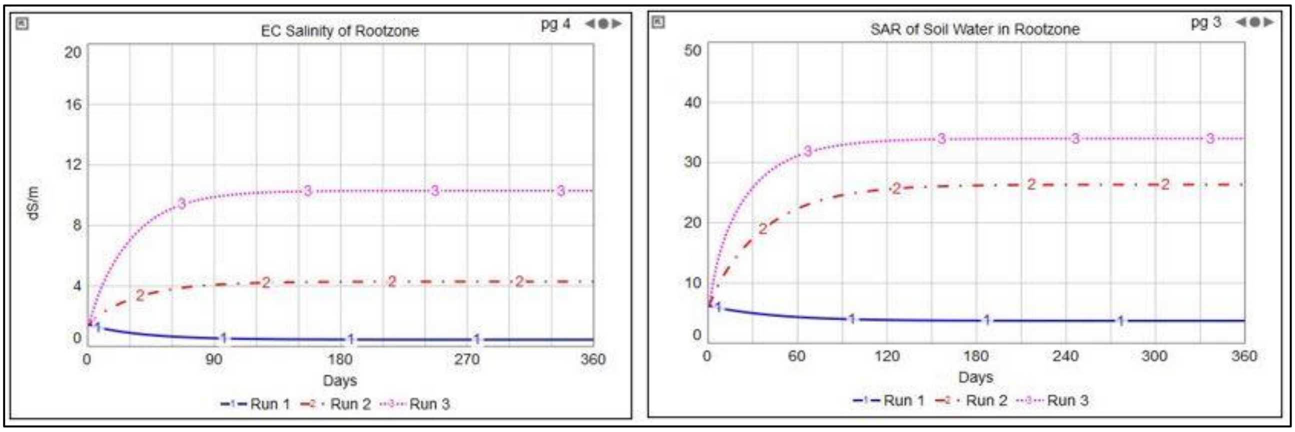

Figure 6.14. Sensitivity Test 2: EC and SAR of Rootzone.

Upon these different equilibrium conditions in rootzone, actual transpiration rate and reduction in hydraulic conductivity percentage are influenced variably. Three simulation runs were performed with 0.3, 3 and 8 EC (dS/m) respectively. The outcome on the rootzone salinity conditions of these irrigation qualities is depicted in Figure 6.14. Accordingly, we expect that the extent of the transpiration is to be negatively impacted in that order as well. In Figure 6.15 the actual transpiration rate is illustrated for three simulation runs on the left side. Based on these results, we can observe that actual transpiration rate is sensitive to the irrigation water quality as it is negatively impacted by highly saline water in the third run.

On the other hand, the sensitivity of reduction in hydraulic conductivity to the quality of irrigation water is more complicated than other comparisons for sensitivity tests. Reduction in hydraulic conductivity is increased parallel to the rise in parameters which express soil sodicity, ESP and SAR values respectively. However, an augmentation in soil salinity conditions ameliorates the hazardous impact of sodic conditions and diminishes the percentage of reduction in hydraulic conductivity. In addition to these, regardless of soil sodicity level, too low rates of soil salinity further reduce hydraulic conductivity (Weil & Brady, 2016). Therefore, we investigate the sensitivity of reduction in hydraulic conductivity parameter to various irrigation qualities. In the first run, we apply a non-saline and non-sodic irrigation water. Afterwards, a slightly saline and sodic water is applied. Lastly, saline and, highly sodic is applied, in the third run.

The sensitivity analysis for different irrigation water qualities to reduction in hydraulic conductivity is depicted in Figure 6.15, on the right side. We can observe the changes in the reduction in hydraulic conductivity parameter over time. Accordingly, we can state that hydraulic conductivity is highly sensitive to low salinity conditions. Besides, we can also observe that sodic and slightly saline water also significantly impact hydraulic conductivity. Nevertheless, the third simulation run indicates that reduction in hydraulic conductivity can be improved to certain extent as higher saline conditions are achieved.

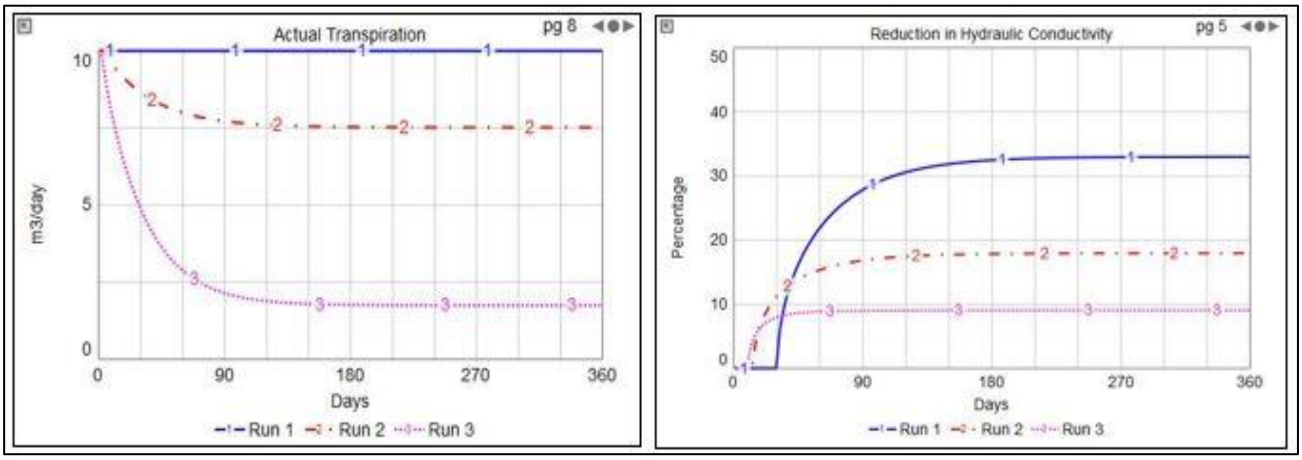

Figure 6.15. Sensitivity Test 2: Transpiration and Reduction in Hydraulic Conductivity.

6.3. Behavior Pattern Test

After having built sufficient confidence in structural validity of the model through previous tests, we apply a test to examine the behavioral pattern validity of the model. Nevertheless, we do not possess any recorded historical data to compare our outputs with measured results in real conditions.

Furthermore, the availability of such data which would represent changes in at least soil salinity and sodicity parameters over time, requires continuous field or experimental measurements. Therefore, we can state that it is not easy to acquire these data records. Consequently, we choose to compare our results with another robust model, Hydrus 1-D, that represents hydraulic and solute transport processes within the soil profile.

Hydrus 1-D is employed by many studies which is capable of accounting water movement and solute transport in soil profile accurately particularly with small spatial and temporal resolution. It also depicts the daily transpiration rate which can be impacted by water and salt stress. However, as mentioned earlier, this model is not convenient for representing long-term processes which comprise variances in crop rotations, and also for fast simulation purposes. Within this scope, we compare the outputs of our model with Hydrus 1-D under the same conditions.

In the simulation run for comparing two models, soil type is assigned as clay loam. Initial conditions for water content, soil salinity and, soil sodicity levels are set as equals. The potential evaporation and transpiration are given as constant rates along the simulation run. The potential evaporation rate equals to 15 m^3/day while potential transpiration corresponds to 10 m^3/day. The same irrigation regime is applied into both models with constant irrigation quality. The irrigation regime signifies three different conditions to test and reflect different behaviors of models in equal time intervals during the simulation. The salinity level of the irrigation water is 1.5 EC (dS/m), and the SAR value of irrigation water set as 6.3.

In these conditions, we observe the changes in volumetric water content, electrical conductivity, sodium adsorption ratio, and actual transpiration rate (root water uptake) over time for both models. In the figures presented below, we can compare the outputs of two models. The outputs of our model are illustrated on the left-hand side of the figures, while Hydrus 1-D outputs are depicted on the right side. We generate the outputs of our model for one representative point through which it is aimed to describe the average conditions of the rootzone. On the other hand, we illustrate the outputs of Hydrus 1-D model generated with three different observation nodes as the model is capable of accounting small spatial differences. The positions for the representative point of our model and for the observation nodes of Hydrus model in the soil profile are demonstrated in Figure 6.16.

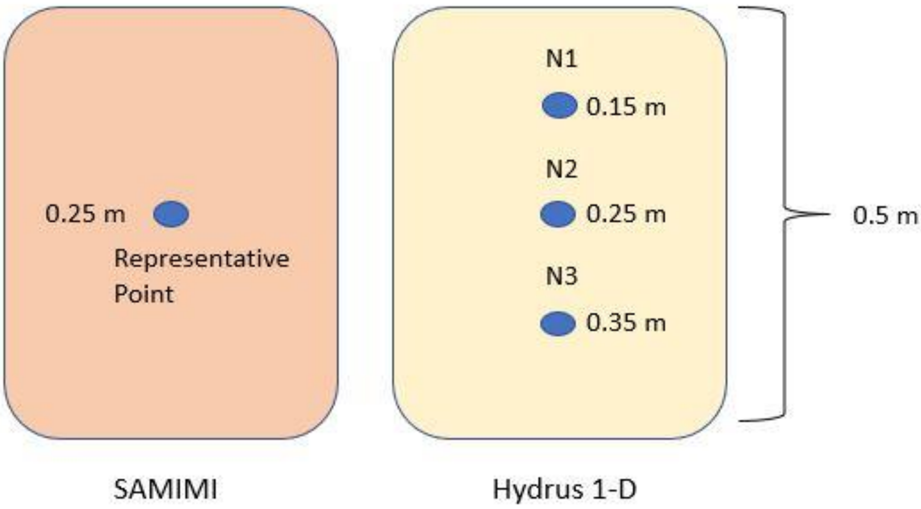

Figure 6.16. Behavior Pattern Test: Observation Points.

Based on these conditions, we applied an irrigation regime with varying rates over time. In the first 120 days, we apply a constant rate of 50 m^3/day, which corresponds to 0.5 cm/day for Hydrus model. Thereafter, we do not apply any water for the next 120 days. In last 120 days of the simulation, we apply 200 m^3/day for 5 days in 40 days of intervals. The irrigation regime is illustrated in Figure 6.17 below.

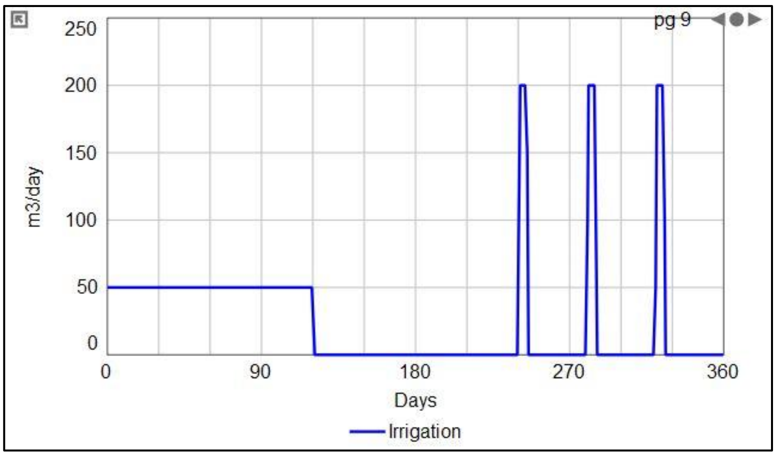

Figure 6.17. Behavior Pattern Test: Applied Irrigation Regime.

Considering the applied irrigation regime, we expect that the volumetric water content to increase and stabilize during the first 120 days. On the other hand, this parameter should diminish during the second 120 days as no water inflow is provided to rootzone. The irrigation application in the last 120 days is supposed to create three peaks, each corresponding to the time irrigation is applied. Figure 6.18 shows the change in volumetric water contents for both models over time. We can view that model behaviors match in pattern and satisfy our expectation.

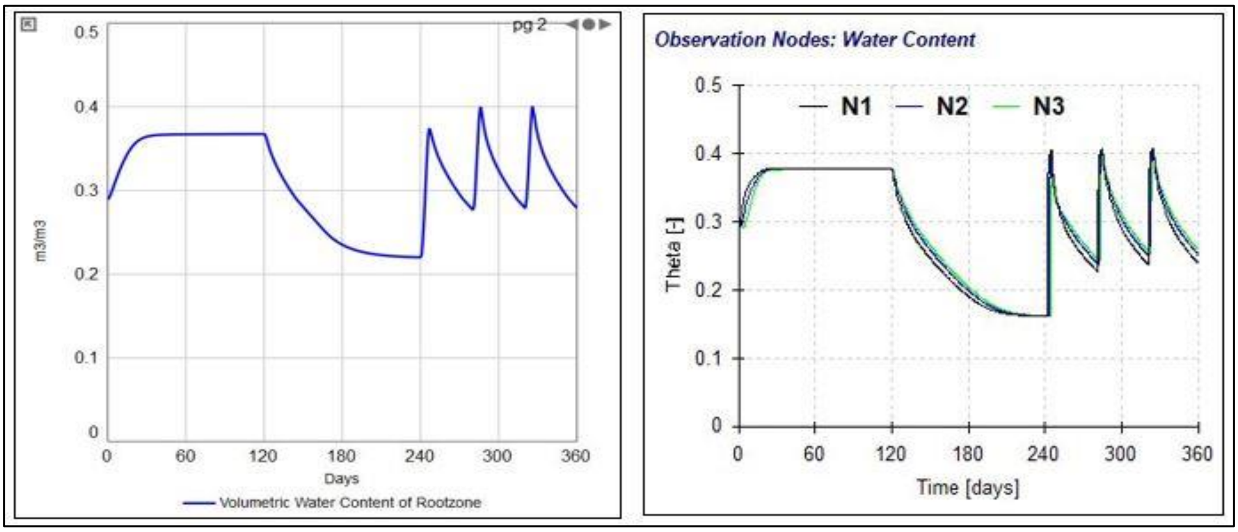

Figure 6.18. Behavior Pattern Test: Volumetric Water Content.

On the other hand, dissolved salt minerals are introduced into the rootzone via irrigation. In these conditions, we expect that EC rates should increase during the first 120 days of simulation as constant irrigation rate bring dissolved salts. In the following 120 days, a further increase in soil salinity rate is expected. The water content is mainly depleted by evaporation and transpiration flows, leaving the dissolved salt minerals in rootzone. However, during the last 120 days of simulation, a fluctuation in the salinity level of rootzone should take place. This fluctuation arises from the introducing more dissolved salts into rootzone which would increase the soil salinity as well as the leaching of the salt minerals from rootzone towards deeper soil layers which leads to reductions in the soil salinity rate. Accordingly, we can observe the changes in soil salinity rates of both models over time in Figure 6.19. In this figure, we can observe that soil salinity increases during the first 120 days in both models. We should note that the magnitude of the increase in soil salinity is also the same during the first 120 days. After then, another increase can be observed parallel to our anticipation. However, the magnitude of the increase slightly differs between the two models. After all, we can view the fluctuations take place in both models as expected. Nonetheless, during the last 120 days we can see that soil salinity levels differ in Hydrus 1-D model based on the depths of the observation nodes. Along with that, we can state that our model is capable of representing the average conditions in rootzone for soil salinity measurements.

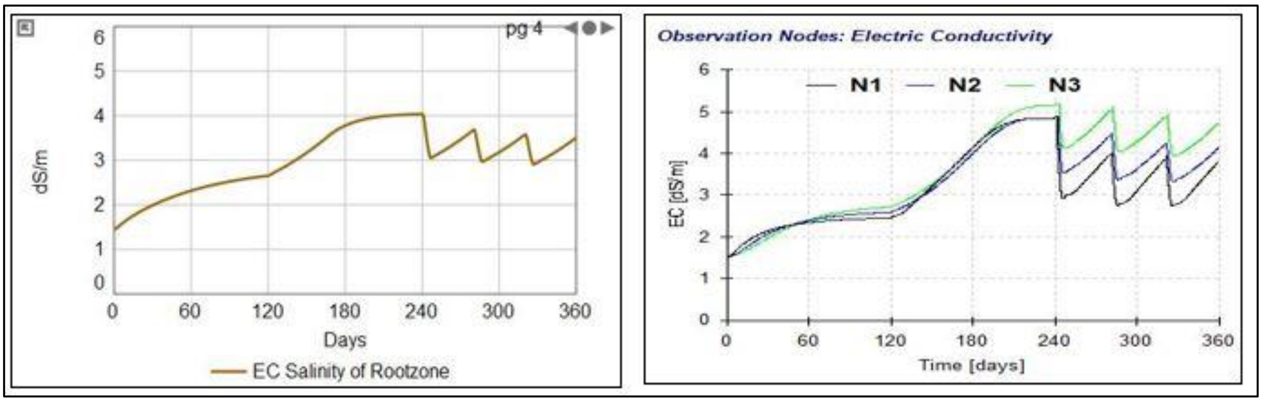

Figure 6.19. Behavior Pattern Test: EC Salinity of Rootzone.

Furthermore, the change in the concentrations of dissolved salt minerals may bring alterations in the soil sodicity levels. Parallel to the above-mentioned patterns of soil salinity conditions, we expect increases and fluctuations in the SAR value of both models over time. As the irrigation water introduces dissolved cations into the rootzone we observe a similar increase pattern in both models in Figure 6.20. Thereafter, we view a further increase in SAR values during the second 120 days of the simulation run where no irrigation applied but the soil salinity increased. Although the behavior of the pattern is like each other, we can see that Hydrus illustrates a bigger increase compared to our model. Furthermore, the SAR values of both models fluctuates three times during the last 120 days depending on the irrigation application. In overall, we can state that the calculation of our model for soil sodicity, represented by SAR value here, indicates a sufficient similarity to the outputs of Hydrus 1-D.

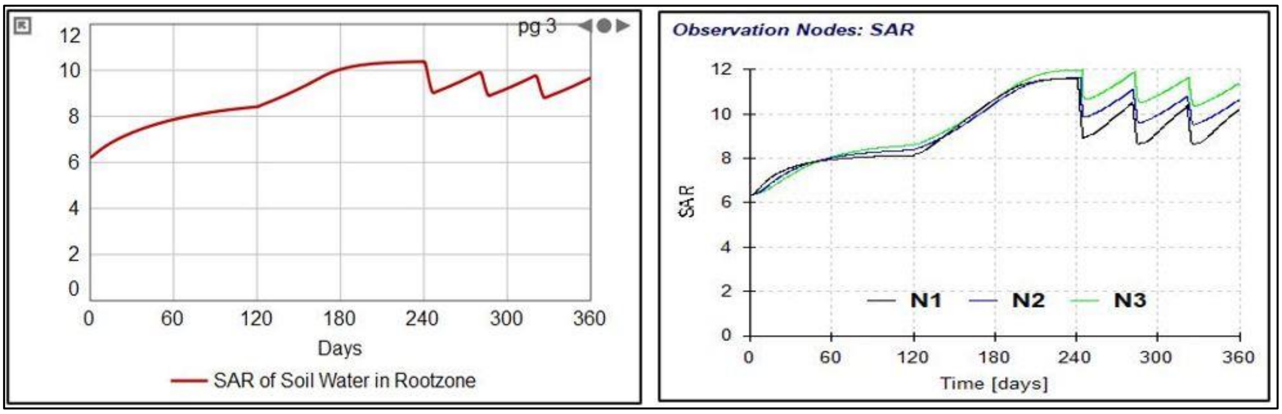

Figure 6.20. Behavior Pattern Test: SAR of Soil Water in Rootzone.

Based on the changes in the volumetric water content and salinity rates in rootzone, we can see to what extent the crop can perform its potential transpiration rate. We anticipate that crop may slightly experience a stress during the first 120 days, since hypothetical crop, maize, is quite sensitive to salinity concentration. However, the actual transpiration rate should definitely diminish during the second 120 days of the simulation run as volumetric water content sharply decreases along with the increase in the soil salinity. In addition to these, crop can experience stress during the last 120 days due to increases in soil salinity and periodic water deficiencies due to fluctuations. Nevertheless, we expect that crop should be able to uptake more water than previous sequence. In Figure 6.21, we can view the daily transpiration rates generated by both models separately. We can state that both models meet our expectations to a large extent. However, we should note that there is a difference during the first 120 days as our model indicates a slight reduction in actual transpiration while in Hydrus model it can perform its potential.

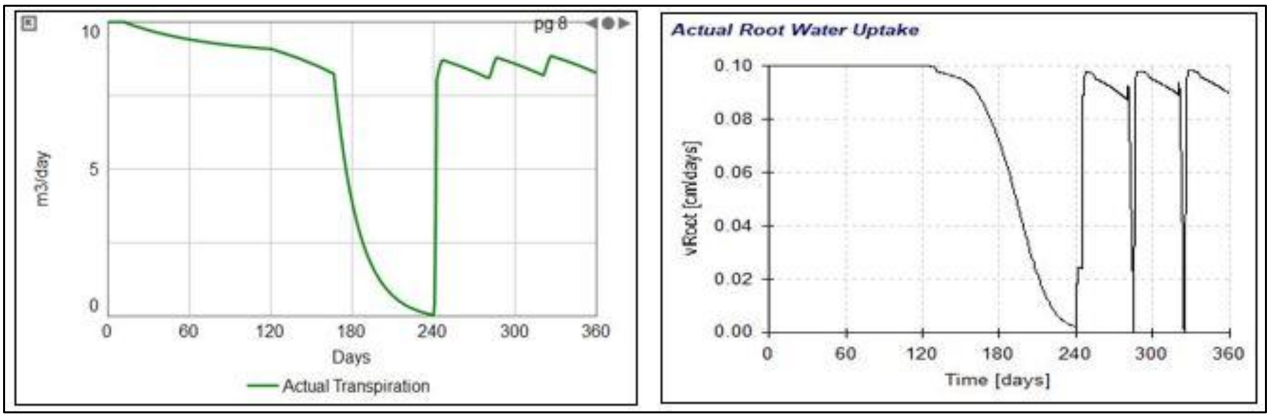

Figure 6.21. Behavior Pattern Test: Transpiration.

6.4. Reference Model Behavior

The reference behavior of the model is presented in this section. Apart from the previous validation tests, the model simulated with parameters which represent field conditions. The simulation time horizon set as 10950 days, i.e., 30 years. The precipitation regime is adapted to represent RCP 2.6 climate pathway. Therefore, we avoid any reduction on the precipitation rate due to climate change scenarios for better representing the reference model behavior. The reference evapotranspiration rate demonstrates the field conditions of Konya, Karapınar. Furthermore, the crop type is set as corn throughout the simulation duration. Therefore, the seasonal dynamics on the reference evapotranspiration and transpiration rates are implemented. Irrigation water quantity is introduced with the sprinkler method. The crop does not experience any stress due to water deficit during the growth season. In this simulation run, irrigation water quality is non-saline and non-sodic, which corresponds to 0.75 dS/m EC, and 1.5 SAR values. The initial conditions for soil salinity and sodicity are the similar to previous tests, 1.5 dS/m and 6.3 SAR value respectively. Under these conditions, we demonstrate the change in the relative soil moisture, soil salinity and sodicity rates, along with the seasonal crop yield loss predictions, and the percentage of reduction on the hydraulic conductivity over time.

In the Figure 6.22 below, the change in relative soil moisture is illustrated with respect to field capacity, water stress threshold, wilting point, and residual water content. We can observe that the relative soil moisture, which indicates level of soil saturation, fluctuates between water stress threshold and saturation level.

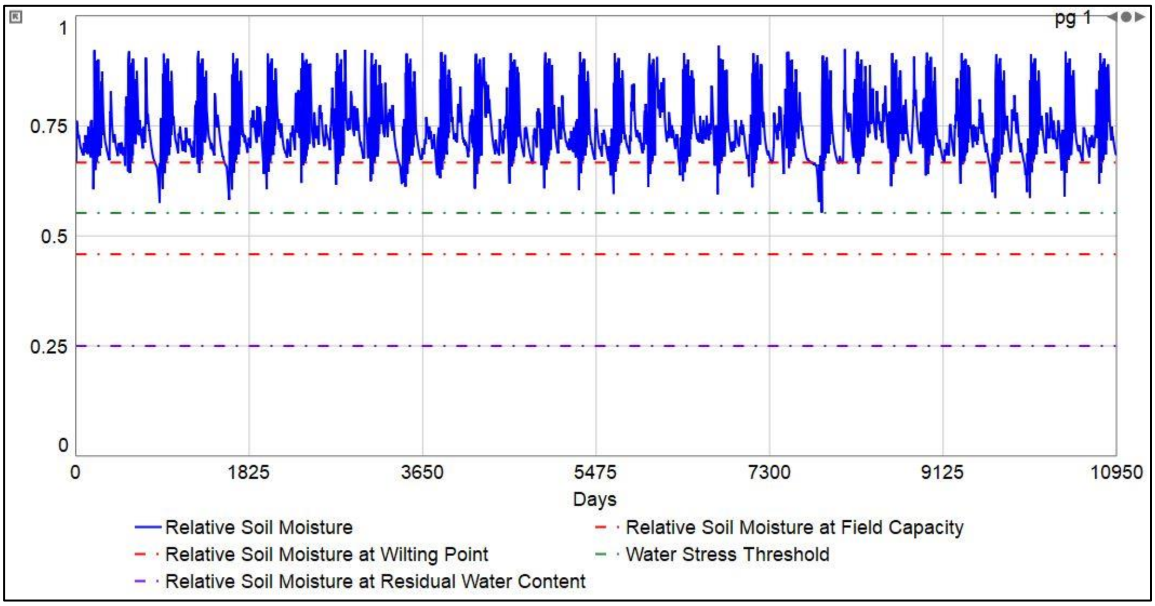

Figure 6.22. Reference Model Behavior of Relative Soil Moisture.

In the Figure 6.23, the change in soil salinity is demonstrated. We can view that soil salinity level fluctuates over time. As the salt minerals are introduced into soil via irrigation water during the crop growth season when evapotranspiration rate is high, while the precipitation level is low. However, after the crop growth season evapotranspiration rate reduces and also, precipitation generally occurs during the winter period. Accordingly, the salt minerals in the rootzone are leached away after the crop growth season. Therefore, the fluctuation in the soil salinity rate takes place based on these dynamics over time.

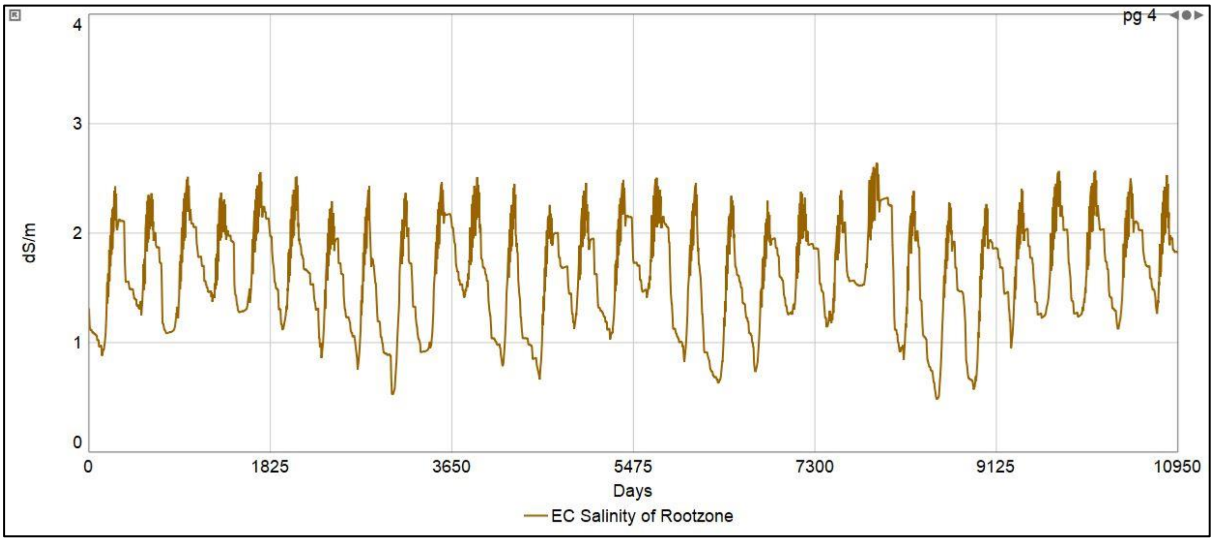

Figure 6.23. Reference Model Behavior of Soil Salinity.

The change in soil sodicity is depicted in the Figure 6.24. The low value of SAR leads to a decrease in sodicity conditions of rootzone initially. However, following the initial reduction, a parallel fluctuation is observed in SAR value over time. These parallel patterns stem from the similar rates of increase in both cations concentration cause an augmentation in SAR value, during the growth season where evapotranspiration rate is quite higher than precipitation as in the first extreme test case. Likewise, after the crop growth season, the dissolved cations are leached down from rootzone to deep layers due to precipitation. Therefore, the similar rates of decrease in both cations' concentrations drives the SAR to lower values.

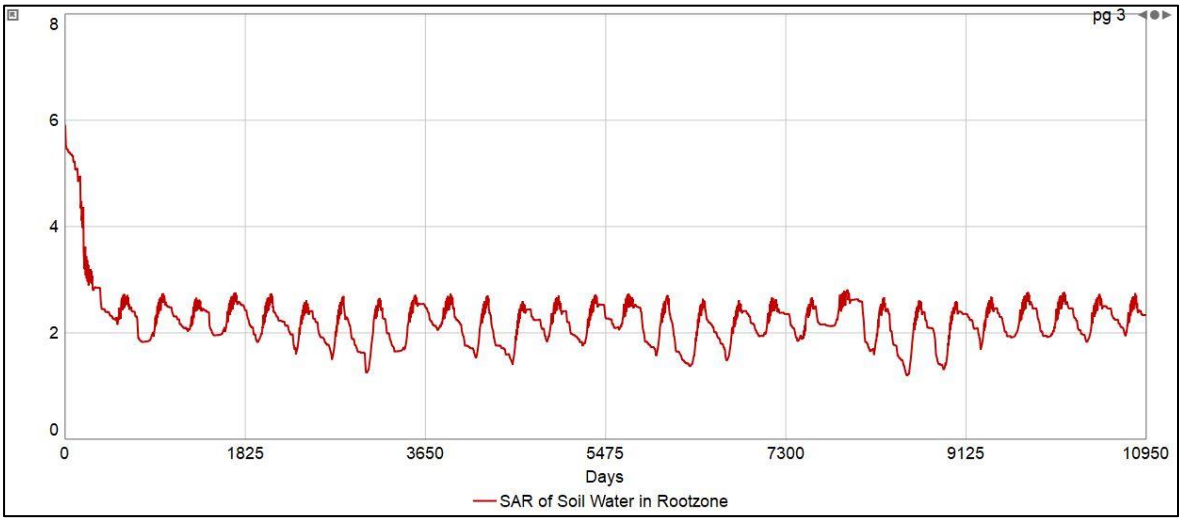

Figure 6.24. Reference Behavior of Soil Sodicity.

The percentages for seasonal loss on crop yield are illustrated in Figure 6.25. The separate minor curves arise each season which indicate that the reduction percentage for obtained yield with respect to the maximum possible yield. However, we should note that crop yield loss percentage is calculated through the comparison of daily actual transpiration rate and the potential transpiration. Therefore, we assess the last value of the curve that points out the level of crop yield loss at the end of the season. Since the corn is a quite sensitive crop type to the soil salinity, we can observe minor losses on the yield on these conditions.

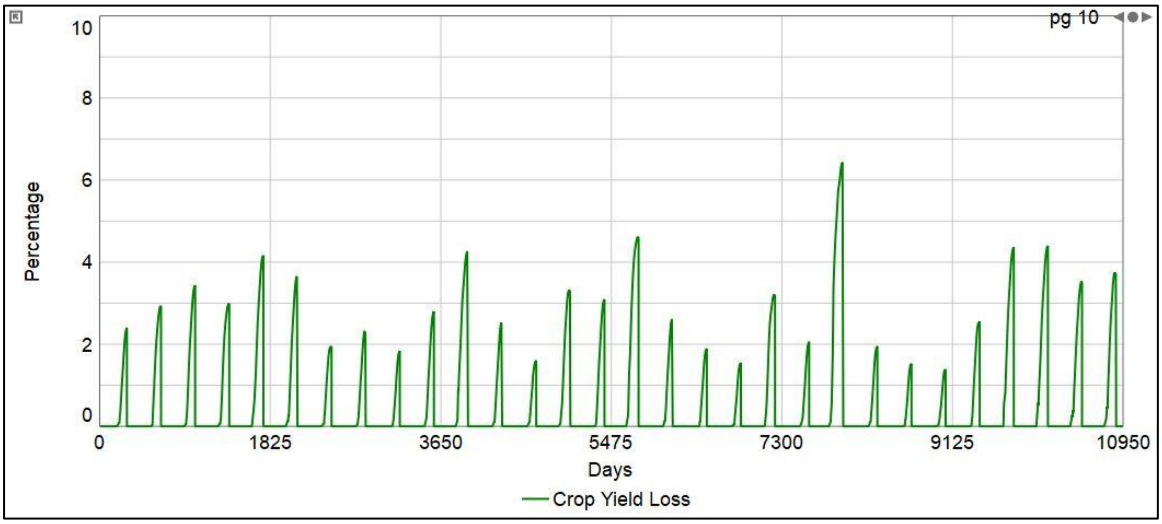

Figure 6.25. Reference Model Behavior: Crop Yield Loss.

In the Figure 6.26, the reduction on hydraulic conductivity through the simulation duration is illustrated. As the irrigation water has a non-sodic characteristic, we do not observe reductions based on soil sodicity. However, as the soil salinity reaches quite low values during the fluctuation, we can view the temporal reductions based on low soil saline conditions.

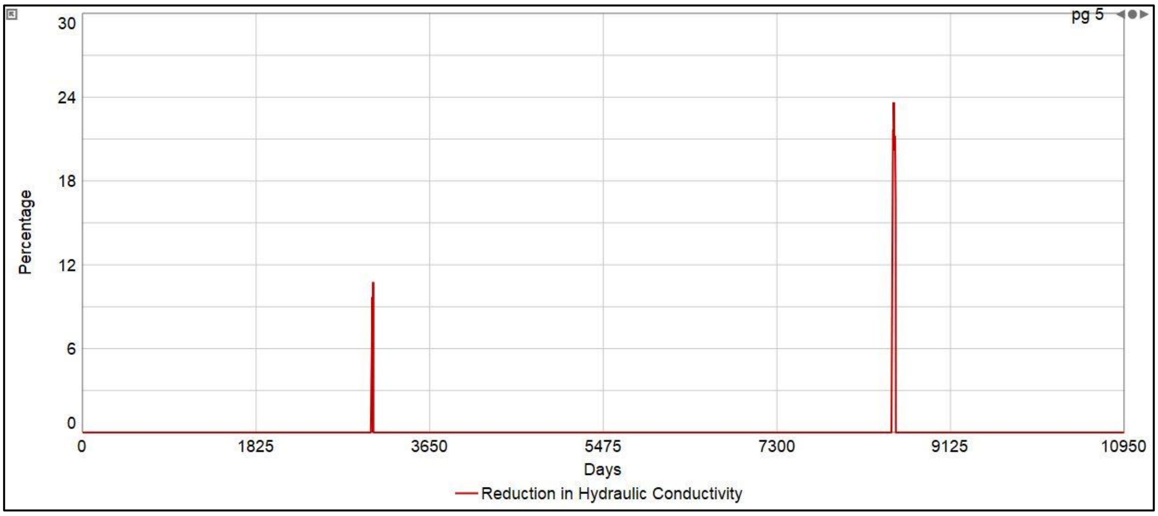

Figure 6.26. Reference Model Behavior: Reduction in Hydraulic Conductivity.

7. SCENARIO RESULTS

Scenario analyses are performed with various hypothetical scenarios to grasp the important dynamics in the complex nature of salt-related problems in farmlands. In this way, we perform different simulation experiments with various irrigation water quality, irrigation method, crop rotations and precipitation regimes to assess their potential impact on soil salinization processes. In these scenarios, the field conditions of Karapınar in Konya Plain are aimed to be represented. The soil specific parameters employed in the hydraulic model are set based on the soil column experiment studies performed by our colleagues in a scientific research project funded by TUBITAK (Project no: 118Y343). All employed parameters are listed in Appendix. The climate related parameters, evapotranspiration, and precipitation are parametrized based on the Karapınar conditions (TAGEM and DSI, 2017).

Furthermore, in the scenarios we employ two different crop rotations of four subsequent growing seasons which are set regarding widely planted crop types in the irrigated areas in the region. The first crop rotation includes corn, sugar beet, sunflower, and potato accordingly. The second one contains corn, wheat, sugar beet and wheat. Therefore, each crop rotation comprises various crop types and lasts for four years. The crop rotations repeat itself along the simulation duration. In addition to that, the applied water amount differs between irrigation methods. The sprinkler irrigation introduces more water than the drip as it is expressed in model description section.

On the other hand, we input two different irrigation water quality characteristics which are set hypothetically as the water quality can highly vary from one well to another across the plain. One type of irrigation water quality corresponds to the non-saline and non-sodic characteristics while the second type indicates a slightly saline and slightly sodic water.

In the Table 7.1, the details of scenario analyses are depicted categorically. In the first case, precipitation regime represents the RCP 4.5 climate pathway. The first crop rotation is applied in this simulation run. The irrigation is applied via sprinkler method while the quality of the water is non-saline and non-sodic. The second scenario analysis is run with the same crop rotation, irrigation method and water quality with the first one. However, the second scenario is simulated with the precipitation regime which bases on RCP 8.5 scenario. On the other hand, the third scenario is run with slightly saline and slightly sodic water while precipitation regime corresponds to RCP 8.5 pathway. Furthermore, the crop rotation and the irrigation method are the same as previous scenarios.

Besides, in the fourth scenario analysis the precipitation regime is set based on RCP 8.5 and the first crop rotation is applied for this case as well. The irrigation water is applied via drip method water which has slightly saline and slightly sodic quality. The fifth scenario analysis is performed under the precipitation regime base on RCP 8.5. The slightly saline and slightly sodic water is applied like the previous scenario. Nevertheless, crop rotation is altered in the scenario, which indicates the second type of rotation.

Table 7.1. Scenario Analysis Characteristics.

	Precipitation Regime	*Crop Rotation*	*Irrigation Method*	*Irrigation Water Quality*
Scenario Analysis 1	RCP 4.5	1	Sprinkler	EC=0.5 SAR=6
Scenario Analysis 2	RCP 8.5	1	Sprinkler	EC=0.5 SAR=6
Scenario Analysis 3	RCP 8.5	1	Sprinkler	EC=1.5 SAR=10
Scenario Analysis 4	RCP 8.5	1	Drip	EC=1.5 SAR=10
Scenario Analysis 5	RCP 8.5	2	Drip	EC=1.5 SAR=10

7.1. Scenario Analysis 1

The outputs for the first scenario analysis are presented below. Firstly, we observe the change in the saturation level of the water demonstrated by the relative soil moisture variable, in Figure 7.1. Accordingly, we can view that moisture level in the rootzone highly fluctuates over time which is caused by the daily precipitation and irrigation rates that can take various values based on the seasonal differences.

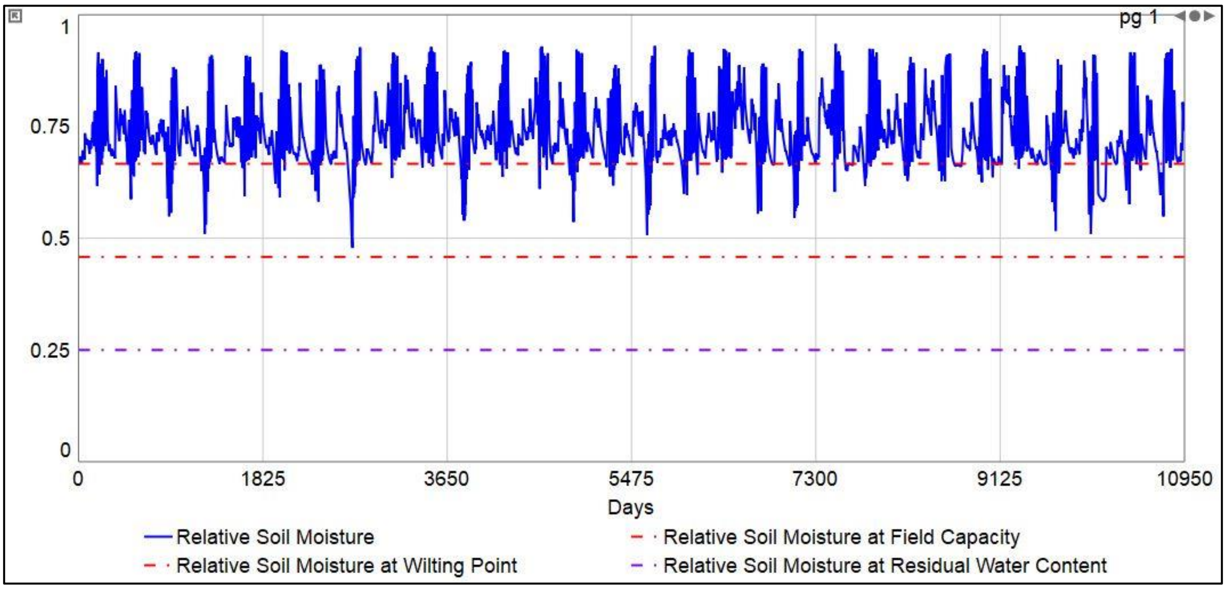

Figure 7.1. Scenario Analysis 1: Relative Soil Moisture.

On the other hand, the changes in the soil salinity are illustrated in the Figure 7.2. The fluctuations based on the seasonal changes in precipitation and evapotranspiration rates can be well observed in the figure. As the irrigation water has a non-saline characteristic, we do not monitor major increases in the salinity rate over time. The soil salinity rate generally takes value between 0.75 and 2 dS/m. Yet, we can view that it can take lower values for multiple times and also reach up to 2.5 dS/m for one time. We can state that there is not a major change over the 30 years of simulation duration.

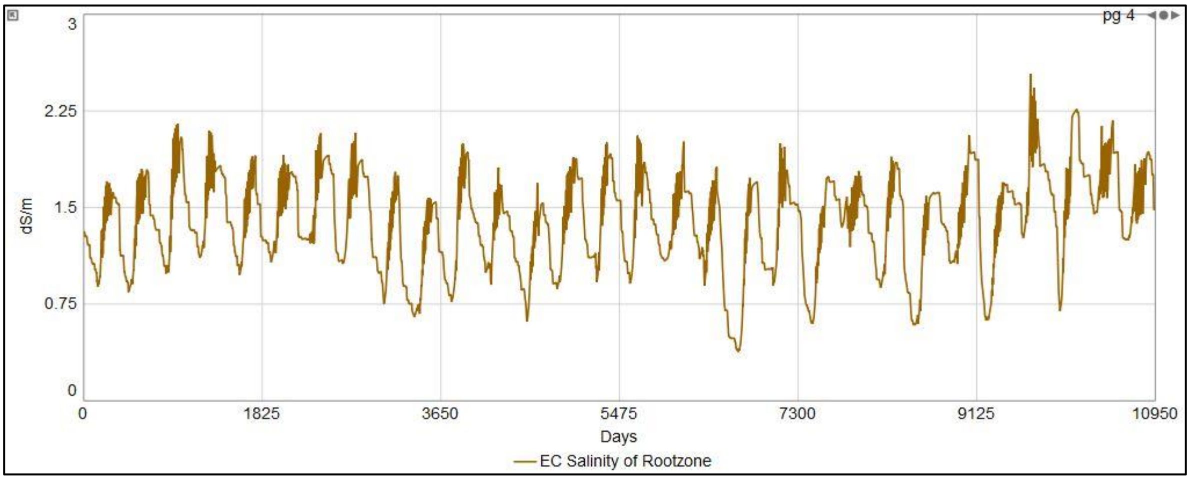

Figure 7.2. Scenario Case 1: EC Salinity of Rootzone.

The result for sodicity level of soil water in rootzone is depicted in Figure 7.3. Similar to the changes in the soil salinity rate, we can view that SAR value also indicates a fluctuation over time which depends on the seasonal changes in the concentrations in the salt minerals in the rootzone. Nevertheless, it is worth to state that, SAR value fluctuates between the values which are significantly higher than its initial condition and sodicity level in irrigation water. Therefore, we observe that SAR value of the rootzone indicates the sodification of soil where 13 SAR value is accepted as a threshold.

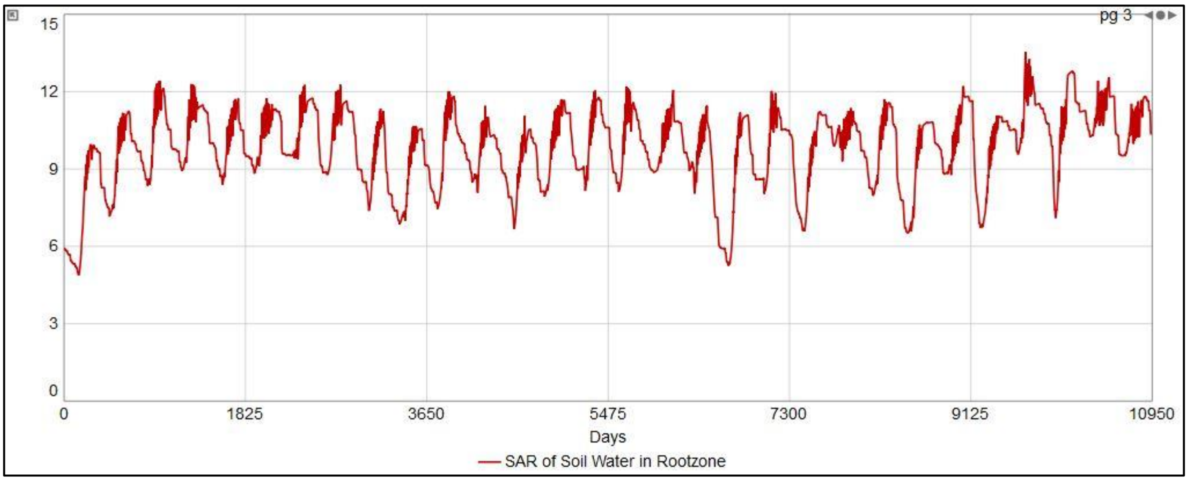

Figure 7.3. Scenario Analysis 1: SAR of Soil Water in Rootzone.

Figure 7.4, the yield loss percentage is demonstrated over time. As it is depicted above, we do not observe high salinity conditions in this scenario analysis and irrigation water is supplied to sufficiently meet crop water requirement. Consequently, we do not view major losses in the yield over time based on these conditions. Yet, we can view one peak around the eighth year which indicates a significant stress during the developmental stage due to water stress. However, the stress seems to be compensated as the last value of yield loss percentage of that season indicates around 6% loss.

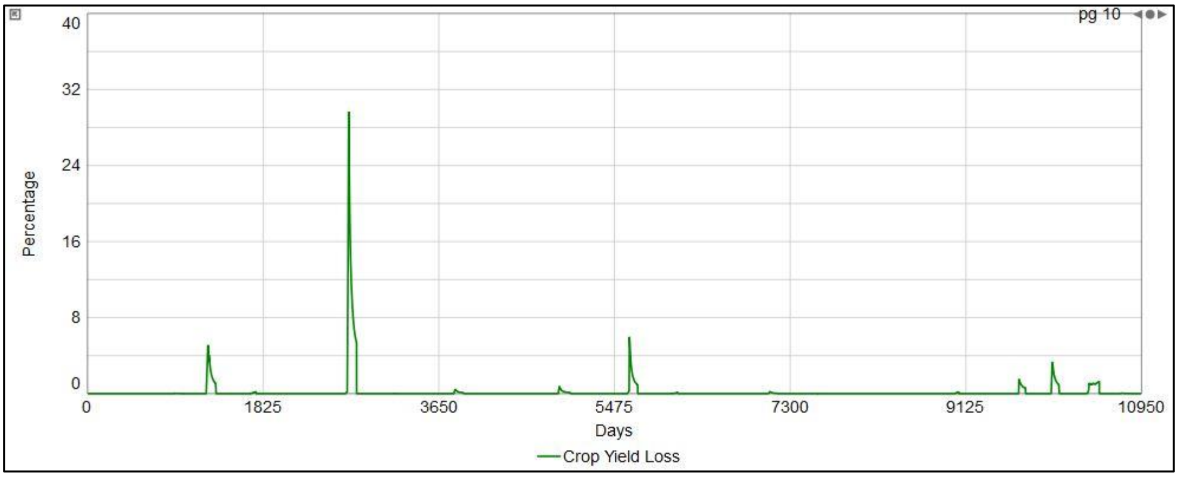

Figure 7.4. Scenario Analysis 1: Yield Loss.

The reduction in hydraulic conductivity over time is demonstrated in the Figure 7.5 below. As it is expressed previously, this parameter is highly dependent on the soil salinity and sodicity levels of the rootzone. Consequently, we can view that the reduction percentage in hydraulic conductivity fluctuates between 10-25 percentages over time generally. Yet it can take values up to 40% for one season and to 30% for multiple seasons. Therefore, we can state that hydraulic conductivity rate is significantly impacted in a negative way in these conditions.

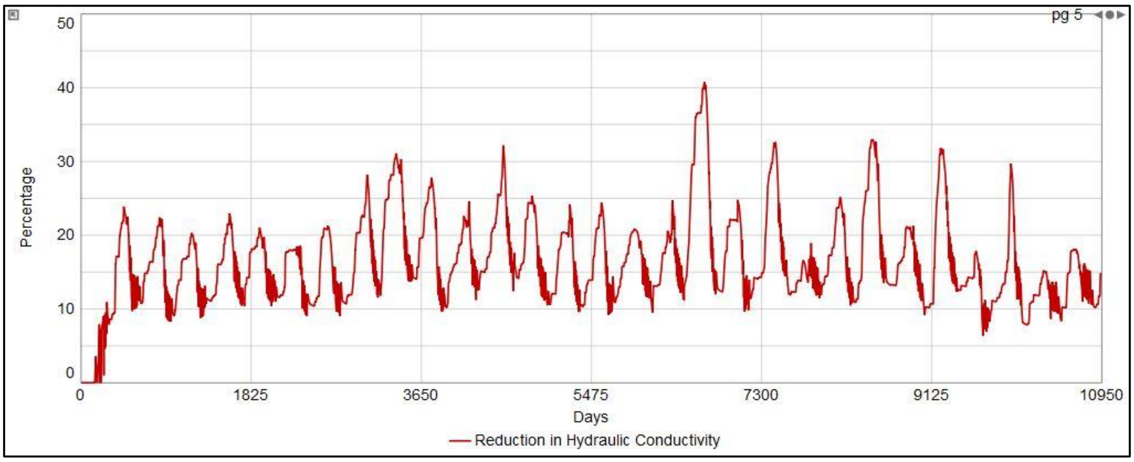

Figure 7.5. Scenario Analysis 1: Reduction in Hydraulic Conductivity.

7.2. Scenario Analysis 2

In this scenario analysis, we run the simulation with the first crop rotation under the precipitation regime for RCP 8.5. We employ sprinkler irrigation method with non-saline and non-sodic water. The outputs for this scenario are displayed below.

Firstly, the soil saturation level is demonstrated in Figure 7.6. The soil moisture level fluctuates over the time horizon between the saturation level and wilting point of the soil. Although, the soil moisture level reaches mostly higher levels than field capacity of the soil, we can observe that it can also reduce near wilting point level. Furthermore, we can state that soil moisture takes low values more frequently in this scenario comparing the first scenario analysis. As the irrigation method is the same for these scenarios, we can suggest that the lower conditions of soil moisture level mainly depend on the precipitation regime.

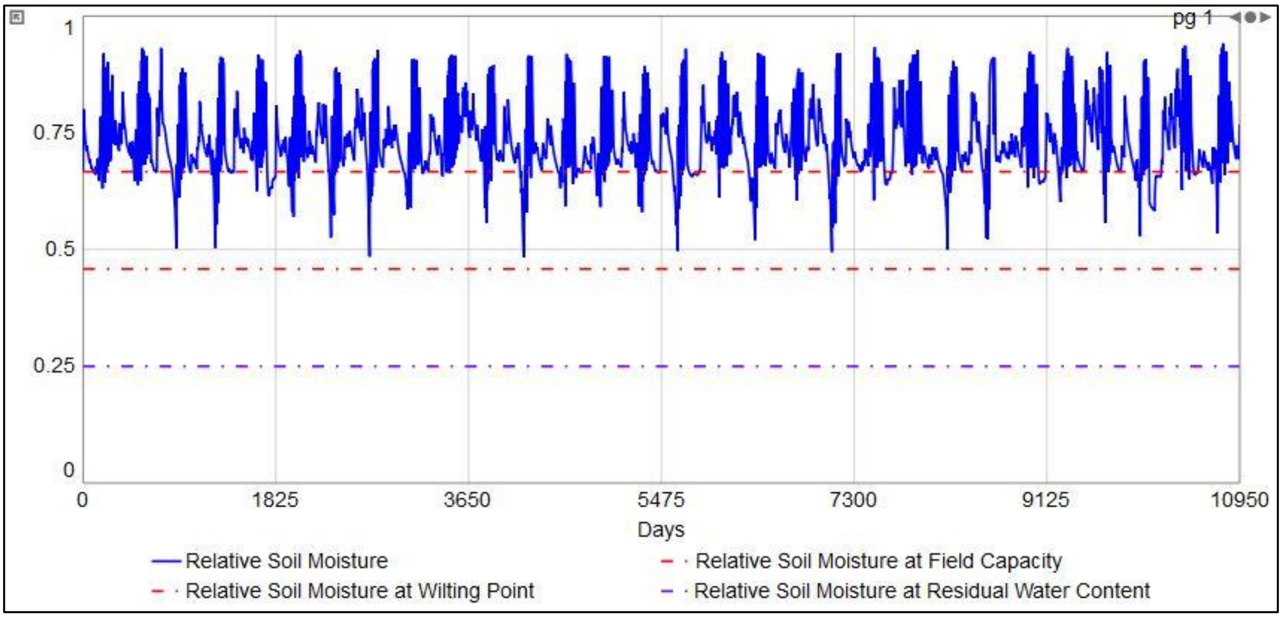

Figure 7.6. Scenario Analysis 2: Relative Soil Moisture.

In the Figure 7.7, soil salinity rate over the time horizon is illustrated. Soil salinity level does not reach high values in this scenario analysis. There are ups and downs in salinity level due to the seasonal differences based on precipitation and evapotranspiration rates, soil salinity rate changes between 0.75 and 2.25 dS/m. Comparing to the previous scenario, soil salinity rate is significantly similar especially in the first half of the simulation duration. However, after the 5475th day, soil salinity rates point out a small degree of increase considering the augmentation in the lowest values.

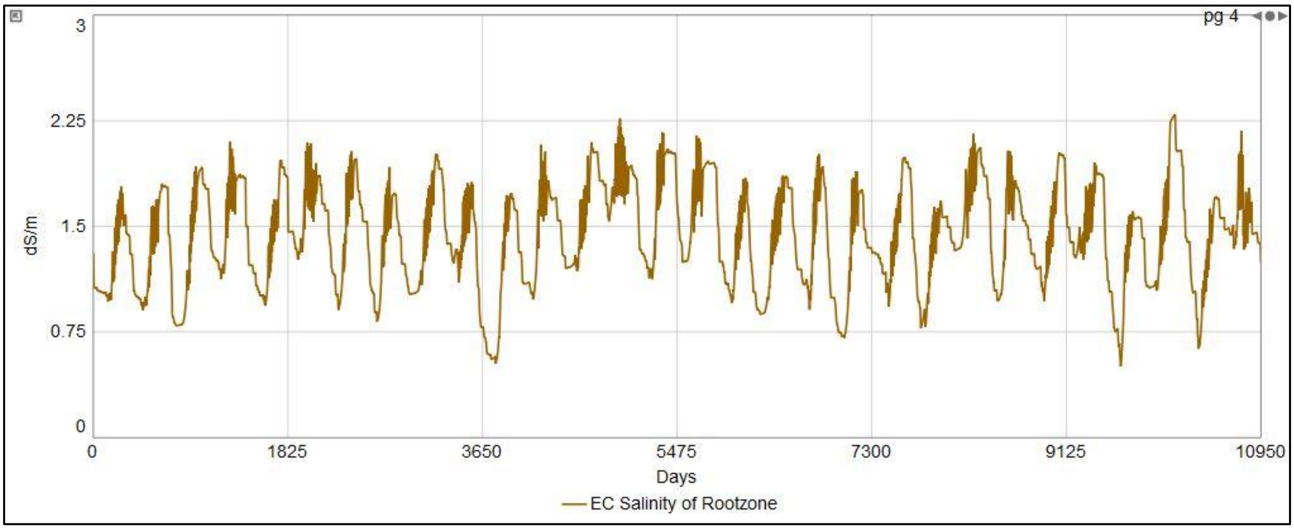

Figure 7.7. Scenario Analysis 2: EC Salinity of Rootzone.

The changes in SAR value of soil water in rootzone is depicted in Figure 7.8. The fluctuations in the SAR value take place quite parallel to the soil salinity rate. On the other hand, these SAR values over time does not indicate a serious sodification problem of the soil profile. The values reach up to 12 and the lowest rate over the time is observed around the 6 SAR value. The changes in the SAR values are very similar to the first scenario.

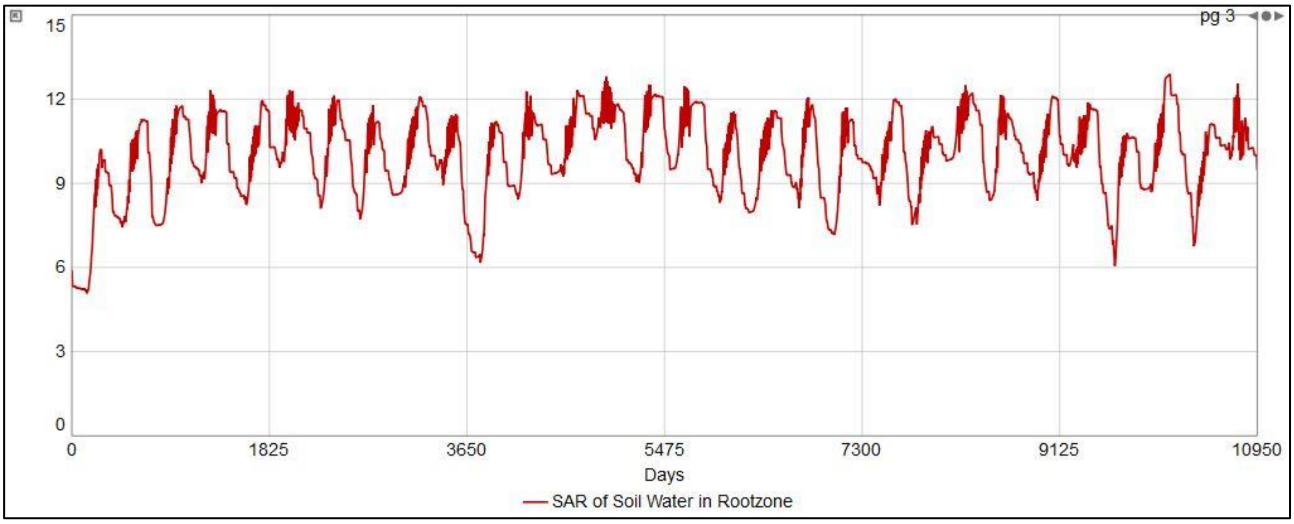

Figure 7.8. Scenario Analysis 2: SAR of Soil Water in Rootzone.

On the other hand, the seasonal yield loss percentages are shown in the Figure 7.9 below. We can observe that the losses on the yield rates are more considerable in this scenario analysis. Although the crops experience stress during the developmental stages, the yield is not negatively impacted profoundly. Nevertheless, we can observe that yield losses are observed more often under this precipitation regime comparing to the previous scenario.

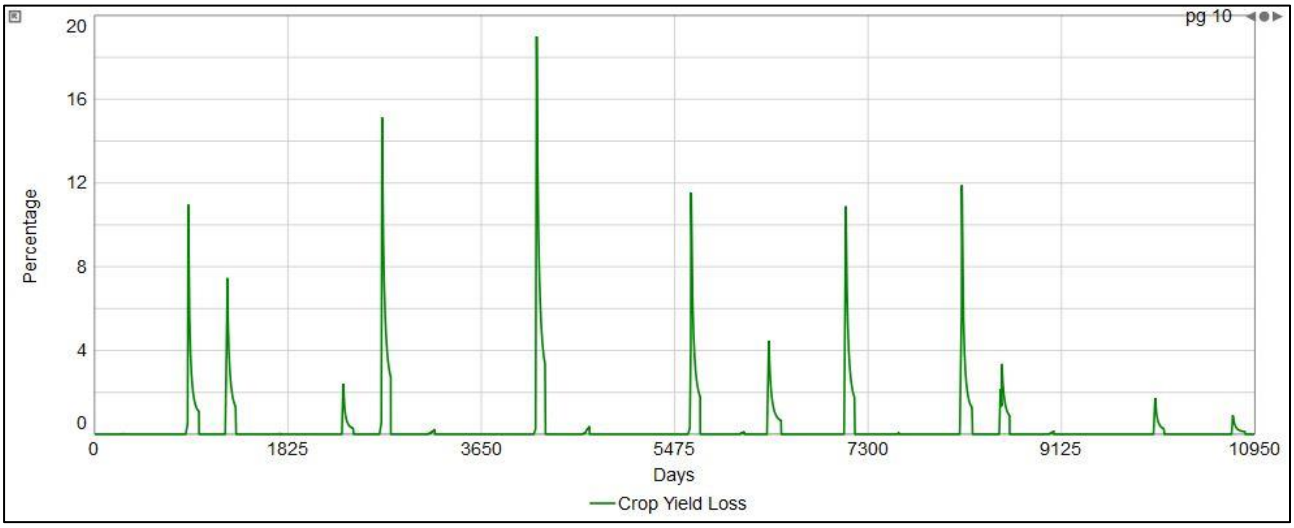

Figure 7.9. Scenario Analysis 2: Yield Loss.

Based on the soil salinity and sodicity rates depicted above, we can observe the reduction in hydraulic conductivity in Figure 7.10. The reduction percentage generally changes between 10% and 25%. However, there two peaks observed which reach up to 35% of reduction. These peaks happen due to the low rates of soil salinity rather than high sodic conditions as illustrated in above figures.

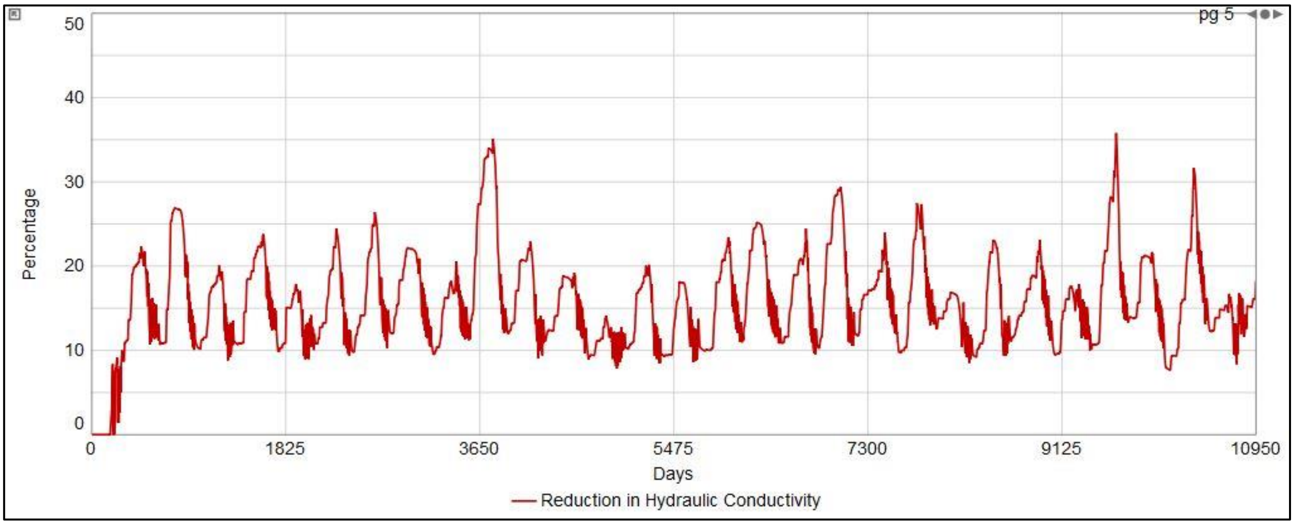

Figure 7.10. Scenario Analysis 2: Reduction in Hydraulic Conductivity.

7.3. Scenario Analysis 3

In this scenario analysis, the first crop rotation is adopted. The precipitation regime represents the RCP 8.5 conditions. The irrigation water is introduced via sprinkler irrigation and irrigation water quality indicates a slightly saline and slightly sodic characteristic. The salinity of irrigation water is 1.5 dS/m, while SAR value corresponds to 10.

In the Figure 7.11, the changes in soil moisture level are demonstrated. The soil moisture level is generally above the field capacity of soil. However, we can observe that it can fall below the field capacity and take values near wilting point of rootzone. Besides, the precipitation regime and the irrigation method are the same with previous scenario run. Therefore, we can view that the changes in soil moisture occur quite parallel to the second scenario.

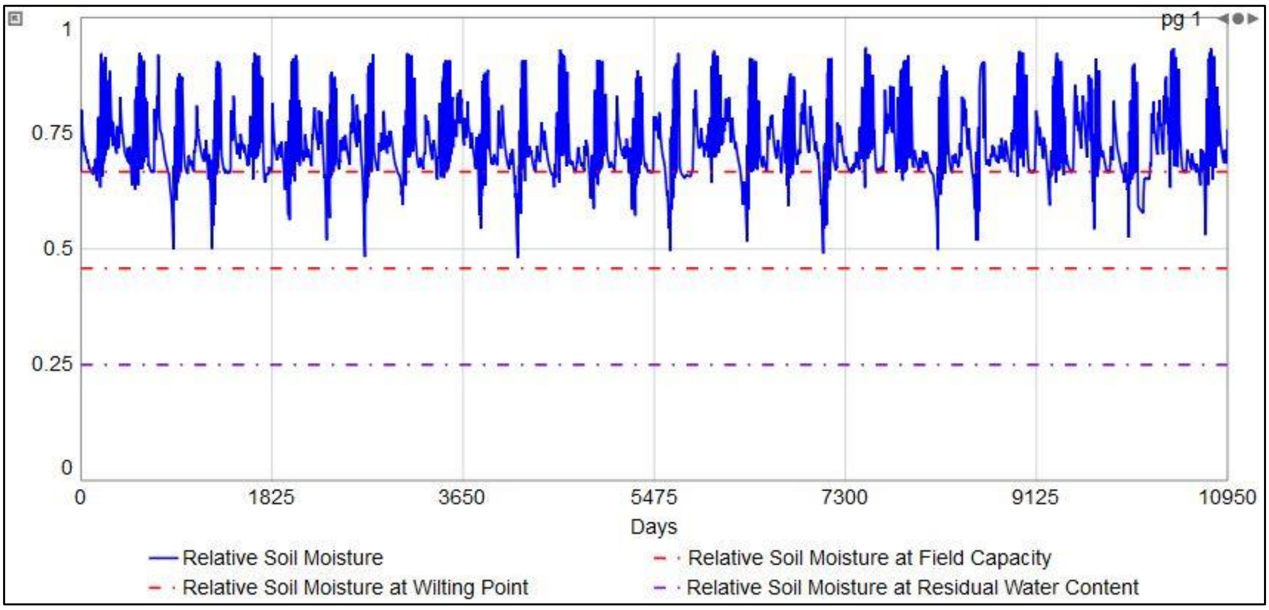

Figure 7.11. Scenario Analysis 3: Relative Soil Moisture.

The soil salinity rate over time is depicted in Figure 7.12. The fluctuations depend on the seasonal differences can be well observed. Furthermore, we can view that soil salinity generally takes values between 1.5 and 4.5 dS/m yet, there are several pick rates that surpass 4.5 dS/m. On the other hand, change in irrigation water quality brings a significant influence in the soil salinity rates across the simulation time. Therefore, we can conclude that irrigation water quality is one of the key factors in salt accumulation in rootzone. In addition to that, we should emphasize that even a slightly saline water can lead to significant increase in soil salinity conditions. Therefore, water quality can be considered as a sensitive factor for soil salinity process.

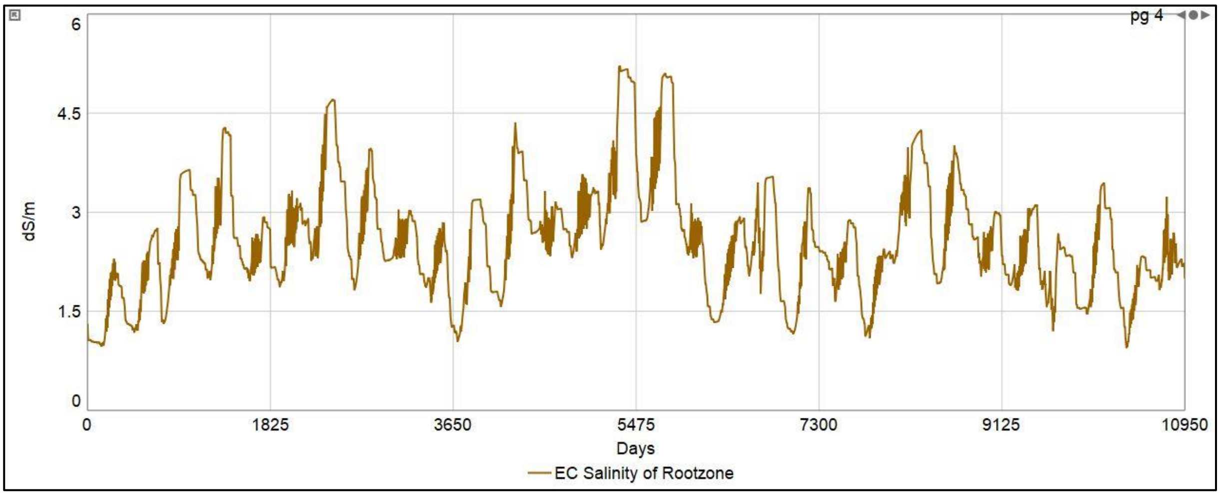

Figure 7.12. Scenario Analysis 3: EC Salinity of Rootzone.

The SAR value of rootzone over time is presented in Figure 7.13 below. The SAR values increases from the initial conditions and achieves high rates which are generally higher than the soil sodicity threshold suggested as 13 SAR value. Therefore, in this scenario analysis we can observe that soil can be ended up with sodic conditions due to the change in irrigation water quality, which indicates 10 SAR value.

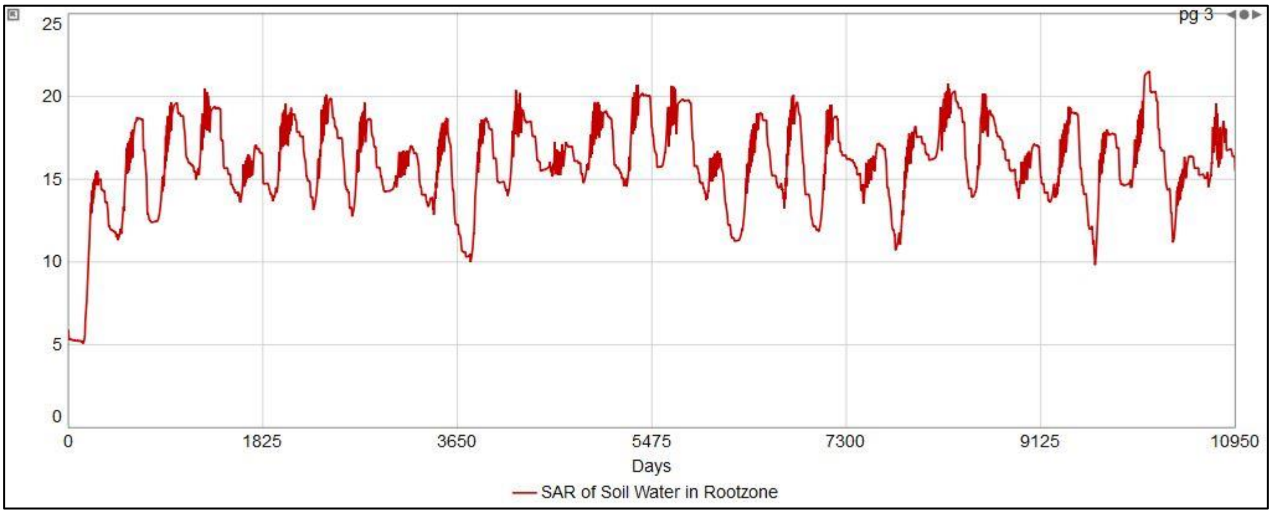

Figure 7.13. Scenario Case 3: SAR of Soil Water in Rootzone.

The percentages of crop yield losses are illustrated in the Figure 7.14 below. We can view that the percentage of loss on crop yield changes from season to season due to varying salt tolerance capacities of the crops, yet it indicates significant losses up to 25%. There are multiple seasons where crops do not suffer even such losses as well. However, we can state that crop growth is highly dependent on the irrigation water quality and soil salinity conditions. Besides, even a slightly saline water can lead to remarkable yield loss rates. Therefore, can say that the quality of water is quite responsive in terms of soil productivity.

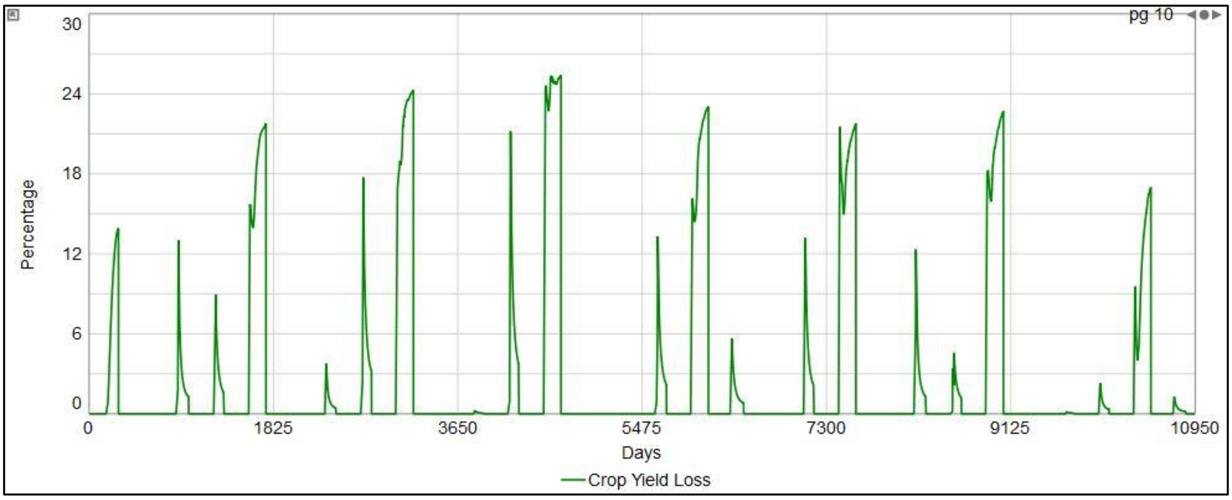

Figure 7.14. Scenario Analysis 3: Yield Loss.

On the other hand, the percentage of reduction on hydraulic conductivity over time is illustrated in Figure 7.15. We can view that there is a minor reduction in hydraulic conductivity rate in overall. However, there are several peaks for reduction percentage where it can achieve up to 15%. This is a quite informative figure where we can view that there are no major reductions which can rise maximum to 15 % for several seasons over 30 years. Despite the high SAR values obtained in scenario analysis. The reduction in hydraulic conductivity is viewed to be much lower than previous scenario. Therefore, we should highlight the counteractive influence soil salinity in the reduction of hydraulic conductivity opposed to sodicity. Consequently, we can state that high salinity rates of the soil prevent the reduction despite the high SAR values.

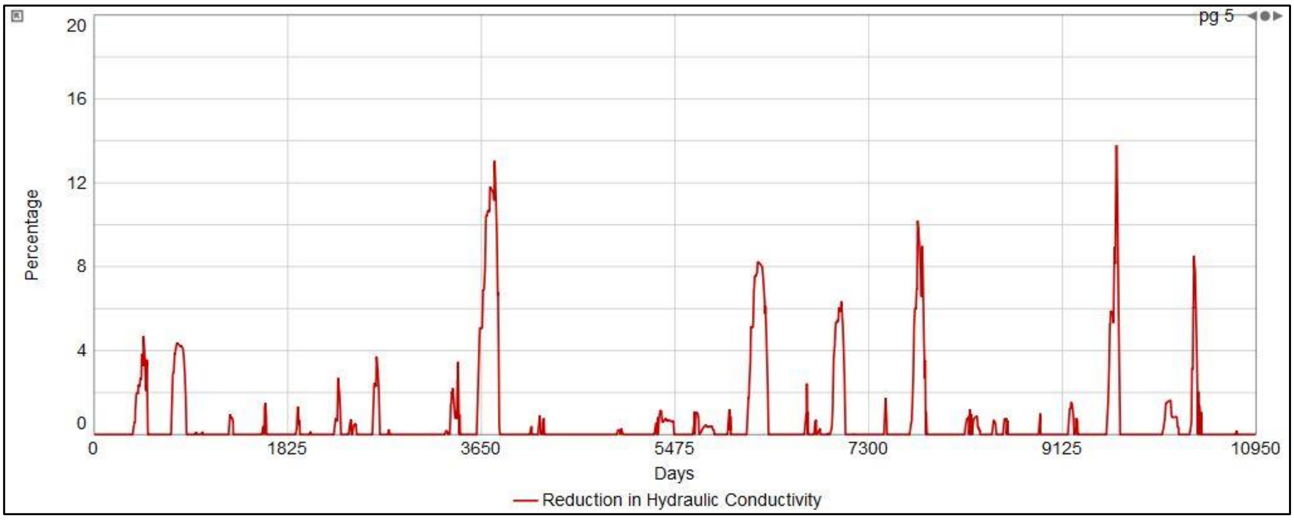

Figure 7.15. Scenario Analysis 3: Reduction in Hydraulic Conductivity.

7.4. Scenario Analysis 4

In this simulation run, we adopted the first crop rotation where corn, sugar beet, sunflower and potato are sown, one after the other. The simulation is run under the precipitation regime which represents RCP 8.5 conditions. The irrigation water method is drip, while the irrigation water quality indicates the slightly saline and slightly sodic properties. Therefore, the difference between this analysis and the previous scenario is the irrigation method.

The change in the soil moisture of the rootzone is depicted in Figure 7.16 below. We can observe that the soil moisture level is generally remains higher than soil field capacity along with the season-based fluctuations. The moisture level can also reduce to wilting point level oftentimes. In addition to that, the moisture level remains in low values for more time than the previous scenario in this run. As the precipitation regime is the same for these scenarios, we can suggest that the lower conditions of soil moisture level mainly depend on the irrigation method.

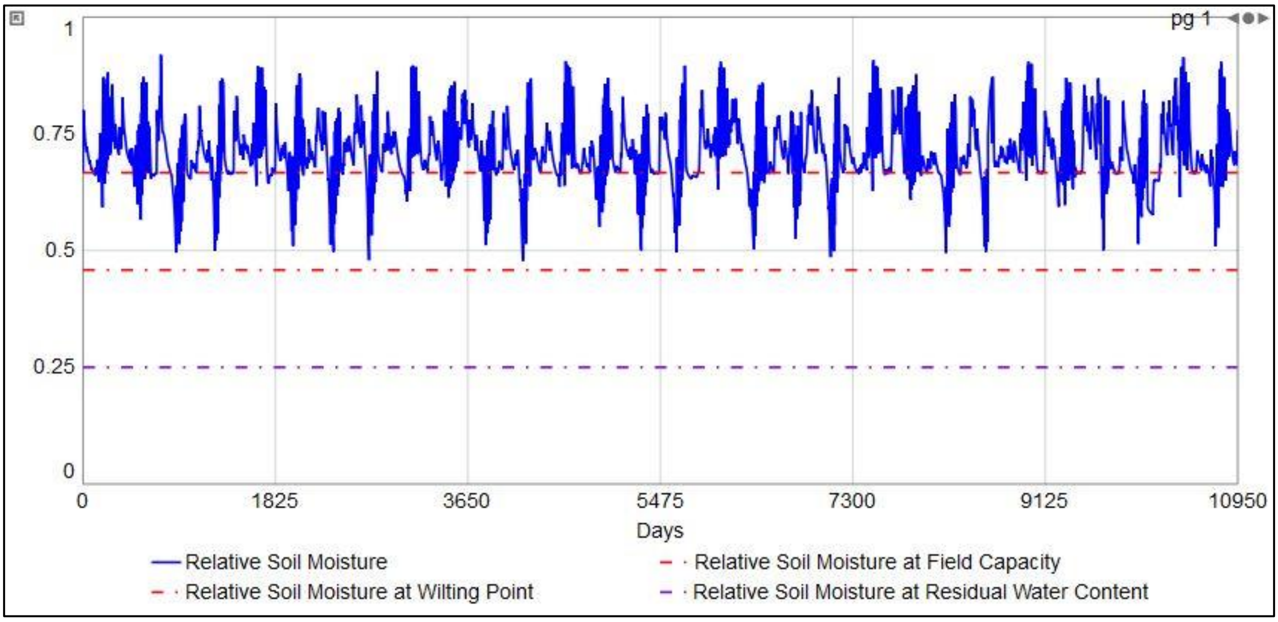

Figure 7.16. Scenario Analysis 4: Relative Soil Moisture.

In Figure 7.17 below, the soil salinity rate over time is illustrated. The salinity rate fluctuates between 2.5 and 9 dS/m along the simulation run. In drip irrigation the main motivation is to supply to water more efficiently than the sprinkler. Therefore, the gap between the plant water uptake and introduced irrigation water amount is aimed to be minimized. In such conditions, the leaching of the salt minerals in the rootzone through the percolation of soil may become harder. Consequently, the salt minerals tend to accumulate in the rootzone and cause soil salinization. With the more saline water and different irrigation method, which corresponds to lower leaching of salts, we can observe how the rootzone gets saline compared to the previous scenario analyses.

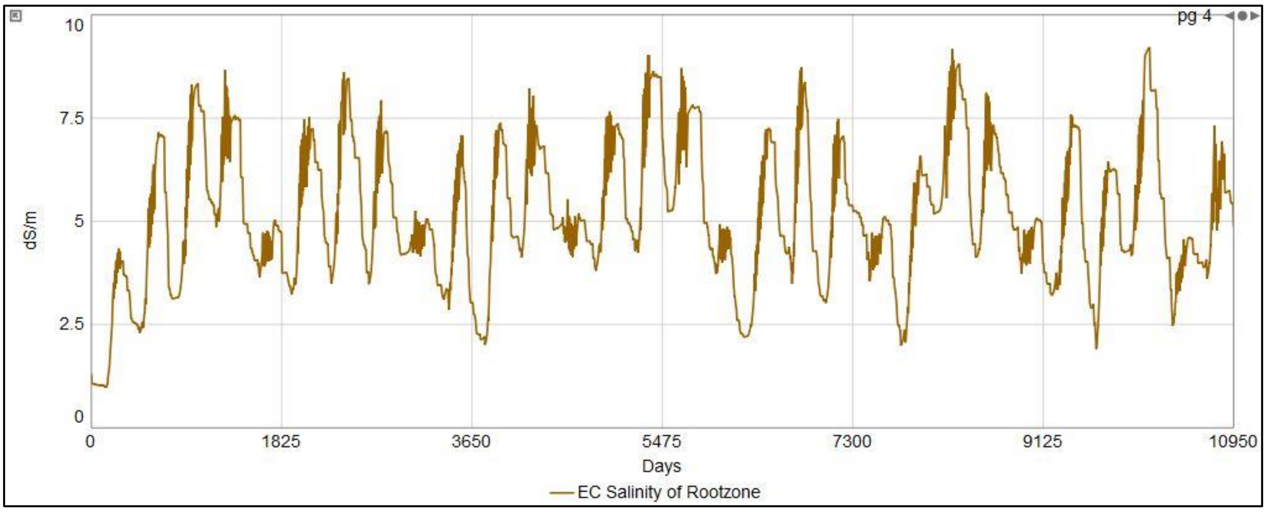

Figure 7.17. Scenario Analysis 4: EC Salinity of Rootzone.

On the other hand, the SAR value of rootzone is presented based on this simulation run in Figure 7.18. We can view that the SAR value indicates a clear soil sodification where it is generally higher than 13. Encore, the pattern of the SAR over time behaves parallel to the soil salinity patterns.

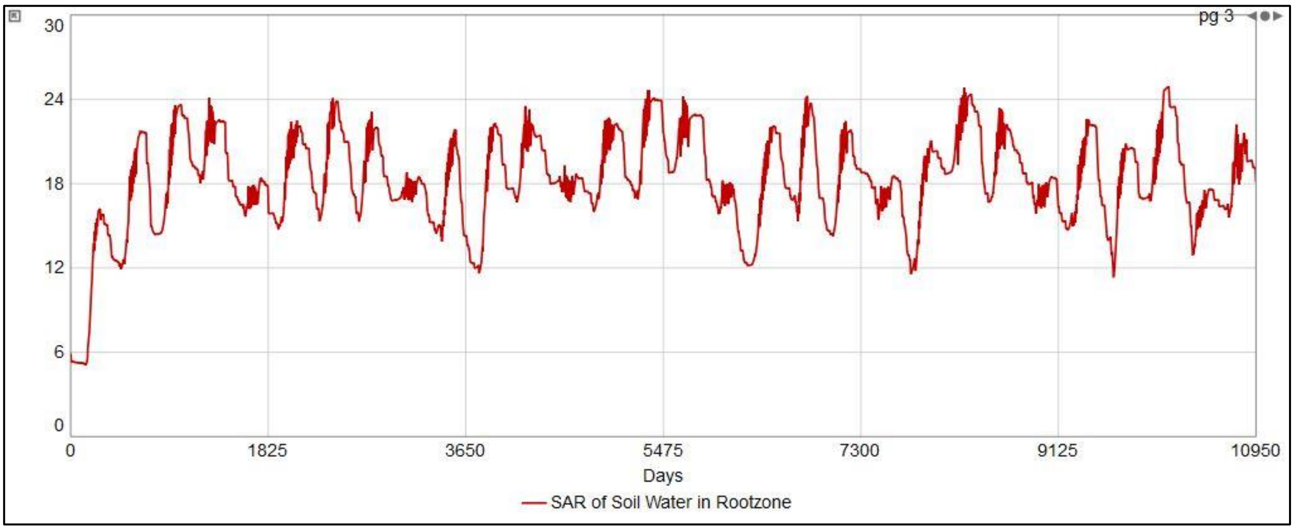

Figure 7.18. Scenario Analysis 4: SAR of Soil Water in Rootzone.

Furthermore, the percentage of yield loss over seasons is depicted in the Figure 7.19 below. We can observe that the loss on crop yield may take 5%, 10% and, 20% and, 40% from season to season. Compared to the previous scenario simulation, we can note the negative impact of drip irrigation on the crop yield ratios through the salt accumulation in rootzone.

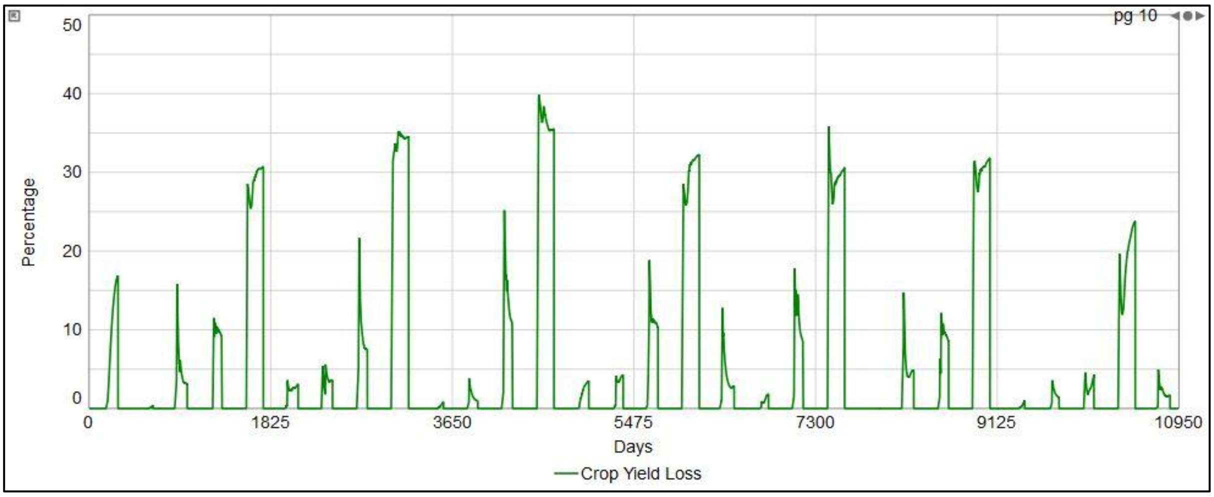

Figure 7.19. Scenario Analysis 4: Yield Loss.

The Figure 7.20 shows the changes in reduction in hydraulic conductivity percentage over time. Accordingly, we can view that there is no major negative impact on the hydraulic conductivity based on this scenario analysis. However, the reduction percentage reaches around 8% for several times, yet it again diminishes later. Interestingly, we can see that lower rate of salinity and sodicity conditions of rootzone in the previous scenarios impact more negatively than the higher saline and sodic conditions that we observe for this scenario analysis. Consequently, we can highlight that the soil salinity rate is as much as influential on the hydraulic conductivity with soil sodicity.

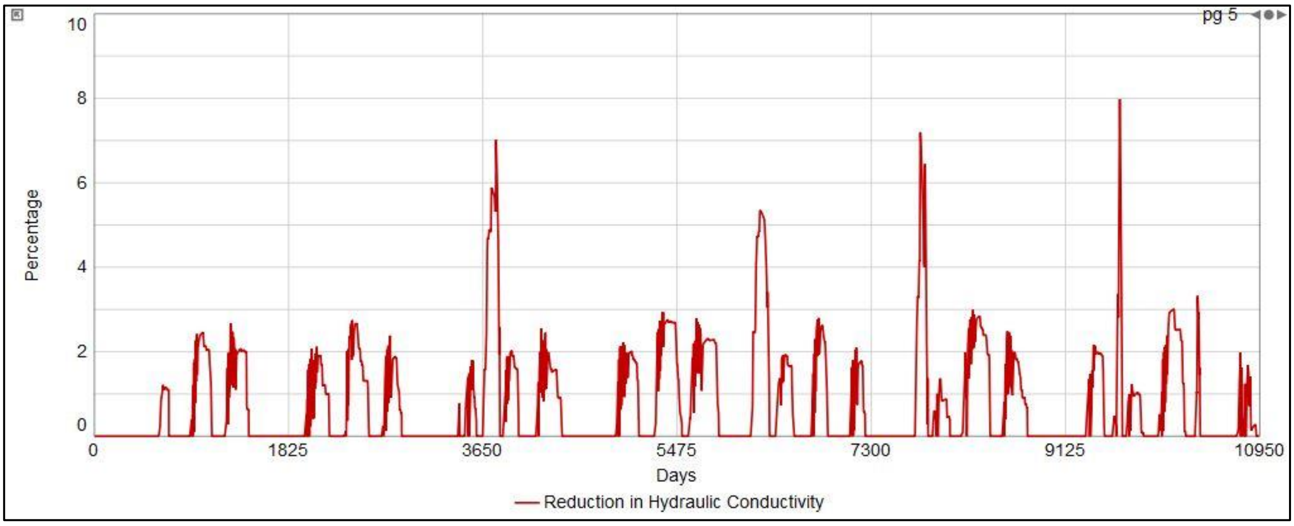

Figure 7.20. Scenario Analysis 4: Reduction in Hydraulic Conductivity.

7.5. Scenario Analysis 5

In this scenario analysis, the second crop rotation adopted includes corn, wheat, sugar beet and wheat, respectively. The precipitation regime represents the RCP 8.5 conditions. The irrigation water is introduced via drip irrigation and irrigation water quality indicates a slightly saline and slightly sodic characteristic. The salinity of irrigation water is 1.5 dS/m, while SAR value corresponds to 10.

In the Figure 7.21, the changes in soil moisture level are illustrated. The soil moisture level is generally above the field capacity of soil. Although, the soil moisture level reaches mostly higher levels than field capacity of the soil, we can observe that it can also reduce to wilting point level. Furthermore, we can state that soil moisture takes lower values in this scenario comparing the previous scenarios. The soil moisture level lasts in low values considerably longer periods than previous simulations. As the irrigation method and precipitation regimes are the same with the fourth scenario, the crucial factor here is the crop rotation.

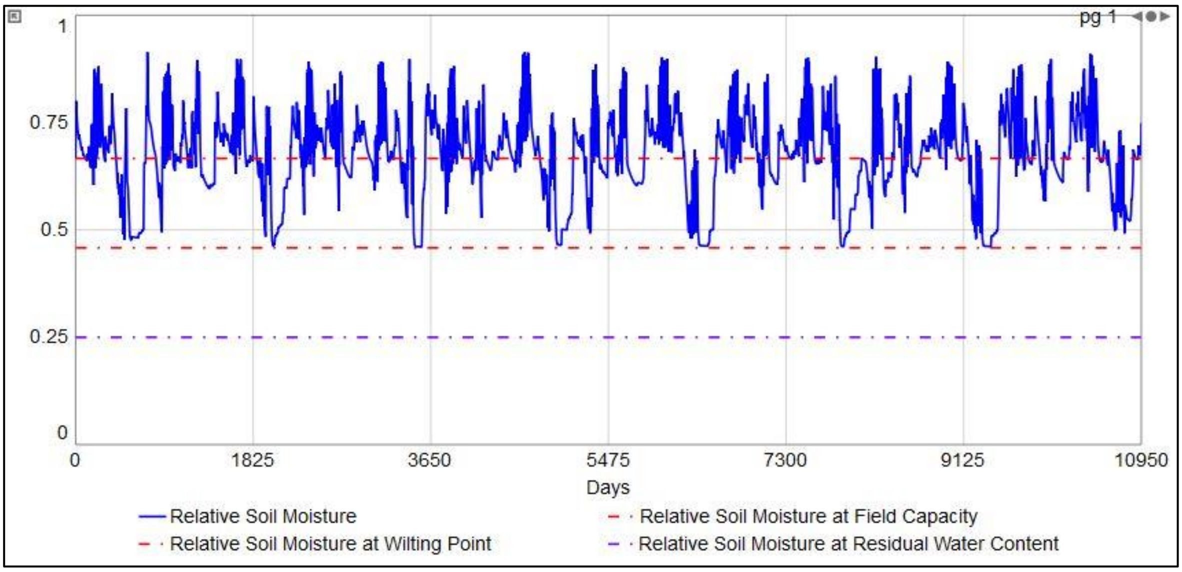

Figure 7.21. Scenario Analysis 5: Relative Soil Moisture.

In the Figure 7.22, soil salinity rate over the time horizon is depicted. Soil salinity level reaches high values in this scenario analysis. Even if there are ups and downs in salinity level due to the seasonal differences based on precipitation and evapotranspiration rates, we can observe several pick rates where soil salinity rate exceeds 9 dS/m. Therefore, we can state that in this scenario analysis salinization of the soil profile significantly experienced.

We suggest that the underlying reason for these rates of salt accumulation in rootzone depends on the change in the crop rotation. We adopt the second crop rotation which include corn, wheat, sugar beet, and wheat accordingly. Wheat and sugar beet are considered as salt tolerant crop types. The salinity stress threshold for wheat is suggested as 6 dS/m while it is indicated as 7 dS/m for sugar beet. Therefore, these salt tolerant crop types can uptake soil water in saline conditions and leave salt minerals in the rootzone even in saline conditions which can further increase soil salinity rates. Along with this, this crop rotation includes almost a fallow period after the wheat is harvested due to its nature of planting schedule. To be more specific, wheat is harvested during June, yet the corn and sugar beet are sown during the springtime, April and May, respectively. Consequently, the time after the wheat is harvested, the soil profile is not planted, therefore not irrigated until the next plant is sowed, in the next summer. Therefore, during the summer period the soil water is prone to vaporize under arid conditions of summer months and leave all salt minerals in the soil profile.

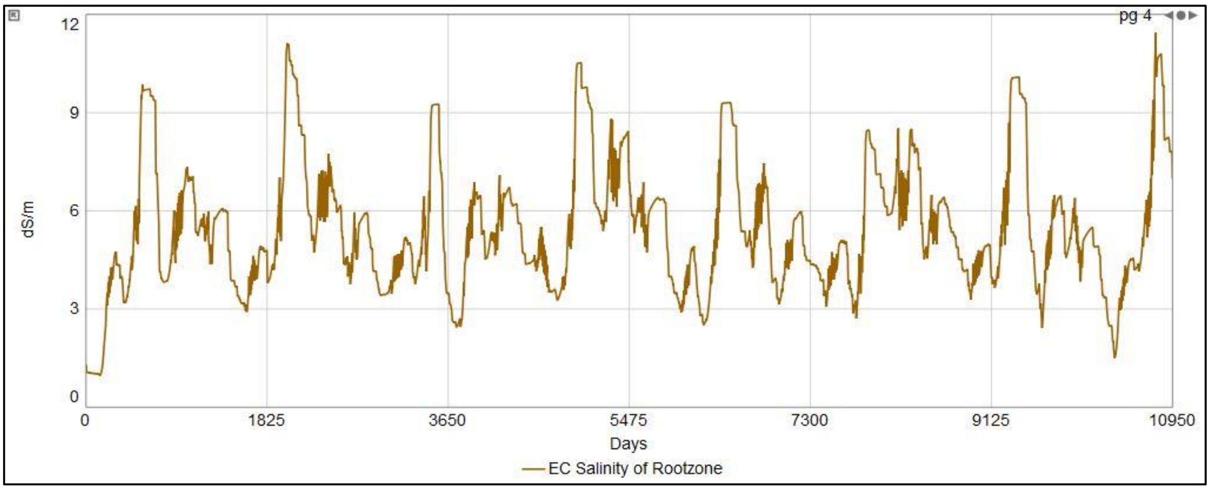

Figure 7.22. Scenario Analysis 5: EC Salinity of Rootzone.

The changes in SAR value of soil water in rootzone is depicted in Figure 7.23. The fluctuations in the SAR value take place quite parallel to the soil salinity rate. On the other hand, these SAR values over time indicate a serious sodification problem of the soil profile. The values exceed 24 and the lowest rate over the time is observed around the 12 SAR value.

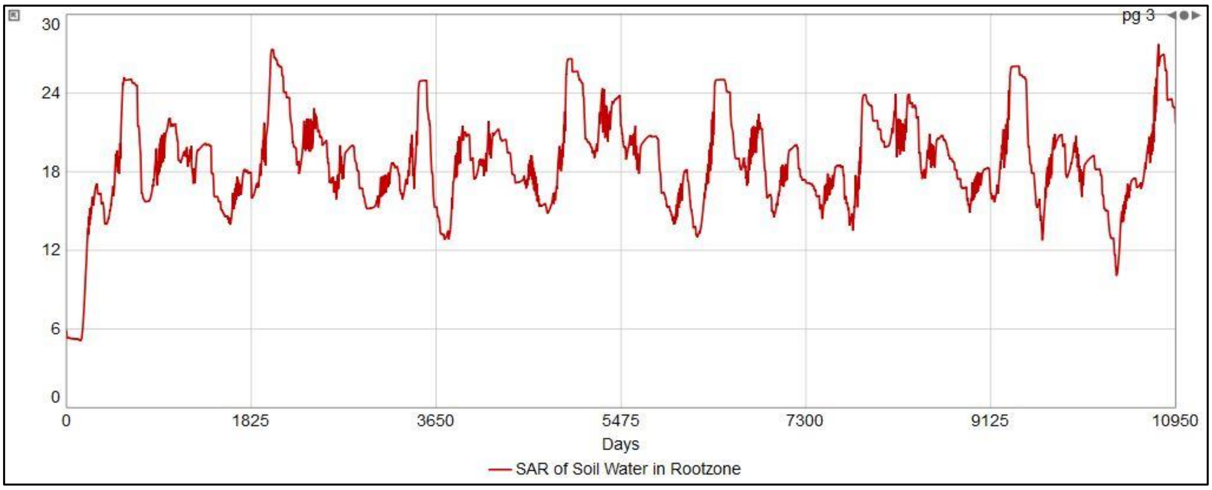

Figure 7.23. Scenario Analysis 5: SAR of Soil Water in Rootzone.

On the other hand, the seasonal yield loss percentages are shown in the Figure 7.24 below. We can observe that the losses on the yield rates are remarkable in this scenario analysis. Although the wheat and sugar beet are salt tolerant crop types, the high saline conditions of soil profile negatively impact the crop growth process. The yield percentage varies from season to season, yet it can take high values up to 50 % over the simulation time.

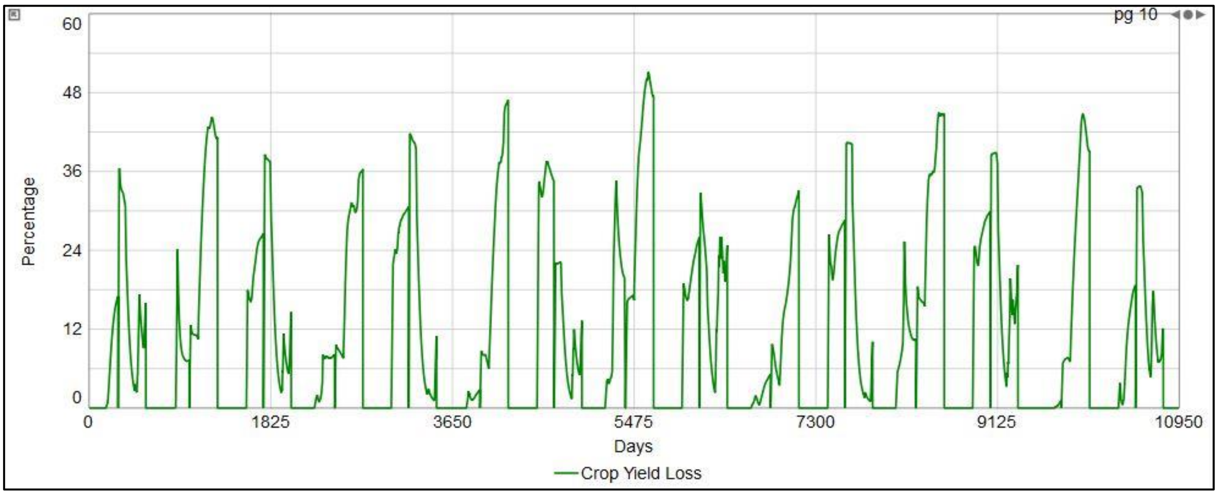

Figure 7.24. Scenario Analysis 5: Yield Loss.

On the other hand, the percentage of reduction on hydraulic conductivity over time is demonstrated in Figure 7.25. We can observe that there is a minor reduction in hydraulic conductivity rate in overall. However, there are several peaks for reduction percentage where it can achieve up to 15%. Nevertheless, we should underline that the soil salinity rate as much as influential on the hydraulic conductivity with soil sodicity.

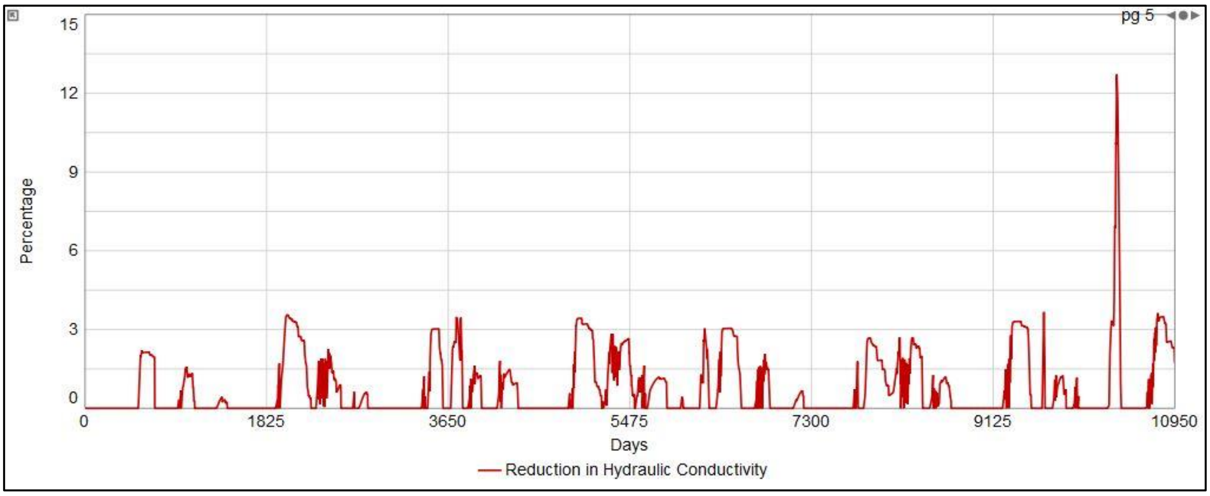

Figure 7.25. Scenario Analysis 5: Reduction in Hydraulic Conductivity.

8. DISCUSSION

In this section, we discuss the main findings of this study based on the reference model outputs and the scenario analyses performed to represent and test the impact of alternative applications in farmlands on the soil salinity, sodicity, crop yield and hydraulic conductivity parameters.

The reference model demonstrates the model behavior under expected real-life conditions. The initial conditions and parameters are set to reference conditions, which are realistic field values. The simulation is performed for 30 years to illustrate patterns for a long-term period. It is observed that the model provides meaningful outcomes. The seasonal fluctuations in the outputs and the sharp increases in soil moisture based on irrigation applications and reductions in the moisture level following the end of crop growth season can be observed. Along with that, we can see that soil salinity rate in the rootzone increases as the salt minerals are introduced via irrigation water during the crop season where the evapotranspiration rates are higher than the precipitation rates. Then, the salinity rate diminishes with the increase in the precipitation and decrease in the evapotranspiration rate due to seasonal differences which facilitates the leaching of the salt minerals away from the rootzone. Nevertheless, we can observe that soil salinity level takes values which are higher than the irrigation water quality parameters even the irrigation water quality corresponds to non-saline conditions. Therefore, we can note that regular and continuous applications of irrigation can lead to salt accumulation in the rootzone in the regions where semi-arid and arid climatic conditions are dominant. On the other hand, we can observe that change in the SAR values of the rootzone generally follows similar pattern to the soil salinity conditions. Furthermore, the yield loss percentage indicates low levels of reductions as the soil salinity rate does not augment significantly. Lastly, we do not observe reduction in hydraulic conductivity as the problematic conditions do not become dominant in the reference simulation. However, it is important to note that, the model is able to demonstrate even temporary reductions which are caused by low soil salinity rates in this case.

After the reference behavior of the model is presented, several scenario analyses are performed to test long-term impact of different applications in terms of precipitation regime, irrigation water quality, irrigation method, and crop rotation on the soil salinization and sodification processes along with the reductions in the crop yield and hydraulic conductivity rates. The results which are presented in the previous chapter in detail and indicate several important points.

To begin with, we can suggest that the model is capable of fast simulating these complex dynamics and represent realistic behavior patterns and outputs for long periods. On the other hand, we can state four important points that model outputs indicate. The first point is that different precipitation regimes in the future may impact the magnitude of soil salinization processes as the leaching of salt minerals from rootzone can be negatively influenced. Based on the comparison of soil salinity rates over time between the first and second scenarios, we can view quite minor increase in the second scenario where precipitation regime is altered and represented more drought conditions. Nevertheless, we strongly highlight that various types of precipitation scenarios from different climate models should be tested to investigate soundness of this argument. On the other hand, we can emphasize that, different precipitation regimes can also affect the yield rates.

Furthermore, the comparison of the second and the third scenarios indicate that irrigation water quality is an essential factor on salt accumulation process over time. In addition to that, irrigation water quality can also play an important role for crop production as it influences the productivity of the soil. Besides, we can note that irrigation method is another critical factor regarding the salt accumulation process in rootzone. Comparing the third and the fourth scenarios, the change in the irrigation method reveals a meaningful aspect about this point. Therefore, we can say that drip irrigation can be a facilitating factor for soil salinization where percolation of the water from rootzone is aimed to be minimized to improve irrigation water efficiency. However, this motivation may lead to accumulation of salt minerals in the rootzone since the leaching of the salt from rootzone is also reduced along with the decrease in percolation rates.

On the other hand, a very interesting point indicated by scenario analyses is the impact of salt-tolerant crop and crop rotation on the soil salinity process. We can clearly detect that the highest values for both soil salinity and sodicity parameters arise in the fifth scenario analysis. Consequently, the seasonal yield loss percentages indicate major losses on the yield rate parallel to the high soil salinity. The fifth scenario analysis includes salt tolerant crops as sugar beet and wheat. In addition to that, the wheat is planted two times based on this crop rotation which lasts for 4 years. This scenario is aimed to represent the idea of incorporating less irrigation water demanding crops in the rotations in a semi-arid region where also irrigation water sources are also under threat. Therefore, the underlying motivation is to reduce applied irrigation amount. In this sense, crop rotation schedule is undergone with mostly salt-tolerant crops. These crops are able to uptake the soil water from the rootzone under saline conditions. As the crops uptake the soil water, the dissolved salt minerals are left in the rootzone and begin to accumulate more. Consequently, their ability of growing in saline conditions via securing the transpiration rate result in increasing the salt concentration of soil water, therefore leads to higher soil salinity rate. In addition to that, in this crop rotation we can view the impact of leaving the farmland to fallow after harvesting the wheat in the beginning of the summer. In these conditions, salt minerals are introduced via irrigation throughout crop development process. Thereafter, the soil is left to dry out due to high atmospheric evaporation demand during the summer which can result in increasing the salt concentration of the soil water in the rootzone. Hence, the leaching of the salt minerals from rootzone may be crucial when such crop rotations are applied for long-terms.

The last take away point from these various scenario analyses is that soil salinity rates are as much influential as soil sodicity level on the soil hydraulic properties. Regarding the soil salinity and sodicity parameters starting from the second scenario, both parameters further increase step by step as the scenario order is followed. We can observe that the percentage of reduction in hydraulic conductivity, however, reduces in the scenario order respectively. Therefore, we highlight that salinity has a counterbalancing role in hydraulic conductivity rate by which is negatively impacted by high sodic conditions.

9. CONCLUSION

In this research, complex and dynamic nature of soil salinization and sodification processes is studied. The soil salinity and sodicity, which frequently accompany each other, can lead to degradation of soil properties, significant reductions on yield rates, and, therefore, can negatively impact the food security and livelihoods of farmers. The soil salinization problems can take place due to natural processes and human actions which are mainly based on the agricultural practices, and irrigation applications. While the salt minerals are mainly transported by the hydraulic flow through the soil profile, the accumulation of salt minerals particularly at the top layers of soil can deteriorate soil hydraulic properties and poses threat to agricultural production as it can inhibit crop evapotranspiration rate as well. The feedback rich mechanism of the problem is highly impacted by the various agricultural practices. Therefore, irrigation method, irrigation water quality and schedule along with the crop choices and rotations can be influential on the salt accumulation process. Moreover, soil salinity and sodicity can be prevalent problems in semi-arid and arid regions where evapotranspiration rates are higher than precipitation which can be a facilitating factor.

To comprehend the feedback rich complex nature of the problem, a dynamic simulation model based on the dynamic systems methodology is developed. The model allows us to represent these complex long-term processes through its fast-simulating ability. The credibility of the model outputs is built by the various validation tests suggested by the system dynamics literature. After the structural validation tests performed, the model behavior patterns are compared with another model in use, Hydrus-1D under the same conditions. Thereafter, the reference model behavior is presented and analyzed.

The model provides an experimental platform to test the impact of alternative scenarios on soil salinization, sodification processes, and therefore crop yield and reduction in hydraulic conductivity rates. Five different scenario analyses are performed. Based on the scenario analysis the importance of precipitation regimes, irrigation methods and crop choices on the salt accumulation on rootzone is discussed. Furthermore, the balancing impacts of soil salinity and sodicity on the reduction in hydraulic conductivity are analyzed based on the scenario cases. The results of these scenario analysis and the experimental platform of the model can guide further discussions and analyses by various stakeholders which take part in the agricultural practices.

The model is developed based on the theoretical knowledge provided by soil physics and system dynamics literature. The model parameters are employed from the literature and field measurements as well. For further research, incorporating the shallow water table into the model and providing an option for irrigation from the groundwater which shares the same aquifer with the water table can improve the model capabilities of representing further feedbacks between saturated zone and rootzone salt concentrations. Furthermore, the representation crop growth process can be ameliorated to include different developmental stages of growth process and their specific necessities. On the other hand, incorporating plentiful precipitation regimes may facilitate the inspection on salt accumulation process in the future under various scenarios. In addition to that, the modelling of irrigation methodologies can be better represented to provide wide options to test different irrigation water quantities with various methods. Besides, incorporating cations uptake by plant may add an affluence on the model as it would represent the ion toxic effect on the crops separately from the osmotic stress due to soil salinity. It also would bring another dimension in the mass balance of cations in rootzone. Additionally, including the crop stress due to air deficit within rootzone may strengthen the realistic representation of the model. Moreover, the online experimental platform should be provided to open the accessibility of the model for further learning of mass audience. All in all, the model suggests important capability to represent long-term soil salinization and sodification problems under different environmental conditions and agricultural practices and for future climatic conditions to better comprehend and manage these problematic processes.

REFERENCES

Allen, R. G., Pereira, L. S., 2009. Estimating crop coefficients from fraction of ground cover and height. Irrigation Science, 28(1), 17–34.

Allen, R. G., Pereira, L. S., Raes, D., Smith, M., 1998. FAO Irrigation and Drainage Paper NO. 56. Rome, Italy.

Bahceci, I., 2021. Tarımsal Drenaj Sistemleri. Harran Üniversitesi Ziraat Fakültesi website: http://web.harran.edu.tr/assets/uploads/other/files/Ziraat_Fakültesi/SULAMA/TARIMSAL_DRENAJ_MÜH.pdf. Data accesed June 2021

Bahçeci, I., Dinç, N., Tari, A. F., Ağar, A. I., Sönmez, B., 2006. Water and salt balance studies, using SaltMod, to improve subsurface drainage design in the Konya-Çumra Plain, Turkey. Agricultural Water Management, 85(3), 261–271.

Tarım ve Orman Bakanlığı., 2015. Konya Havzası Kuraklık Yönetim Planı: EK II/II - Havza Su Potansiyeli ve Su Potansiyelindeki Değişimin Tespiti: Hidrolojik Modelleme. Vol. 2. Ankara, Turkey.

Barlas, Y., 1996. Formal aspects of model validity and validation in system dynamics. System Dynamics Review, 12(3), 183–210.

Barlas, Y., 2002. System Dynamics: Systemic Feedback Modelling for Policy Analysis. In Encyclopedia for Life Support Systems. UNESCO Publishing.

Brouwer, C., Prins, K., Heibloem, M., 1989. Irrigation Water Management: Irrigation Scheduling. Food and Agriculture Organization of the United Nations.

Butcher, K., Wick, A. F., Desutter, T., Chatterjee, A., Harmon, J., 2016. Soil salinity: A threat to global food security. Agronomy Journal, 108(6), 2189–2200.

Carsel, F. R., Parrish, R. S., 1988. Developing Joint Probability Distributions of Soil Water Retention Chracteristics. Water Resources, 24(5), 755–769.

Clapp, R. B., Hornberger, G. M., 1978. Emprical Equations for Some Soil Hydraulic Properties. Water Resources Research, 14(4), 4.

Daliakopoulos, I. N., Tsanis, I. K., Koutroulis, A., Kourgialas, N. N., Varouchakis, A. E., Karatzas, G. P., Ritsema, C. J., 2016. The threat of soil salinity: A European scale review. Science of the Total Environment, 573, 727–739.

de Meester, T., 1970. Soils of the Great Konya Basin, Turkey. In Agricultural Research Reports (Vol. 740). https://library.wur.nl/WebQuery/wurpubs/fulltext/304248. Data accessed June 2021

Dingman, S. L., 2015. Physical Hydrology. 3rd Edition. Waveland Press Inc. U. S. A.

Doorenbos, J., Kassam, A. H., 1979. Yield Response to Water. FAO. Rome, Italy.

Ezlit, Y. D., Bennett, J. M., Raine, S. R., Smith, R. J., 2013. Modification of the McNeal Clay Swelling Model Improves Prediction of Saturated Hydraulic Conductivity as a Function of Applied Water Quality. Soil Science Society of America Journal, 77(6), 2149–2156.

FAO-ITPS., 2015. Status of the World ’s Soil Resources: Main Report. Rome, Italy.

Foth, D. H., 1990. Fundamentals of Soil Science. 8th Edition. John Wiley & Sons. U. S. A.

Frenken, K., 2009. Irrigation in the Middle East Region in Figures, Aquastat Survey -FAO Water Report 34. In Fao Water Reports., Vol. 34. Rome, Italy.

Hillel, D., 1998. Environmental Soil Physics. 1st Edition. Academic Press. U. S. A.

Hillel, D., 2000. Salinity Management for Sustainable Irrigation Integrating Science, Environment, and Economics. The World Bank. Washington, DC, U. S. A.

Huang, P. M., Li, Y., Summer, M. E., 2012. Handbook of Soil Sciences: Resource Management and Environmental Impacts. Second Edition. CRC Press. U. S. A.

Ivushkin, K., Bartholomeus, H., Bregt, A. K., Pulatov, A., Kempen, B., de Sousa, L., 2019. Global mapping of soil salinity change. Remote Sensing of Environment, 231, 111260.

Jacobson T., Adams, R. M., 1958. Salt and silt in Ancient Mesopotamian Agriculture Progressive changes in soil salinity and sedimentation contributed to the breakup of past civilizations. Science, 128(3334), 1251–1258.

Jiang, J., Feng, S., Huo, Z., Zhao, Z., Jia, B., 2011. Application of the SWAP model to simulate water-salt transport under deficit irrigation with saline water. Mathematical and Computer Modelling, 54(3–4), 902–911.

Jones, P. G., Thornton, P. K., Diaz, W., Wilkens, P. W., 2002. MarkSim: A Computer Tool That Generates Simulated Weather Data for Crop Modelling and Risk Assessment. Volume 1. Centro International de Agricultura Tropical. Cali, Columbia.

Kale, S., 2011. Field-evaluation of DRAINMOD-S for predicting soil and drainage water salinity under semi-arid conditions in Turkey. Spanish Journal of Agricultural Research, 9(4), 1142.

Kalkınma Bakanlığı, T. C., 2018. On Birinci Kalkınma Planı: Tarımda Toprak ve Sulama Suyunun Sürdürülebilir Kullanımı Özel İhtisas Komisyonu Raporu. Ankara, Türkiye.

Kanber, R., Cullu, M. A., Kendirli, B., Antepli, S., Yılmaz, N., 2005. SULAMA, DRENAJ ve TUZLULUK. Türkiye Ziraat Mühendisliği VI. Teknik Kongresi Bildirileri, 1–44. Milli Kütüphane, Ankara, Türkiye.

Kandil, H. M., Skaggs, R. W., Abdel Dayem, S., Aiad, Y., 1995. DRAINMOD-S: Water management model for irrigated arid lands, crop yield and applications. Irrigation and Drainage Systems, 9(3), 239–258.

Khan, S., Yufeng, L., Ahmad, A., 2007. Analyzing complex behavior of hydrological systems through a system dynamics approach. Environmental Modelling and Software, 24(12), 1363–1372.

KOP., 2017. KOP - Son Durum Raporu. Konya Ovası Projesi Bölge Kalkınma İdaresi Başkanlığı. Türkiye.

KOP., 2020. KOP Bölgesi Sosyo-Ekonomik Göstergeler. Konya Ovası Projesi Bölge Kalkınma İdaresi Başkanlığı. Türkiye.

Kramer, I., Mau, Y. 2020. Soil Degradation Risks Assessed by the SOTE Model for Salinity and Sodicity. Water Resources Research, 56(10), 1–17.

Kroes, J. G., Van Dam, J. C., Groenendijk, P., Hendriks, R. F. A., Jacobs, C. M. J., 2009. SWAP version 3.2. Theory description and user manual. In SWAP version 3.2. Theory description and user manual. http://www.swap.alterra.nl/ Data accessed June 2021

Levy, R., Hillel, D., 1968. Thermodynamic equilibrium constants of sodium-calcium exchange in some Israel soils. Soil Science, 106, 393–398.

Luo, Y., Khan, S., Cui, Y., Peng, S., 2009. Application of system dynamics approach for time varying water balance in aerobic paddy fields. Paddy and Water Environment, 7(1), 1–9.

Maas, E. V., Hoffman, G. J., 1977. Crop Salt Tolerance - Current Assessment. Journal of the Irrigation and Drainage Division, 103, 115–134.

Mau, Y., Porporato, A., 2015. A dynamical system approach to soil salinity and sodicity. Advances in Water Resources, 83, 68–76.

Mau, Y., Porporato, A., 2016. Optimal control solutions to sodic soil reclamation. Advances in Water Resources, 91, 37–45.

McNeal, B. L., 1968. Prediction of the Effect of Mixed-Salt Solutions on Soil Hydraulic Conductivity. Soil Science Society of America Journal, 32(2), 190–193.

Meier, J., Zabel, F., Mauser, W., 2018. A global approach to estimate irrigated areas - A comparison between different data and statistics. Hydrology and Earth System Sciences, 22(2), 1119–1133.

Mein, R.G., Larson, C., 1973. Modeling Infiltration during a Steady Rain. Water Resources Research, 9(2), 384–394.

Oosterbaan, R. J., 2002. SALTMOD: Description of Principles, User Manual, and Examples of Application. (May), 81. http://www.waterlog.info/pdf/saltmod.pdf. Data Accessed June 2021

Qadir, M., Oster, J. D., 2004. Crop and irrigation management strategies for saline-sodic soils and waters aimed at environmentally sustainable agriculture. Science of the Total Environment, 323(1–3), 1–19.

Qadir, M., Quillérou, E., Nangia, V., Murtaza, G., Singh, M., Thomas, R. J., Noble, A. D., 2014. Economics of salt-induced land degradation and restoration. Natural Resources Forum, 38(4), 282–295.

Richards, L. A., 1954. Diagnosis and Improvement of Saline and Alkaline Soils. Soil Science, 64(5), 432.

Rodriguez-Iturbe, I., Porporato, A., 2007. Ecohydrology of Water-Controlled Ecosystems Soil Moisture and Plant Dynamics. Cambridge University Press. U. K.

Shahid, S. A., Zaman, M., Heng, L., 2018. Soil Salinity: Historical Perspectives and a World Overview of the Problem. In Guideline for Salinity Assessment, Mitigation and Adaptation Using Nuclear and Related Techniques. Springer. 43–53.

Simunek, J., Sejna, M., Saito, H., Sakai, M., van Genuchten, M. T., 2018. The HYDRUS-1D Software Package for Simulating the One-Dimensional Movement of Water, Heat, and Multiple in Variably-Saturated Media. Riverside, California: Department of Environmental Sciences, University of California Riverside. U. S. A.

Steduto, P., Hsiao C., T., Fereres, E., Raes, D., 2012. Crop Yield Response to Water. FAO. Rome, Italy.

Sterman, J. D., 2000. Bussiness Dynamics: Systems Thinking and Modeling for a Complex World. McGraw Hill. U. K.

TAGEM., DSI., 2017. Türkiye'de Sulanan Bitkilerin Bitki Su Tüketimleri. Tarımsal Araştırmalar ve Politikalar Genel Müdürlüğü, Devlet Su İşleri Genel Müdürlüğü, Ankara, Türkiye.

Tanji, K. K., 2002. Salinity in the Soil Environment. In Salinity in the Soil Environment. Springer, Dordrecht. 21–51.

TUIK., 2021a. Agricultural Production Data. https://biruni.tuik.gov.tr/medas/?kn=92&locale=tr Data Accessed June 2021

TUIK., 2021b. Agriculture Portal. https://data.tuik.gov.tr/ Data Accessed June 2021

van Genuchten, M. T., 1980. A Closed-form Equation for Predicting the Hydraulic Conductivity of Unsaturated Soils. Soil Science Society of America Journal, 44(5), 892–898.

Vengosh, A., 2003. Salinization and Saline Environments. Environmental Geochemistry: Treatise on Geochemistry, 9(9), 1–35.

Weil, R. R., & Brady, C. N., 2016. The Nature and Properties of Soil (15^{th} Edition). Pearson. U.K.

WWF., 2014. Konya'da Suyun Bugünü Raporu. World Wide Fund-Türkiye. Türkiye.

Yaron, B., Danfors, E., Vaadia, Y., 1973. Arid Zone Irrigation. Ecological Studies 5. Springer - Verlag Berlin. Germany.

Yılmaz, A. M., Okumuş, Ş., 2015. Water Quality of Groundwater Affect on Soil Salinization in Konya-Eregli Province of Turkey. Extensive Journal of Applied Sciences, 144–152.

Zeng, W. Z., Xu, C., Wu, J. W., Huang, J. S., 2014. Soil salt leaching under different irrigation regimes: HYDRUS-1D modelling and analysis. Journal of Arid Land, 6(1), 44–58.

APPENDIX: MODEL EQUATIONS AND PARAMETERS

Water_in_Surface(t) = Water_in_Root_Zone(t - dt) + (irrigation + precipitation + capillary rise to surface- runoff -
surface evaporation_- infiltration) * dt

INIT Water_in_Surface = 5
UNITS= m3

INFLOWS:
Precipitation = IF Climate_Scenario_Preference=1 THEN "Precipitation_RCP_2.6" ELSE IF Climate_Scenario_Preference=2 THEN "Precipitation_RCP_4.5" ELSE IF Climate_Scenario_Preference =3 THEN "Precipitation_RCP_8.5" ELSE 0
UNITS= m3/day

Irrigation = IF Climate_Scenario_Preference=1 THEN "Irrigation_for_RCP_2.6" ELSE IF Climate_Scenario_Preference=2 THEN "Irrigation_for_RCP_4.5" ELSE IF Climate_Scenario_Preference=3 THEN "Irrigation_for_RCP_8.5" ELSE 0
UNITS= m3/day

Capillary Rise to Surface = Evaporation_Gap*Evaporation_Kr_coeffcient
UNITS= m3/day

OUTFLOWS
Surface Evaporation = MIN (Potential_Evaporation, Water_in_Surface*Evaporation_Fraction)
UNITS= m3/day

Runoff = MAX (((Water_in_Surface - Maximum_Water_Amount_in_Surface)*Runoff_Fraction), 0)
UNITS= m3/day

Infiltration =
MIN(Area_of_the_land*Saturated_Hydraulic_Conductivity_in_Rootzone*Relative_Hydraulic_Conductivity*((Suction_in_Rootzone+Distance)/Distance), Water_in_Surface*Infiltration_Fraction)

UNITS= m3/day

Water_in_Root_Zone(t) = Water_in_Root_Zone(t - dt) + (infiltration- percolation – actual transpiration – capillary rise to surface) * dt

INI = 1600

UNITS= m3

INFLOWS

Infiltration

OUTFLOWS

Percolation = IF Relative_Soil_Moisture > Relative_Soil_Moisture_at_Field_Capacity THEN Area_of_the_land*Hydraulic_Conductivity_in_Rootozone*Relative_Hydraulic_Conductivity ELSE 0

UNITS= m3/day

Actual Transpiration= Potential_Transpiration*Ks

UNITS= m3/day

Capillary Rise to Surface

Na Dissolved in Surface(t) = Na Dissolved in Surface(t - dt) + (Na in Irrigation Water + Capillary Rise of Na to Surface - Na Runoff – Na Infiltration) * dt

INITIAL = 0.5

UNITS = equivalents

INFLOWS =

Na in Irrigation Water = Na_Concentration_in_Irrigation_Water*Irrigation

UNITS = equivalents/day

Capillary Rise of Na to Surface =

Na_Concentration_in_Soil_Water_in_Rootzone*Capillary_Rise_to_Surface

UNITS = equivalents/day

OUTFLOWS

Na Runoff = Runoff*Na_Concentration_in_Surface

UNITS = equivalents/day

Na Infiltration= Na_Concentration_in_Surface*Infiltration

UNITS = equivalents/day

Na Dissolved in Rootzone(t) = Na Dissolved in Rootzone(t - dt) + (Na Infiltration - Capillary Rise of Na to Surface – Na Leaching) * dt

INI= 1400

UNITS = equivalents

INFLOWS

Na Infiltration

OUTFLOWS

Capillary Rise of Na to Surface

Na Leaching = Na_Concentration_in_Soil_Water_in_Rootzone*Percolation

UNITS = equivalents/day

Ca Dissolved in Surface(t) = Ca Dissolved in Surface(t - dt) + (Ca in Irrigation Water + Capillary Rise of Ca to Surface - Ca Runoff – Ca Infiltration) * dt

INITIAL = 0.25

UNITS = equivalents

INFLOWS =

Ca in Irrigation Water = Ca_Concentration_in_Irrigation_Water*Irrigation

UNITS = equivalents/day

Capillary Rise of Ca to Surface =

Ca_Concentration_in_Soil_Water_in_Rootzone*Capillary_Rise_to_Surface

UNITS = equivalents/day

OUTFLOWS

Ca Runoff = Runoff*Ca_Concentration_in_Surface

UNITS = equivalents/day

Ca Infiltration= Ca_Concentration_in_Surface*Infiltration

UNITS = equivalents/day

Ca Dissolved in Rootzone(t) = Ca Dissolved in Rootzone(t - dt) + (Ca Infiltration - Capillary Rise of Ca to Surface – Ca Leaching) * dt

INI= 7000

UNITS = equivalents

INFLOWS

Ca Infiltration

OUTFLOWS

Capillary Rise of Ca to Surface

Ca Leaching = Ca_Concentration_in_Soil_Water_in_Rootzone*Percolation

UNITS = equivalents/day

Cumulative Potential Transpiration (t) = Cumulative Potential Transpiration (t - dt) + (Potential Transpiration – Cumulative Potential Transpiration Outflow) * dt

INFLOWS

Potential Transpiraiton= ETo*Kcb

OUTFLOWS = IF Kcb = 0 THEN cumulative_potential_transpiration/DT ELSE 0

UNITS= m3/day

Cumulative Actual Transpiration (t) = Cumulative Potential Transpiration (t - dt) + (Actual Transpiration – Cumulative Actual Transpiration Outflow) * dt

INFLOWS

Actual Transpiration= Potential_Transpiration*Ks

OUTFLOWS

IF Kcb = 0 THEN Cumulative_Transpiration/DT ELSE 0

UNITS= m3/day

A Constant= 0.442 {Dimensionless}

A parameter = 2.2 {1/meter}

A value for Rootzone=
(EsCA_in_Rootzone*Selectivity_Coefficient_for_Rootzone)/((EsNA_in_Rootzone^2)*Salts_Concentration_in_Soil_Water_in_Rootzone/1000) {Dimensionless}

B Constant = 1 {Dimensionless}

B Constant for RHC = 0.242 {Dimensionless}
B Value Salinity Tolerance = IF Crop_Rotation_Preference=1 THEN B_Value_for_Crop_Rotation_2 ELSE IF Crop_Rotation_Preference=2 THEN B_Value_for_Crop_Rotation_1 ELSE IF Crop_Rotation_Preference=3 THEN B_Value_for_Crop_Rotation_3 ELSE 0
{m/dS}

C Value for RHC = G_Constant*(Euler_constant^(M_Constant*(ESP_of_Rootzone/100)))
{Dimensionless}

Ca Concentration in Irrigation Water = 2.9 {equivalent/m3}

Ca Concentration in Soil Water in Rootzone = Ca_Dissolved_in_Rootzone/Water_in_Rootzone
{equivalent/m3}

Ca Concentration in Surface = Ca_Dissolved_in_Surface/Water_in_Surface
{equivalent/m3}

Climate Scenario Preference = 1
{Dimensionless}

Concentration Threshold= 300

{equivalent/m3}

Crop Rotation Preference= 1
{Dimensionless}

D Value= IF Salts_Concentration_in_Soil_Water_in_Rootzone<Concentration_Treshold THEN 356.4*(Salts_Concentration_in_Soil_Water_in_Rootzone^-0.5)-20.58 ELSE 0
{Dimensionless}

Depth of Rootzone= 0.5
{meter}

Distance= Depth_of_Rootzone/2
{meter}

Drip Irrigation RCP 2.6 = IF Crop_Rotation_Preference=1 THEN "Drip_Irrigation_Crop_Rotation_1_RCP_2.6" ELSE IF Crop_Rotation_Preference=2 THEN "Drip_Irrigation_Crop_Rotation_2_RCP_2.6"ELSE IF Crop_Rotation_Preference=3 THEN "Drip_Irrigation_Crop_Rotation_3_RCP_2.6"ELSE 0
{m3/day}

Drip Irrigation RCP 4.5= IF Crop_Rotation_Preference=1 THEN "Drip_Irrigation_Crop_Rotation_1_RCP_4.5" ELSE IF Crop_Rotation_Preference=2 THEN "Drip_Irrigation_Crop_Rotation_2_RCP_4.5" ELSE IF Crop_Rotation_Preference=3 THEN "Drip_Irrigation_Crop_Rotation_3_RCP_4.5" ELSE 0
{m3/day}

Drip Irrigation RCP 8.5 = IF Crop_Rotation_Preference=1 THEN "Drip_Irrigation_Crop_Rotation_1_RCP_8.5" ELSE IF Crop_Rotation_Preference=2 THEN "Drip_Irrigation_Crop_Rotation_2_RCP_8.5" ELSE IF Crop_Rotation_Preference=3 THEN "Drip_Irrigation_Crop_Rotation_3_RCP_8.5" ELSE 0
{m3/day}

Ec Conversion Unit= 10
{equivalent/(dS*m2)}

EC Salinity in Rootzone= Salts_Concentration_in_Soil_Water_in_Rootzone/EC_Conversion_Unit
{dS/m}

EC Salinity in Surface= Salts_Concentration_in_Surface/EC_Conversion_Unit
{dS/m}

EC Salinity of Irrigation Water = Salts_Concentration_in_Irrigation_Water/EC_Conversion_Unit
{dS/m}

EsCa in Rootzone=
Ca_Concentration_in_Soil_Water_in_Rootzone/Salts_Concentration_in_Soil_Water_in_Rootzone
{Dimensionless}

EsNa in Rootzone=
Na_Concentration_in_Soil_Water_in_Rootzone/Salts_Concentration_in_Soil_Water_in_Rootzone
{Dimensionless}

ESP Adjusted= ESP_of_Rootzone-
(L_constant+S_constant*LN(Salts_Concentration_in_Soil_Water_in_Rootzone))
{Dimensionless}

ESP of Rootzone= Multiplier_for_ESP*ExNA_in_Rootzone
{Dimensionless}

Euler Constant= 2.71
{Dimensionless}

Evaporation Gap= Potential_Evaporation- Surface_Evaporation
{m3/day}

ExCa in Rootzone= Z_Value_for_Rootzone-ExNA_in_Rootzone
{Dimensionless}

ExNa in Rootzone=
{Dimensionless}

F Constant= 0.182
{Dimensionless}

G Constant= 2.07
{Dimensionless}

Infiltration Fraction= 1
{1/day}

Irrigation for RCP 2.6=IF Irrigation_Method=1 THEN "Sprinkler_Irrigation_RCP_2.6" ELSE IF Irrigation_Method=2 THEN "Drip_Irrigation_RCP_2.6" ELSE 0
{m3/day}

Irrigation for RCP 4.5= IF Irrigation_Method=1 THEN "Sprinkler_Irrigation_RCP_4.5" ELSE IF Irrigation_Method=2 THEN "Drip_Irrigation_RCP_4.5" ELSE 0
{m3/day}

Irrigation for RCP 8.5= IF Irrigation_Method=1 THEN "Sprinkler_Irrigation_RCP_8.5" ELSE IF Irrigation_Method=2 THEN "Drip_Irrigation_RCP_8.5" ELSE 0
{m3/day}

Irrigation Method= 1
{Dimensionless}

Kc max= 1.25
{Dimensionless}

Ke= Kc_max – Kcb
{Dimensionless}

Ks = Ks_Water_Stress*Ks_Salinity_Stress
{Dimensionless}

Ks Water Stress= IF Relative_Soil_Moisture <Water_Stress_Threshold THEN MAX((Relative_Soil_Moisture-Relative_Soil_Moisture_at_Wilting_Point)/(Water_Stress_Threshold-Relative_Soil_Moisture_at_Wilting_Point), 0) ELSE 1
{Dimensionless}

Ks Salinity Stress= IF EC_Salinity_of_Rootzone > Salinity_Stress_Treshold THEN MAX(1-B_Value_Salinity_Tolerance*(EC_Salinity_of_Rootzone-Salinity_Stress_Treshold)/(Ky_Factor*100), 0) ELSE 1
{Dimensionless}

Ky Factor= IF Crop_Rotation_Preference=1 THEN Ky_Factor_for_Crop_Rotation_2 ELSE IF Crop_Rotation_Preference=2 THEN Ky_Factor_for_Crop_Rotation_1 ELSE IF Crop_Rotation_Preference=3 THEN Ky_Factor_for_Crop_Rotation_3 ELSE 0
{Dimensionless}

L Constant= -11.42
{Dimensionless}

M constant= 4.801
{Dimensionless}

M parameter= 1-(1/N_parameter)
{Dimensionless}

Multiplier for ESP= 100
{Dimensionless}

N parameter= 1.2
{Dimensionless}

N Value for RHC= ((ESP_of_Rootzone/100)^A_Constant)+B_Constant_for_RHC
{Dimensionless}

Na Concentration in Irrigation Water= 12.1
{equivalent/m3}

Na Concentration in Soil Water in Rootzone= Na_in_Dissolved_in_Rootzone/Water_in_Rootzone
{equivalent/m3}

Na Concentration in Soil Water in Surface= Na_Dissolved_in_Surface/Water_in_Surface
{equivalent/m3}

P Value= IF Crop_Rotation_Preference=1 THEN P_value_for_Crop_Rotation_2 ELSE IF Crop_Rotation_Preference=2 THEN P_value_for_Crop_Rotation_1 ELSE IF Crop_Rotation_Preference=3 THEN P_value_for_Crop_Rotation_3 ELSE 0
{Dimensionless}

Porosity= 0.48
{Dimensionless}

Potential Evaporation= ETo*Ke
{m3/day}

Reduction in Hydraulic Conductivity= (1-Relative_Hydraulic_Conductivity)*100
{Percentage}

Relative Hydraulic Conductvity= IF X_value_for_RHC_in_Rootzone >0 THEN (1-((C_value_for_RHC*X_value_for_RHC_in_Rootzone^N_value_for_RHC)/(1+C_value_for_RHC*X_value_for_RHC_in_Rootzone^N_value_for_RHC))) ELSE 1
{Dimensionless}

Relative Soil Moisture = MIN(Volumetric_Water_Content_of_Rootzone/Saturated_Water_Content_of_Rootzone, 1)
{Dimensionless}

Relative Soil Moisture at Field Capacity=
Water_Content_at_Field_Capacity_in_Rootzone/Saturated_Water_Content_of_Rootzone
{Dimensionless}

Relative Soil Moisture at Residual Water Content=
Residual_Water_Content/Saturated_Water_Content_of_Rootzone
{Dimensionless}

Relative Soil Moisture at Wilting Point=
Water_Content_Wilting_Point_in_Rootzone/Saturated_Water_Content_of_Rootzone
{Dimensionless}

Residual Water Content= 0.12
{m3/m3}

S Constant= 7.678
{Dimensionless}

Salinity Stress Threshold= IF Crop_Rotation_Preference=1 THEN
Salinity_Stress_Treshold_for_Crop_Rotation_2 ELSE IF Crop_Rotation_Preference=2 THEN
Salinity_Stress_Treshold_for_Crop_Rotation_1 ELSE IF Crop_Rotation_Preference=3 THEN
Salinity_Stress_Treshold_for_Crop_Rotation_3 ELSE 0
{dS/m}

Salts Concentration in Soil Water in Rootzone=
Na_Concentration_in_Soil_Water_in_Rootzone+Ca_Concentration_in_Soil_Water_in_Rootzone
{equivalent/m3}

Salts Concentration in Soil Water in Surface=
Na_Concentration_in_Irrigation_Water+Ca_Concentration_in_Irrigation_Water
{equivalent/m3}

SAR of Irrigation Water=
Na_Concentration_in_Irrigation_Water/((Ca_Concentration_in_Irrigation_Water/2)^0.5)
{(equivalent/m3)^0.5}

SAR of Soil Water in Rootzone=
Na_Concentration_in_Soil_Water_in_Rootzone/((Ca_Concentration_in_Soil_Water_in_Rootzone/2)^0.5)
{(equivalent/m3)^0.5}

Saturated Hydraulic Conductivity in Rootzone= 0.831
{meter/day}

Saturated Water Content of Rootzone= (Volume_of_Rootzone*Porosity)/Volume_of_Rootzone
{m3/m3}

Selectivity Coefficient for Rootzone= 4
{equivalent/m3}

Sprinkler Irrigation RCP 2.6= IF Crop_Rotation_Preference=1 THEN "Sprinkler_Irrigation_Crop_Rotation_1_RCP_2.6" ELSE IF Crop_Rotation_Preference=2 THEN "Sprinkler_Irrigation_Crop_Rotation_2_RCP_2.6" ELSE IF Crop_Rotation_Preference=3 THEN "Sprinkler_Irrigation_Crop_Rotation_3_RCP_2.6" ELSE 0
{m3/day}

Sprinkler Irrigation RCP 4.5 = IF Crop_Rotation_Preference=1 THEN "Sprinkler_Irrigation_Crop_Rotation_1_RCP_4.5" ELSE IF Crop_Rotation_Preference=2 THEN "Sprinkler_Irrigation_Crop_Rotation_2_RCP_4.5" ELSE IF Crop_Rotation_Preference=3 THEN "Sprinkler_Irrigation_Crop_Rotation_3_RCP_4.5" ELSE 0
{m3/day}

Sprinkler Irrigation RCP 8.5= IF Crop_Rotation_Preference=1 THEN "Sprinkler_Irrigation_Crop_Rotation_1_RCP_8.5" ELSE IF Crop_Rotation_Preference=2 THEN "Sprinkler_Irrigation_Crop_Rotation_2_RCP_8.5" ELSE IF Crop_Rotation_Preference=3 THEN "Sprinkler_Irrigation_Crop_Rotation_3_RCP_8.5" ELSE 0
{m3/day}

Suction in Rootzone= (1/A_parameter)*((1-(Relative_Soil_Moisture^(1/M_parameter)))^(1/N_parameter))

{meter}

Volume of Rootzone= Area_of_the_land*Depth_of_Rootzone
{m3}

Volumetric Water Content of Rootzone= Water_in_Rootzone/Volume_of_Rootzone
{m3/m3}

Water Content at Field Capacity in Rootzone= 0.32
{m3/m3}

Water Content at Wilting Point in Rootzone= 0.22
{m3/m3}

Water Stress Threshold= Relative_Soil_Moisture_at_Field_Capacity-P_Value*(Relative_Soil_Moisture_at_Field_Capacity-Relative_Soil_Moisture_at_Wilting_Point)
{Dimensionless}

X Value for RHC in Rootzone= F_constant*(0.00036*ESP_Adjusted)*D_Value
{Dimensionless}

Z Value for Rootzone= 1
{Dimensionless}